LEIDSE GEOLOGISCHE MEDEDELINGEN, Deel 28 1963 blz. 1—102 pre-issued 10-10-1962

A FABRIC STUDY OF LHERZOLITES
WITH SPECIAL REFERENCE TO ULTRABASIC NODULAR INCLUSIONS IN THE LAVAS OF AUVERGNE (FRANCE)

by

A. L. G. COLLEE

CONTENTS

CHAPTER VI

CHAPTER VII

CHAPTER I

INTRODUCTION AND DELIMITATION OF THE STUDY

1. *Introduction*

This paper deals with the petrofabrics of some ultrabasic rocks of lherzolitic composition. The aim of the study has been to collect both more detailed and more diverse information on the fabric and through this on the origin of nodular inclusions of ultrabasic composition in certain basaltic lavas. The problems related with the genesis of ultrabasic rocks can be tackled from many different angles. Actually nowadays there is a constant flow of publications dealing with the mineralogical, petrographical, chemical, thermodynamical or other aspects of these rocks. For the individual research worker it is almost impossible to involve all these aspects in a study of a limited scope. To avoid the risk of dealing with problems which are beyond his competence, the author has restricted this study as much as possible to the fabric of these rocks. In doing so he realizes that he draws a one-sided picture but it seemed preferable to collect extensive information on one aspect rather than to get lost in the multitude of problems related with the study of ultrabasic rocks in general. Lherzolites are ultrabasic rocks which contain olivine as well as ortho- and clinopyroxene. The name is derived from the Pyrenean type locality: Etang de Lhers, where these rocks occur along the north Pyrenean fault zone, in a number of rather small bodies.

The problem of the genesis of nodular inclusions of ultrabasic composition in certain basaltic lavas, has given rise to much controversy. Nowadays two opinions about their origin predominate. Some authors consider them to be endogenous autoliths i.e. early crystallization products of the basalts in which they occur, others look at them as exogenous xenoliths i.e. fragments of deeply burried ultrabasic rocks or of the peridotite layer of the upper mantle, carried to the surface by the eruptive action of the lavas in which they occur. The theoretical interest of the study of these rocks lies in the fact that, if the latter origin could be proved, these rocks might yield valuable information on the geological, chemical, and tectonic environment of the deeper parts of the crust, if not of the upper part of the mantle.

The studied samples mainly come from the Chaîne des Puys in Auvergne, France, from a collection Professor W. P. de Roever kindly put at my disposal, for the purpose of this study. One sample is from the well known German occurrence at Dreiser Weiher, it forms part of the collection Professor J. Frechen was so kind to supply me with. It seemed logical to include in this study an investigation of material from the Pyrenean type locality, mainly because the literature does not provide many examples in which there exists a clear relationship between the crystal orientation in ultrabasic rocks and the tectonic environment in which the peridotites occur. In the Pyrenean lherzolite there proved to be a close relationship between both.

2. *Previous authors*

It is beyond the scope of this paper to give a complete summary of all the work that has been done on ultrabasic rocks. However it seems useful to mention the main theories bearing on the origin of nodular inclusions in lavas, and to summarize the petrofabric work carried out on ultrabasic rocks in general.

Theories on the origin of ultrabasic inclusions in lavas are numerous. However two main tendencies can be recognized: the endogenous and the exogenous theories. The former look at the nodules as products of the lavas in which they occur, the latter consider the lavas only as means of transport. In the hypothesis based on the endogenous nature of the inclusions, the crystals which build up the nodules are thought to be early crystallization products of the lavas. The accumulation of the crystals may then be due to gravity settling, or to deposition from convection currents in the magma chamber.

Hypotheses based on the exogenous origin of the inclusions break up in two theories. The first advocates an accidental incorporation in the lava of fragments of ultrabasic rocks which intruded in the vicinity of the magma chamber, or are broken through by the lava in the higher levels. The second explains the xenoliths as solid fragments of the peridotite layer, from which the magma originated through anatexis.

Readers interested in a critical review of these theories can refer to Wilshire and Binns (1961).

The petrofabrics of olivine have first been studied by Andreatta in 1934. Later investigators such as Ernst, Phillips, Turner, Ladurner, Paulitsch and Brothers greatly increased the information on the subject. An attempt will now be made to summarize the results of their investigations. The following modes of occurrence will be dealt with:

a. Metamorphic occurrences (tectonite fabrics).
b. Nodular inclusions in lavas.
c. Large, mostly deformed peridotite bodies.
d. Crystal accumulations due to flow in a liquid (appositional fabrics).
e. Crystal accumulations under influence of gravity (depositional fabrics).

a. Andreatta (1934) studied some samples from the Ortles-Cevedale massif in the Italian Alps, which are believed to be of metamorphic origin. The fabric proved to be dominated by a strong maximum of X_{ol} [1]) perpendicular to the macroscopically visible schistosity. Y_{ol} and Z_{ol} did not show a strong preferred orientation within this plane. The same results were obtained by Ernst (1935) who published a diagram of an olivine-schist from Norway. From these results it was concluded that in S-tectonites {010} tends to be oriented parallel to the plane of schistosity, while the Y_{ol} and Z_{ol} have only a weak preferred orientation within this plane.

b. The nodular inclusions in lavas from European occurrences have also been analyzed with regard to their fabrics by Ernst (1935). From the fact that the orientation of olivine in these nodules is of the same type as in the above cited olivinites, he concluded to a tectonic origin of these nodules. In

[1]) For an explanation of the abbreviations: X_{ol}, Y_{ol}, Z_{ol} see page 10.

fact most of the diagrams published in his paper show strong concentrations of X_{ol}. According to the author, the tendency of X_{ol} to form girdles is strongest in samples which show abundant translation lamellae. The olivine crystals are tabular parallel to {010} and thus also show good dimensional orientation.

Turner (1942) mentions an analogous result for a nodule from Prussia in which Y_{ol} and Z_{ol} tend to form perpendicular concentrations in the plane occupied by {010}. In contrast however his diagrams of non-European nodular inclusions do not, or do only weakly confirm the above mentioned rule. For instance his sample 5100, a lherzolite from a pliocene basalt of Kokonga, only shows a faint indication of three such perpendicular maxima. The same holds for sample 6655, a nodule of lherzolitic composition from Kakanui, NE. Otago. Neither rock shows signs of dimensional orientation of the crystals. A completely different orientation has been found in a sample from Auckland (7503). X_{ol} forms a girdle the axis of which is the main Z_{ol} concentration, and to a minor extent also a Y_{ol} concentration. The crystals do not show evidence of dimensional orientation.

c. Petrofabric data of large peridotite bodies are rather abundant. The first to work on this subject was Phillips (1938). His diagrams made of samples from Rum and Skye, suggest a strong relation between the banding of the rock and the orientation of the composing minerals. Three of his samples show strong concentrations of X_{ol} perpendicular to the plane of fissility, only in one of the three diagrams Z_{ol} shows a preferred orientation in this plane. All these samples also show dimensional orientation, the crystals being tabular parallel to {010}. In one of these samples, an allivalite, X_{ol} coincides with the normal to {010} of plagioclase. Strong evidence for the fabric actually being determined by a dimensional orientation of the crystals is suggested by the fact that a rock from the same locality, which is composed of equidimensional crystals, does not show any preferred orientation of its constituents. Phillips concludes that "the stresses acting during the emplacement of an olivine-rich intrusive, already largely crystalline, can develop in the rock precisely those features of the fabric, which have been considered to indicate a metamorphic origin". Thus, based on the same type of diagrams, Phillips and Ernst come to completely different conclusions on the origin of these rocks. This controversy has ever since dominated the interpretation of the fabric of ultrabasic rocks.

It was Turner (1942) who made it clear that the problem is even more complicated. In his study he enlisted a sample (7497) from Rum, the same locality as the rocks studied by Phillips came from. This fissile, slightly linear rock shows a girdle of X_{ol} with its main concentration approximately in the plane of fissility, and a minimum perpendicular to it. Y_{ol} also has its main concentration in this plane, Z_{ol} has not a strong preferred orientation. The crystals do not show signs of dimensional orientation. From this sample it became clear that samples from one locality may yield completely different fabrics, and that the lattice orientation of olivine is not necessarily linked with a dimensional orientation of the crystals. This fact is even more directly confirmed by a diagram Turner obtained from an unbanded non-fissile harzburgite (1380). The fabric shows the usual strong X_{ol} concentration perpendicular to the Y_{ol} and Z_{ol} girdle, in absence of any sign of dimensional orientation. Other samples from Skye (Turner 7496 and 7498) confirmed the rule of a strong X_{ol} concentration perpendicular to the banding or fissility,

with only a weak orientation of Y_{ol} and Z_{ol} in this plane, the rocks being devoid of a strong dimensional orientation of the crystals.

Several diagrams of samples from Dun Mt. Nelson are published by Turner (7493, 7494, 7495, 7505). Again it was demonstrated that the fabrics of samples from one locality may strongly diverge. Both the samples 7494 and 7495 confirm the usual pattern in absence of strong dimensional orientation, but the first (7493) shows a rather well developed girdle of Z_{ol} in S, a strong Y_{ol} concentration perpendicular to S, and a distribution of X_{ol} both in S and perpendicular to S. From this sample which shows strong evidence of deformation it becomes clear that the olivine fabric of peridotites is rather sensitive to deformation. In the fourth sample (7505), composed of equant grains, a relation may be assumed to exist between fabric and tectonic geometry. Turner supposes that the strong Z_{ol} concentration coincides with the tectonic *b* axis, and the well developed girdle of X_{ol} and the weaker one of Y_{ol} with the *ac* plane. The same locality was recently investigated by Battey (1960), who published seven diagrams of oriented samples. His work derives its importance from the fact that a distinct relation between the fold axis and the olivine orientation could be established. The results confirm the above mentioned assumption of Z_{ol} being parallel to the tectonic *b* direction, and X_{ol} forming a girdle in the *ac* plane.

A strong lattice orientation was also reported by Paulitsch (1953) in a dunite from Anghida, which also suffered post crystalline deformation. In this sample a strong Z_{ol} concentration in the banding (S) is the pole of a complete girdle of X_{ol} and Y_{ol}. The highest concentration of X_{ol} occupies a position 50°—70° away from S. The crystals are tabular parallel to {001}. The Z_{ol} maximum probably coincides with the tectonic *b* axis, and the X_{ol} and Y_{ol} girdle with the *ac* plane.

The question arises whether a diagram published by Ladurner (1956) of a banded dunite from Bursa, which he explained by a rather complicated assumption of a dimensional orientation of {011} in S and the occurrence of twinning upon {110} to account for a double Z_{ol} concentration in S, is not to be regarded as a tectonite. This would require a deformation subsequent to solidification, a view rejected by Ladurner, amongst other reasons because of the inhomogeneity of the fabric. Olivine in the chromite-rich layers shows a weaker orientation than in the olivine-rich bands. However it will be demonstrated in the course of this study, that inhomogeneity of the fabric can occur in olivine tectonites as well. The crystals in this rock show an unusual habit, they are tabular parallel to {100} and elongate parallel to [001]. The fabric is dominated by a double Z_{ol} maximum, 47° apart in S, X_{ol} and Y_{ol} occupy broad girdles with mutually perpendicular maxima 30° and 60° respectively from S.

The most extensive study, dealing with the structural petrology of a large peridotite body has been published by Yoshino (1961). The author gives over thirty olivine fabric diagrams, comprising several thousands of measurements. It is impossible here to review all the data collected in that paper. The following conclusions can however be drawn from these data:

1. The olivine fabric is symmetrical with regard to the tectonic geometry of the country rock, in such a way that the Y_{ol} axes tend to be parallel to the regional *b* axis and the X_{ol} axes perpendicular to the regional schistosity plane.
2. The X_{ol} axes tend to be perpendicular to chromite bands in the peridotite.

3. The olivine crystals are equidimensional, and do not show any sign of deformation.

The combination of these facts incited the author to interprete the observed fabric as the result of a neocrystallization of olivine.

A comparable type of fabric has been described by Ladurner (1956) in a pyroxene-rich peridotite from the Seefelder Alps (Austria). The Y_{ol} axes tend to be parallel to the tectonic *b* axis, while X_{ol} and Z_{ol} form girdles in the *ac* plane, probably in relation with visible shear planes intersecting at 80 degrees. The crystals are elongate parallel to [001].

From the foregoing synopsis the following conclusions can be drawn:

- — The fabrics of peridotites, which show no evidence of post-emplacement deformation are mostly characterized by a strong concentration of X_{ol}. Both other olivine axes do not always show a strong preferred orientation in the plane perpendicular to X_{ol}. This type of orientation is not limited to rocks with a strong banding or fissility. Strong orentation of X_{ol} is not always coupled with a dimensional orientation of the crystals.
- — Large deformed peridotite bodies are mainly b-tectonites. They are characterized by either a Z_{ol} or Y_{ol} concentration parallel to the *b* axis. The X_{ol} axes generally form a short girdle in the *ac* plane.
- — Rocks from one locality may show completely different fabrics. This phenomenon is probably due to the fact that olivine reacts quickly to any local deformation.
- — Metamorphic olivinites, when S-tectonites, are characterized by a strong X_{ol} concentration perpendicular to the S plane.
- — Most nodular inclusions in lavas from European occurrences show the same type of preferred orientation as do undeformed peridotites and S-tectonites. As a rule this orientation is coupled with a dimensional orientation of the crystals.

This summary clearly demonstrates that it is rather rash to draw conclusions regarding the genesis of ultrabasic rocks, from petrofabric data only. Yet the fabric of ultrabasic rocks often has served as circumstantial evidence in support of the theory of Bowen which postulates that ultrabasic rocks intrude the country rock as a highly crystalline mass. In doing so, the fact that the same fabric can be the result of completely different processes is disregarded. Furthermore it has not been proved conclusively that a mechanism, such as proposed by Bowen, can actually cause the strong preferred orientation observed in many ultrabasic rocks.

d. In this respect studies of flow orientation of olivine are very interesting. Turner (1942) was the first to publish data bearing on this subject. Huang and Merritt (1952) and Brothers (1959) later did the same.

Turner (5561) did not find indications of dimensional orientation of olivine in a mugearite although the plagioclase laths showed parallel alignment in the rock.

Huang and Merritt (1952) dealt with flow banded troctolites from Oklahoma. Although the authors describe their X_{ol} maxima as being perpendicular to the flow plane, a close examination of their diagrams reveals a clear divergence from the perpendicular position, resulting in a monoclinic symmetry of the

diagrams. This departure of the X_{ol} axes from an orientation normal to the flow plane is important because it implies an imbricate structure of the crystal aggregate, as found in edgewise conglomerates. This orientation is to be expected from flat particles settling in a medium subject to laminar flow.

Extensive work on flow orientation of olivine has been done by Brothers (1959). In this paper diagrams of six different samples are listed. Two of them show very strong orientation of olivine. Brothers claims that in these cases the main X_{ol} concentration is perpendicular to the flow plane. From his diagrams however it seems also possible to infer a small departure of X_{ol} from this perpendicular position, just as was suggested for the diagrams of Huang and Merritt. In this respect the first sample is particularly convincing. Furthermore it is well demonstrated in the paper of Brothers that flow does not always cause a strong orientation of the olivine phenocrysts: "Not all dyke forms reveal the typical flow orientation of olivine phenocrysts, and in the present study 10 intrusions yielded only 5 recognizable patterns". This phenomenon is probably to some extent due to the fact that movements other than flow affected the olivine fabric. Especially gravitational settling must have influenced the diagrams to some extent.

e. It was Turner (1942), and later Huang and Merritt (1952), who studied the orientation of olivine due to gravitational settling from a liquid medium, the former in the gravitationally differentiated sill of Lugar in Ayrshire, the latter in a troctolite. They reached the same conclusion, namely that such a mechanism fails to cause a preferred orientation. However the fact that in both cases the crystals involved were probably equidimensional makes these results little conclusive.

Jackson (1961) in his study on the Stillwater complex, established a direct relationship between grain shape and dimensional orientation, in the case of crystal settling due to gravity and flow. His diagrams leave little doubt that the preferred orientation of both olivine and enstatite increases according as the grain shape stronger deviates from equidimensional. The flat surfaces of the crystals tend to be parallel to the layering plane, the elongate directions show alignment within this plane. The stronger the departure from the equidimensional form, the stronger is the observed preferred orientation. The author also mentions the imbricate structure of some of these rocks. The study of Jackson leaves no doubt that a dimensional orientation of the crystals always implies a direct relationship between the observed orientation and the shape of the grains. If the observed orientation does not agree with the grain shape, the latter cannot be the main cause of the fabric. This conclusion has probably not been given enough consideration in the interpretation of the fabrics of ultrabasic rocks.

Brothers (1960) published three diagrams of nodules from lavas in New Zealand. Although he concluded, mainly on petrographical grounds, to an endogenous origin of the inclusions, he also claims to have found indications for flow movements in the fabric diagrams. However, none of the diagrams of the three samples seems very convincing in this respect. The first shows a rather strong X_{ol} concentration near the banding, a feature not yet observed in flow-banded peridotites. The second shows a rather strong X_{ol} concentration with Y_{ol} and Z_{ol} in an incomplete girdle, an orientation also known from rocks in which flow did probably not occur. The third sample hardly shows any sign of preferred orientation.

3. *Outline of the study*

The preceding summary of the literature leaves no doubt that there still exists a controversy concerning the interpretation of ultrabasic rock fabrics, particularly of the nodular inclusions in lavas. The writer realizes that the best way to tackle these problems, is in following some new approaches in this study.

In the first place it seemed useful to increase the information on the fabric of these rocks by measuring more than one mineral species in any one sample. This is the reason why this study deals with lherzolites rather than with dunites. The mineralogical composition of the former makes it possible to construct fabric diagrams of both olivine and pyroxene. It will be clear from the fact that enstatite is orthorhombic, that it is easier to deal with enstatite rather than with monoclinic pyroxene in petrofabric work. A not too coarse-grained rock containing about twenty percent enstatite yields sufficient grains to construct reliable diagrams.

A second method, not previously applied to rocks consisting of biaxial crystals will be used in this study. It consists in making an "Axial Distribution Analysis". The object in view is to obtain a more detailed and specific insight into the structure of the rock involved. The technique of making an A. D. A. consists in measuring the orientation of all the crystals of one species, present in a given surface of the sample. The resulting fabric diagram is then divided into a number of different areas, each comprising crystals of a specific orientation. On the photograph of the thin section the locations of the crystals of similar orientation are then given a specific shade or colour. The resulting picture gives a clear insight in the distribution in space of similarly oriented crystals in the rock. In doing so, planar or linear structures and their tectonic significance can be visualized.

Only a few authors published more than one diagram of the samples they studied, and most of them found indications for the fabric to be inhomogeneous. In this study diagrams of three perpendicular faces, of samples from both the Eifel and Auvergne occurrences will be published. Thus the question whether these rocks are homogeneous and whether there exists some influence from the "Schnitteffekt" will be broached and an answer sought.

Attention is being paid in this investigation to the grain shape of both olivine and enstatite. In order to avoid long descriptions, the results of these observations are plotted in the fabric diagrams. In all the samples where such proved to be possible, the direction of the long diameter of each inequidimensional crystal has been measured. In the centre of the corresponding diagram, these directions are plotted. Thus the relation between grain shape and fabric is visualized.

In the literature, the problem of the number of measurements required to construct reliable fabric diagrams of ultrabasic rocks has never been treated statistically. Most authors construct their diagrams from fifty or a hundred grains. In the course of this study it has been proved empirically, that the shape of diagrams which show only weak preferred orientation is apt to change when the number of measurements is extended. In this respect it is important to note, that a correct

representation of the orientation of the Y_{ol} and Z_{ol} axes needs a greater number of measurements than the usually stronger oriented X_{ol} axis. In enlarging the number of measurements the strength of the maxima often also decreases, causing a spreading in the diagrams, hence the numerical value of the maxima is not significant, they are only of interest for comparative purposes of different diagrams, based upon the same number of measurements. But for practical reasons it is impossible to extend the number of measurements of biaxial crystals very far. The above mentioned observations induced the writer to base his diagrams on hundred readings. In diagrams based on this number, the one percent density contour proved to be insignificant of preferred orientation. For that reason these lines are not represented, consequently the lowest density line in all diagrams based on hundred grains, is the two percent line.

For a good understanding of the following chapters, a quick description of the minerals this study deals with, might be useful. The fact that both olivine and enstatite are orthorhombic greatly simplifies the petrofabric work. The orientation of the optical indicatrix with respect to the crystallographic axes in olivine is the following:

X_{ol} (α) = b = [010]
Y_{ol} (β) = c = [001]
Z_{ol} (γ) = a = [100]

Most of the olivine crystals show a well developed {010} parting. The well known translation lamellae, which occur in almost all the olivine crystals are invariably normal to Z. Both these features greatly facilitate work with the universal stage. If the mineral is in the extinction position, the orientation of the parting or the lamellae immediately reveals which of the axes, X or Z is parallel to the E.—W. direction of the universal stage. Furthermore the Y axis is easily recognized by the fact that on rotation around this axis, the extinction does not remain complete, due to the high birefringence of olivine. On this account it becomes superfluous to check with the gypsum plate for the measured axis.

The orientation of the optical indicatrix with respect to the crystallographic axes in enstatite is the following:

X_{en} (α) = b = [010]
Y_{en} (β) = a = [100]
Z_{en} (γ) = c = [001]

The crystals have the usual {110} cleavages, and sometimes a {001} parting. Measuring of enstatite turned out to be more time consuming than olivine, because of the lower birefringence of the mineral, which hampers the quick recognition of small departures from the extinction position. In some samples it was difficult to find a hundred enstatite crystals. However with the aid of photographs, on which each measured grain can be noted, it becomes possible to locate and measure all the enstatite crystals in a given thin section.

CHAPTER II

A NODULE OF LHERZOLITIC COMPOSITION FROM DREISER WEIHER, EIFEL, GERMANY

1. *Introduction*

The mineralogical composition of the ultrabasic ejecta at Dreiser Weiher covers a wide range. Almost all transitions between monomineralic rocks consisting of olivine, orthopyroxene, or diopside are known. Picotite mostly occurs as an accessory mineral in the rocks of ultrabasic composition. The chemical composition of the minerals is rather constant: the olivine has a composition of about 90 Fo/10 Fa, the orthopyroxene is a bronzite, and the monoclinic pyroxene is a chromium-diopside.

From the collection kindly put at my disposal by Professor J. Frechen, the fabric of one nodule which approached the lherzolitic composition conveniently, has been studied. It would seem rather superfluous to investigate a rock type from a locality of which samples have already been analyzed, not only as regards their petrofabrics (Ernst 1935) but also concerning their petrographical (Frechen 1948) and chemical properties (Ross, Foster, Myers, 1954). There are, however, several considerations which incited the author to a further study of these rocks. There is, for instance, no doubt that a comparative study of the fabrics of enstatite and olivine has to start with relatively simple patterns. The fact that the fabric of the nodules from Dreiser Weiher is rather simple, makes them an ideal starting-point for an investigation of the orientation of enstatite. Furthermore, the homogeneity of the fabric had to be tested. From the literature it is known that the more complicated fabrics often are inhomogeneous. In order to explain this phenomenon, it is important to know if the simpler mineral orientation pattern found in the nodules from this German locality, also displays the said inhomogeneity. To find this out, fabric diagrams have been made from three mutually perpendicular sections of one sample. The orientation of the thin sections has been chosen in such a manner, that each of them is sub-normal to the main point-maximum of preferred orientation of a different axis of olivine. In doing so, the influence of grain shape on preferred orientation which is likely to occur in the diagrams if the crystals are inequidimensional, can also be evaluated.

2. *Description of the fabric diagrams*

The diagrams 1—31 refer to this lherzolitic nodule (D.W. 1) of Dreiser Weiher. The three faces of the rock of which sections have been studied are referred to as front, top, and side face; see figure 1. The arrows on the cube are drawn to coincide with those on top of the diagrams. In each thin section 100 olivine and 100 enstatite crystals have been measured.

The results of measurements of the direction of the long diameter of the crystals are represented in the centres of the diagrams. In each thin section the direction of the long diameter of each inequidimensional grain has been

measured. These directions are then grouped in units comprising ten degrees of the compass. For each group the percentage of total readings is calculated, and represented in a rose in the centre of the diagram. In this way, the rose figure directly visualizes the grain shape. However, no information on the grain size is given.

The olivine fabric of the front face of figure 1 is represented in the first three diagrams. A strong linear concentration of X_{ol} dominates the fabric, there is however a tendency of X_{ol} to form an incomplete girdle normal to the main common point maximum of Y_{ol} and Z_{ol}. The Z_{ol} orientation although weaker than X_{ol}, is mainly concentrated along the eastern and western [2]) margins of the diagram, in the plane normal to the main X_{ol} concentration.

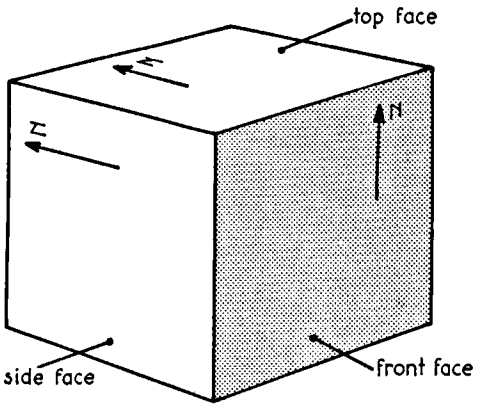

Figure 1.
The three faces of the sample cube D.W. 1., described in chapter II.

The diagrams 4, 5, 6, refer to the enstatite orientation in the front section of figure 1. (for comparative purposes diagram 4 represents Y_{en}, diagram 5: X_{en} and diagram 6: Z_{en}) Z_{en} shows the most pronounced preferred orientation coinciding with that of Z_{ol}. Both other axes have a weaker orientation; however Y_{en} roughly coincides with X_{ol}, while the orientation of X_{en} seems to depend on the orientation of both other axes of the enstatite indicatrix. Before discussing the interpretation of these data, it is more advantageous to deal with the fabric of the other faces of the sample cube.

The diagrams 7—12 refer to the top section. Numbers 7, 8, 9 have been made from the olivine crystals. As should be expected X_{ol} prefers a central position

[2]) The use of the terms north, south, east and west, in the description of the fabrics of nodular inclusions in lavas, does not refer to the geographical azimuths. The fact that the nodules occur scattered in lavas excludes the possibility of establishing a relation between the fabric and any such a direction. For descriptive purposes however, it is convenient to use these terms. The directions are chosen in such a way, that north always coincides with the top of the diagrams, west with the left hand side and so on.

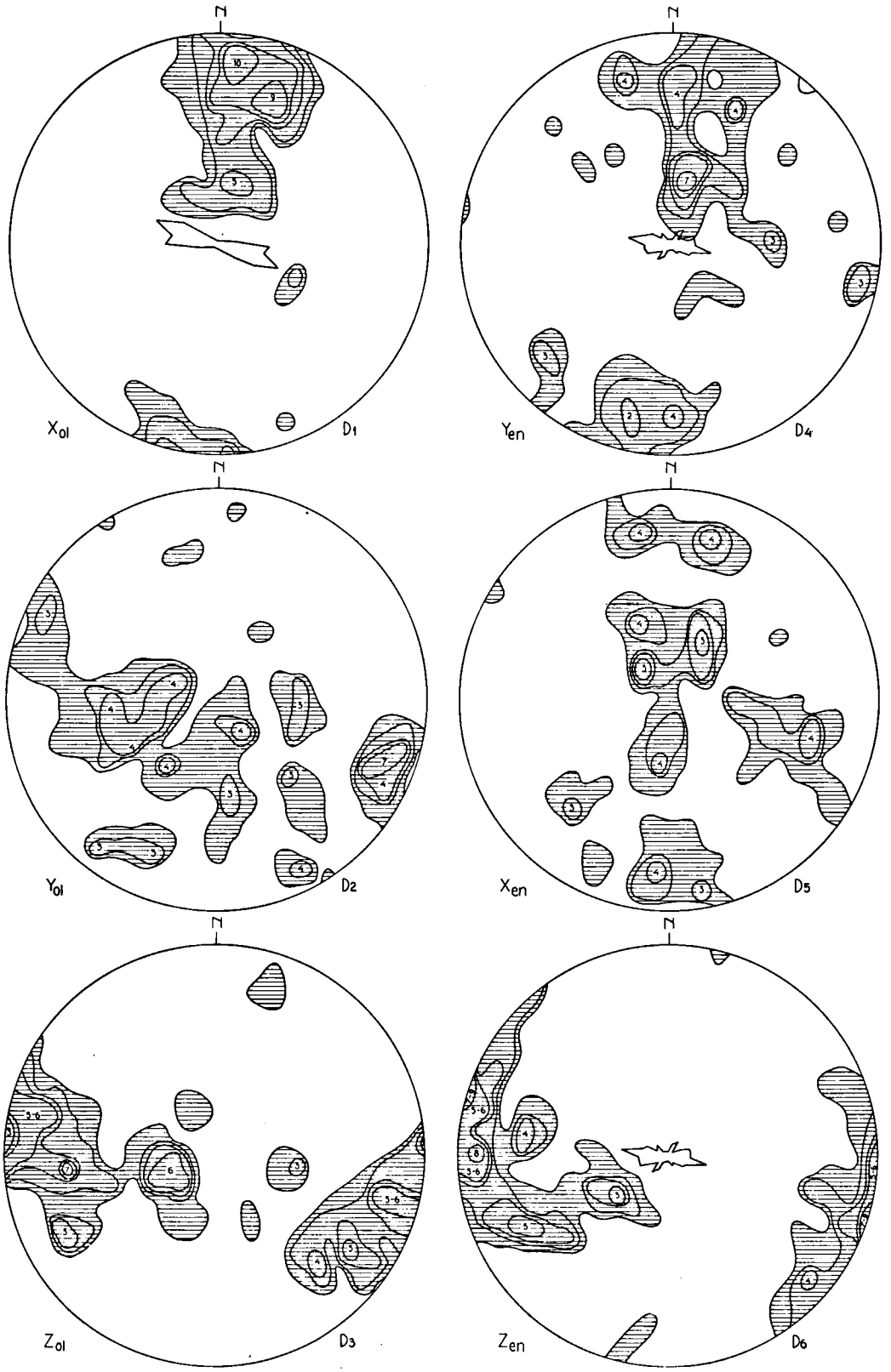

D. 1.: D.W., 100 X_{ol}, front face.
D. 2.: D.W., 100 Y_{ol}, front face.
D. 3.: D.W., 100 Z_{ol}, front face.
D. 4.: D.W., 100 Y_{en}, front face.
D. 5.: D.W., 100 X_{en}, front face.
D. 6.: D.W., 100 Z_{en}, front face.

The projections are lower hemisphere projections.
The numbers refer to the concentrations per 1 % area.
D.W. = Dreiser Weiher.
ol. = olivine, en. = enstatite.

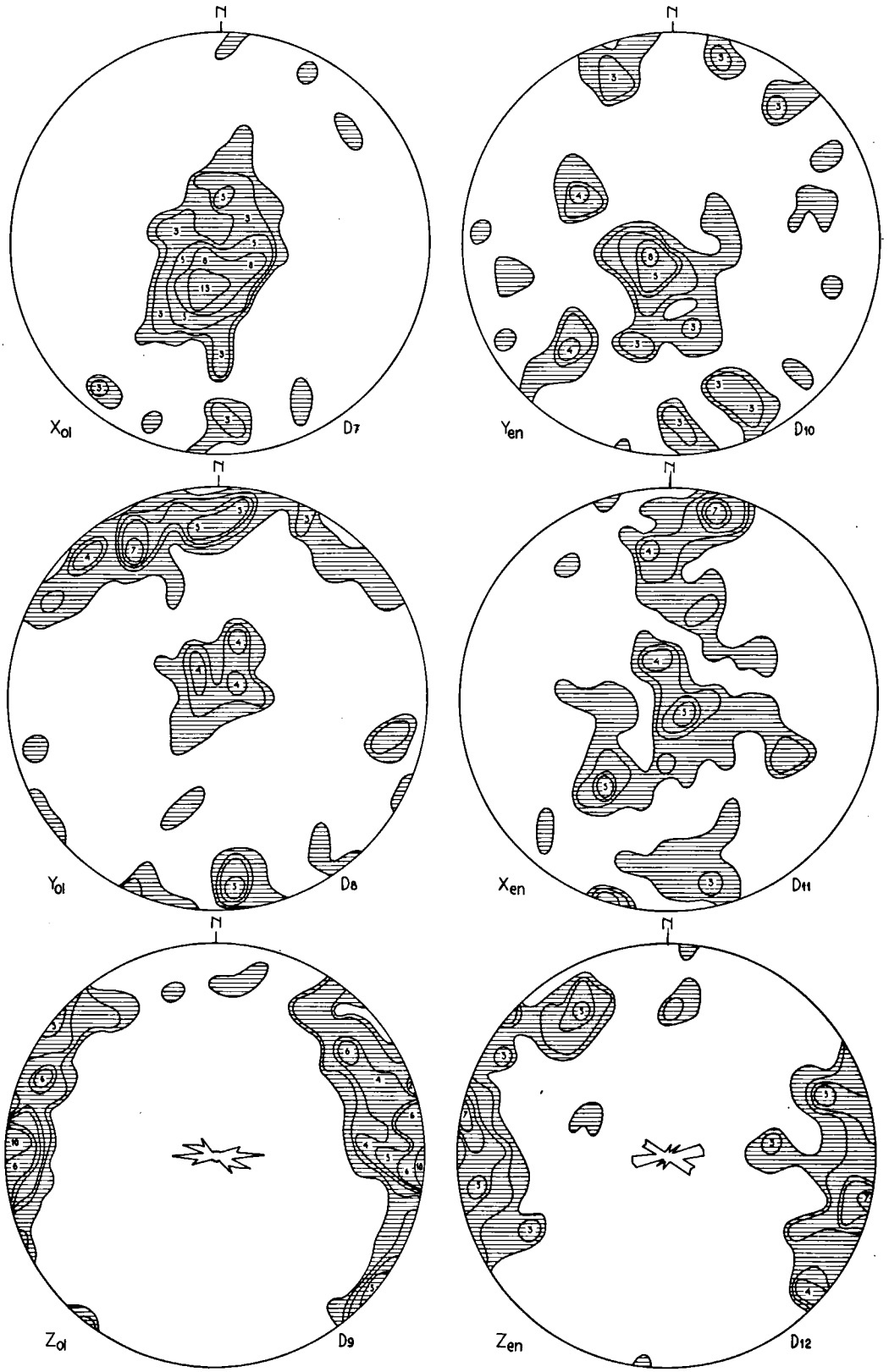

D. 7.: D.W., 100 X_{ol}, top face.
D. 8.: D.W., 100 Y_{ol}, top face.
D. 9.: D.W., 100 Z_{ol}, top face.

D. 10.: D.W., 100 Y_{en}, top face.
D. 11.: D.W., 100 X_{en}, top face.
D. 12.: D.W., 100 Z_{en}, top face.

and has an even greater concentration per unit area than in the front face. Z_{ol} is concentrated in an E.—W. direction along the margin of the diagram. The fact that the direction of Y_{ol} depends on that of both the other axes is clearly demonstrated by a central and marginal distribution of this axis.

As in the front face, the fabric of enstatite in the top section is dominated by an E.—W. direction of Z_{en} (D. 12). A central maximum of Y_{en} (D. 10) exists, but is less pronounced than the similar X_{ol} orientation (D. 7). X_{en} (D. 11) has hardly any preferred orientation within the broad girdle to which it is bound by the strong concentration of Z_{en} (D. 12).

The diagrams 13—18 represent the fabric of the side face of the sample. The main X_{ol} concentration (D. 13) has its anticipated position on the margin of the diagram, close to the E.—W. diameter. The Z_{ol} axes (D. 15) however reveal a rather strong departure from the expected central position. In fact Z_{ol} forms an almost complete two percent girdle, trending roughly N.—S. such as is found for the distribution of Y_{ol} (D. 14).

Such a departure from the anticipated orientation is not shown by Z_{en} (D. 18), the central maximum is strong and there is hardly any indication of spreading in a N.—S. girdle. Both the other enstatite axes, X_{en} (D. 17) and Y_{en} (D. 16) consequently are concentrated in more or less complete girdles along the margins of the diagrams. The preferred orientation of Y_{en} is probably weaker in the side face than in both the other faces of the sample.

The grain shape of olivine may be appreciated from the central rose figures in the diagrams. From the frontal diagrams (D. 1—D. 3) it becomes clear that the X_{ol} direction of all inequidimensional grains, which form by far the greater part, is the short diameter of the grains. The rose diagram of the top face (D. 9), normal to X_{ol} leaves no doubt that of the other two axes Z_{ol} is parallel to the longer diameter. The readings in the side face (D. 13) confirm this rule. From the foregoing it may be concluded that the olivine crystals are tabular parallel to { 010 } and elongate parallel to [100].

Enstatite, on the contrary, does not show such a striking grain shape. From the rose figures in the front face (D. 4, D. 6) it becomes clear that the diameter parallel to Z_{en} is longer than those in the Y_{en} and X_{en} directions. The top face (D. 12) confirms this rule. The rose figures in the diagrams of the side face (D. 16, D. 17) in which about fifty percent of the grains are equidimensional, approaches a circular form. This means an almost equidimensional section normal to Z_{en}. Consequently there seems to be no reason to suppose a tabular grain shape of enstatite. It may be concluded that enstatite is elongate parallel to [001] and equidimensional in { 001 }.

3. *Sampling errors*

To a first approximation, the anomaly observed in the Z_{ol} fabric of the side face may be due to the following causes: to isotropism or inhomogeneity of the fabric or to sampling errors. The former two causes may be excluded. If the fabric were really isotropic or inhomogeneous, the other two faces would probably not have yielded such strongly resembling diagrams.

Sampling errors are bound to influence fabric diagrams of rocks which are composed of inequidimensional crystals, due to the fact that the probability to encounter and thus measure the orientation of a crystal, increases if this

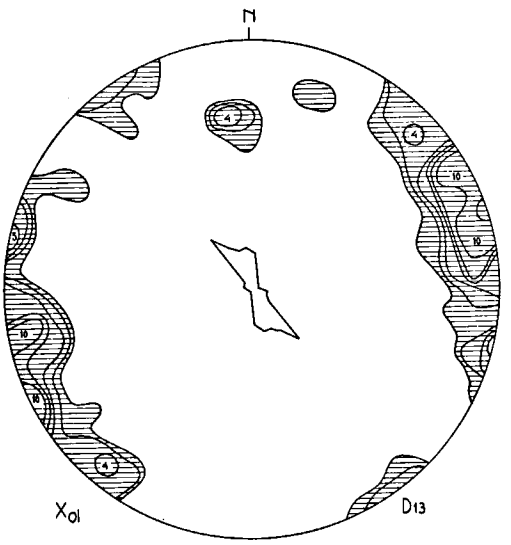

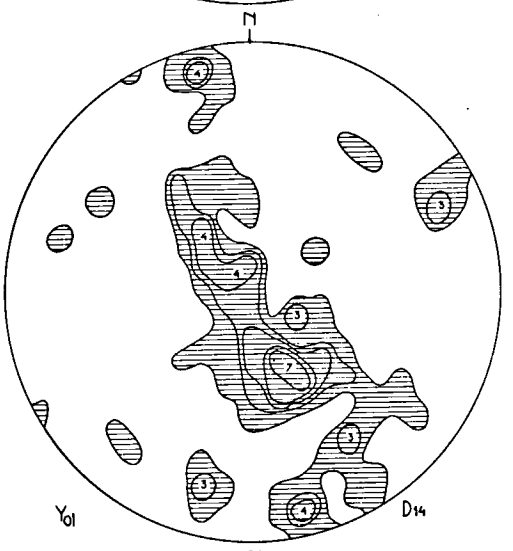

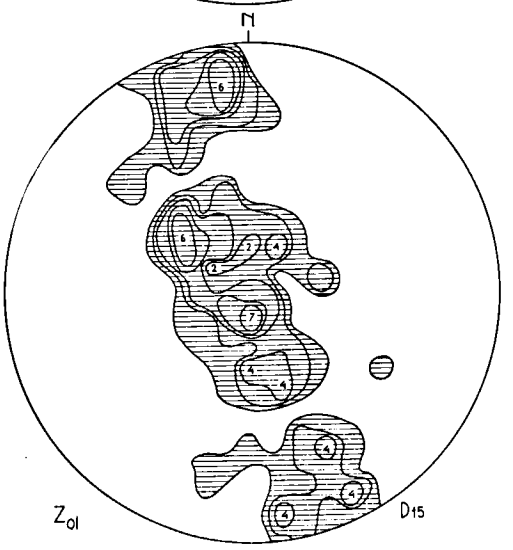

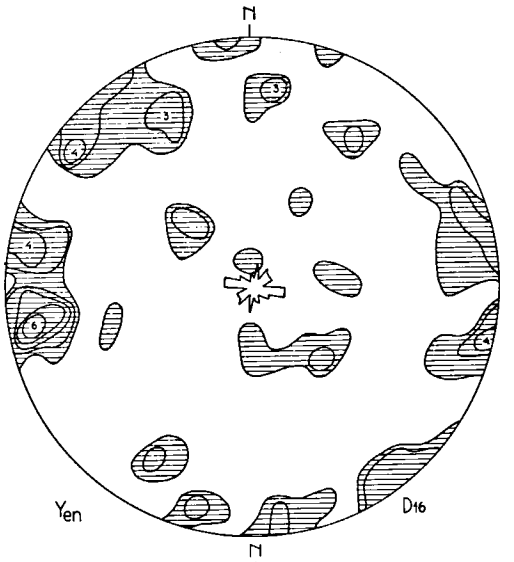

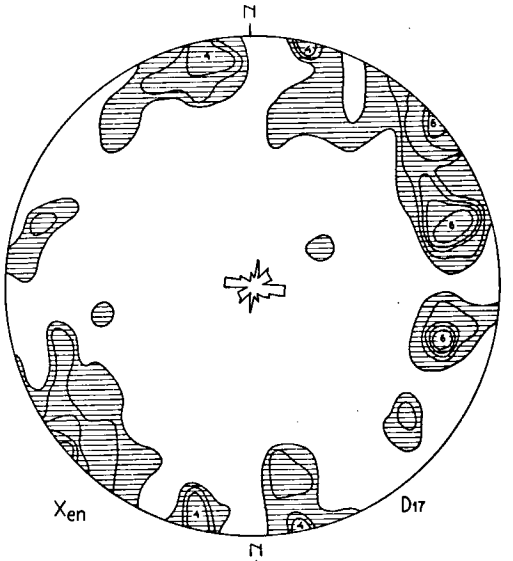

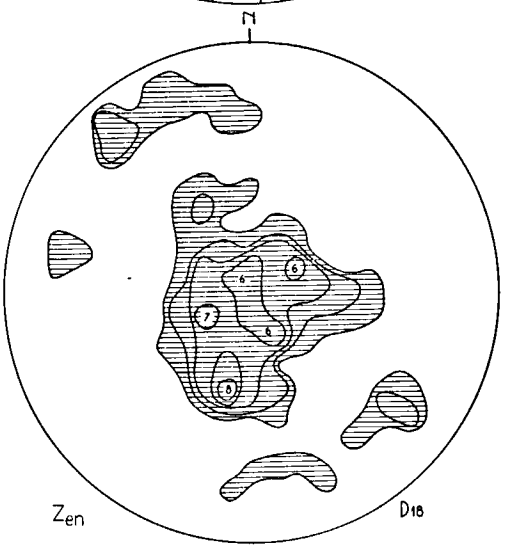

D. 13.: D.W., 100 X_{ol}, side face.
D. 14.: D.W., 100 Y_{ol}, side face.
D. 15.: D.W., 100 Z_{ol}, side face.

D. 16.: D.W., 100 Y_{en}, side face.
D. 17.: D.W., 100 X_{en}, side face.
D. 18.: D.W., 100 Z_{en}, side face.

orientation implies that the crystal in the thin section covers a bigger surface. In the same way, the chance of being measured decreases, if the orientation of the crystal implies that the section in the slide is smaller. The fact that the X_{ol} axes, and hence the short diameters of the grains have a single preferred orientation in the rock, almost restricts the error to the diagrams of one face of the rock. In the top face for instance, nearly all olivine crystals have { 010 } in the plane of the thin section. The surface area of the { 010 } section is independent of the orientation of Y_{ol} and Z_{ol} in this face. A fabric diagram of this face will therefore yield a true picture of the orientation of both these axes. In the diagrams of the side face however, X_{ol} occupies an E.—W. position. Consequently in the thin section { 001 } and { 100 } occur, of which { 001 } has the larger area. From the E.—W. orientation of Z_{ol} in the front face (D. 3), one may expect that crystals with { 100 } in the plane of the thin section of the side face will predominate. The larger surface of { 001 }, however, enhances the probability of measuring olivine crystals with Z_{ol} in the plane of the side face, since X_{ol} has a strong E.—W. orientation. This effect causes the unexpectedly strong concentration of Z_{ol} along the northern and southern margin of the side face (D. 15). In the foregoing description the term „Schnitteffekt" has been expressly avoided, because the definition of the „Schnitteffekt" as given by Sander, Kastler and Ladurner (1954) does not altogether apply to the here mentioned effect [3]).

The difference between both effects can be summarized as follows: in the case of a „Schnitteffekt" in the sense of Sander, the thin section does not represent a true picture of the rock fabric. Fabric diagrams constructed from such a thin section are consequently not representative for the rock fabric. In the case of a sampling error as described in this chapter, the thin section represents the true fabric, but the error is introduced during the sampling procedure.

The sampling error can be reduced by eliminating the influence of the grain size on the sampling, i. e. by avoiding the double measuring of grains and by selecting the grains to be measured along lines rather than by random sampling of a hundred grains. It will, however, be difficult to eliminate the error completely, not to mention the preference of every universal stage worker to measure the larger grains.

So far no attention has been paid in the literature to the influence of sampling errors on olivine fabric diagrams. However most of the published diagrams with strong X_{ol} preferred orientations are oriented in such a way that X_{ol} occupies a marginal position in the diagrams. In these diagrams, provided that the long diameter of the grains, which is not always parallel to Z_{ol}, is normal to the plane of observation, sampling errors may cause a wrong representation of both the Y_{ol} and Z_{ol} axes in the plane normal to X_{ol}. According to the present author, the often reported lack of preferred orientation of Y_{ol} and Z_{ol} in this plane may be due to this effect.

[3]) The definition of Sander et al. says: Der Schnitteffekt ist der Effekt, durch welchen ein wie üblich im Schliffe eingemessenes Diagramm von der wirklichen Lagenkugelbesetzung abweicht, dadurch, dass formanisotrope (Scheiben, Stäbe usw.) Gefügeelemente vom Schliff nicht mit gleicher Wahrscheinlichkeit, sondern mit der von dem Winkel ihrer eingemessenen Achse zur Dünnschliffebene abhängigen Wahrscheinlichkeit getroffen und der Messung zugänglich werden.

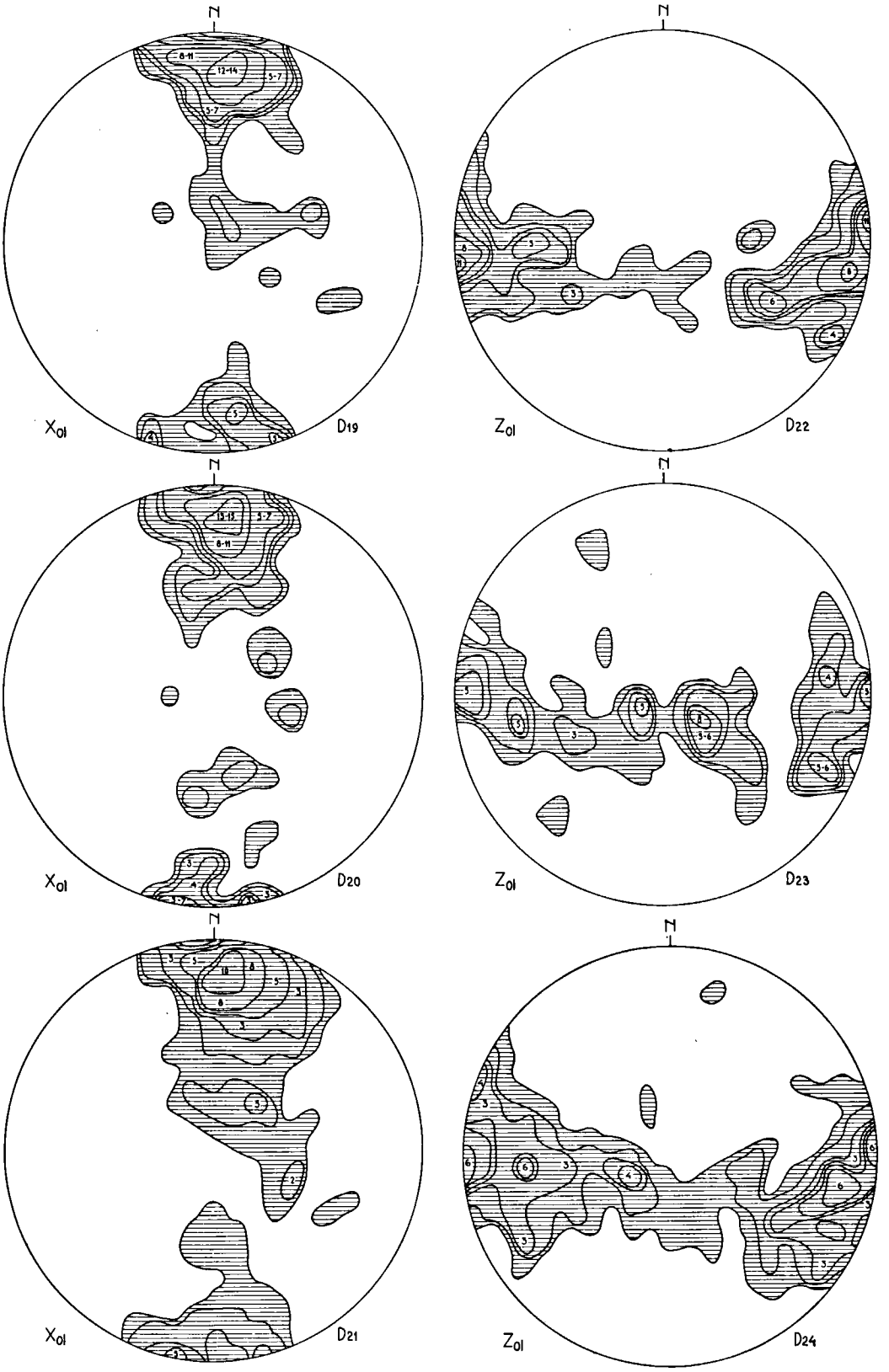

D. 19.: D.W., 100 X_{01}, top face rotated to front face.
D. 20.: D.W., 100 X_{01}, side face rotated to front face.
D. 21.: D.W., 300 X_{01}, collective diagram. Lowest contour: 1 %.
D. 22.: D.W., 100 Z_{01}, top face rotated to front face.
D. 23.: D.W., 100 Z_{01}, side face rotated to front face.
D. 24.: D.W., 200 Z_{01}, collective diagram front and top face.
Lowest contour: 1 %.

In the above analyzed case the difficulty can easily be avoided by relating the diagrams to the top face, i. e. to a section normal to X_{ol}. In the following description of the same rock type from another locality (Auvergne), however, it will become clear that such a solution is not always applicable, because of the fact that the fabric of peridotites is often inhomogeneous. In such a case only a threedimensional fabric analysis of the specimen will yield the required information.

4. *Rotated diagrams*

The diagrams 19 and 20 represent the X_{ol} diagrams of the top and side face respectively, rotated to the front face. Their mutual resemblance as well as their resemblance with the original X_{ol} diagram of the front face (D. 1) is striking. These diagrams clearly demonstrate the anisotropism and homogeneity of the fabric; they are also a valuable proof that hundred grains are sufficient to make reliable fabric diagrams of the X_{ol} axis. Diagram 21 is the collective diagram of X_{ol} of the three faces rotated to the front face. The somewhat broader spreading observed in this diagram, is due to the fact that the lowest density contour is a one percent line.

The same rotation is carried out for the Z_{ol} diagrams of both the top and side faces. The results are represented in the diagrams 22 and 23. The sampling error is well demonstrated in diagram 23. The central Z_{ol} concentration is much too strong. The collective diagram 24 is therefore constructed from two partial diagrams only, those of the front and top face. Although Z_{ol} forms a complete girdle along the E.—W. diameter, the main concentration has a marginal position in the diagrams.

The enstatite diagrams of the top and side face are also rotated to the front face. The diagrams 25 and 26 refer to the Y_{en} axes; they are the results of a rotation from the top and side face respectively. It is obvious that Y_{en} does not yield such a regular pattern as X_{ol}. The mutual differences between diagram 25 and 26 are rather strong. Diagram 25 shows a rather good resemblance with the original Y_{en} diagram of the front face (D. 4). A collective diagram of Y_{en} is constructed (D. 27) which shows a complete one percent girdle with a stronger concentration near the northern and southern margin in the same direction as the main X_{ol} concentration. Some 55° towards the centre of the diagram a second concentration occurs which also has its counterpart in the X_{ol} diagram (D. 21).

The diagrams 28 and 29 give the result of the rotation of Z_{en} from both the top and side face to the front face. Both show a strong concentration along the eastern and western margins of the diagrams. The more central concentration in diagram 29 may be due to a sampling error, which is certainly of less importance than in the case of olivine. This may be caused by the fact that enstatite is less elongate in the Z direction than olivine. On the other hand, the low percentage of enstatite in the rock makes it necessary to measure almost all the grains present in a given thin section. This excludes the influence of the grain size. Diagram 30 is the collective diagram of Z_{en} of the three faces of the specimen. The resemblance of this diagram with the Z_{ol} diagram (D. 24) is striking. However the concentration of Z_{en} along the periphery is stronger and the tendency to form a girdle weaker than for olivine.

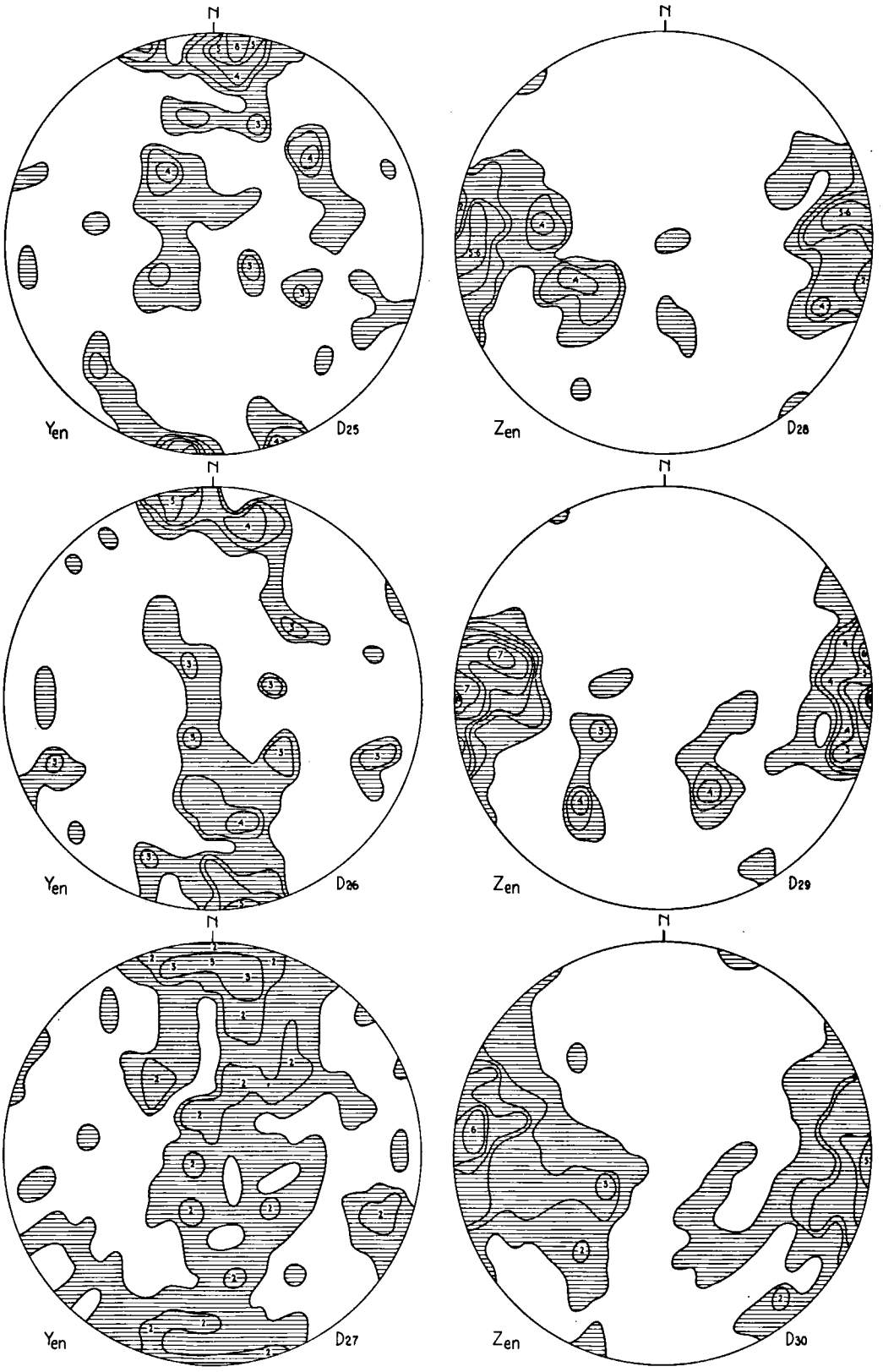

D. 25.: D.W. 100 Y_{en}, top face rotated to front face.
D. 26.: D.W. 100 Y_{en}, side face rotated to front face.
D. 27.: D.W. 300 Y_{en}, collective diagram. Lowest contour: 1 %.
D. 28.: D.W. 100 Z_{en}, top face rotated to front face.
D. 29.: D.W. 100 Z_{en}, side face rotated to front face.
D. 30.: D.W. 300 Z_{en}, collective diagram. Lowest contour: 1 %.

5. *Discussion*

The foregoing description clearly demonstrates the close relation between the fabrics of olivine and enstatite. Z_{en} has a rather fixed orientation in the plane (S) normal to the main X_{ol} concentration. This Z_{en} concentration coincides almost with Z_{ol}. The incomplete X_{ol} girdle is parallel with the broad complete X_{en} (D. 31) and Y_{en} (D. 27) girdle. The Y_{en} orientation however, approximates the X_{ol} orientation more closely than X_{en} does.

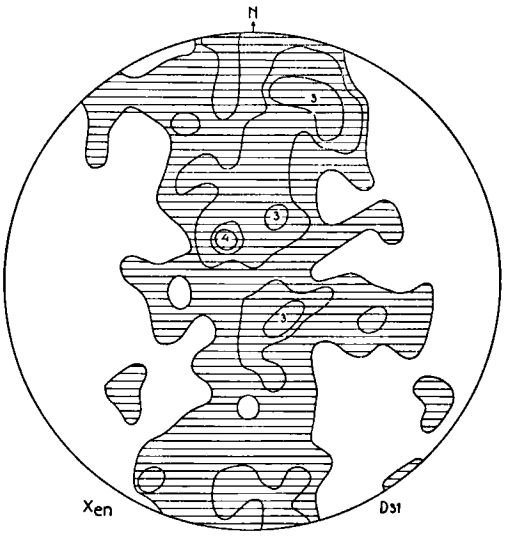

D. 31 Collective diagram. 300 X_{en} of three faces of sample D.W.1. projected on front face.

There is no doubt that the preferred orientation of the crystallographic axes of both olivine and enstatite, is linked with a dimensional orientation of these crystals. Olivine is tabular parallel to {010} and elongate parallel to [100]. This grain shape is expressed in the fabric: {010} of most of the olivine crystals is parallel to S, and [100] has a rather fixed orientation in this plane. The long diameter of enstatite, Z, is parallel to Z_{ol}. The fact that the section normal to Z_{en} is equidimensional, and consequently could not give rise to a dimensional orientation, is expressed in a girdle-shaped orientation of X_{en} and Y_{en}.

It seems obvious to conclude from these observations that the shape of the crystals actually was the cause of their preferred orientation. Most authors seem to prefer such an interpretation, but according to the present writer, cause and effect are confused in doing so. Some arguments against the view that the observed fabric has been controled by the shape of the crystals will now be developed.

The most obvious objection against a theory which explains the observed fabric as the result of a dimensional orientation is the fact that the preferred orientation is not restricted to crystals of the above mentioned shape. Olivine

crystals with another shape, mostly do not have the different orientation one would expect, if the orientation were governed by their habit only. In this respect the equidimensional crystals, which should have a random orientation, are of special interest. Furthermore it appears from the rose diagrams and from observations in the thin sections, that enstatite has a less pronounced long diameter than olivine. The orientation of the long diameter of enstatite however, is stronger than that of olivine. This observation is difficult to reconcile with the theory of a dimensional orientation. A third objection may be found in the fact that in the X_{ol} diagram (D. 21) a subsidiary concentration occurs at 55° from the main maximum. Both the X_{en} and Y_{en} collective diagrams (D. 27, D. 31) show comparable concentrations. In the case of olivine one might suppose that this concentration stands for an orientation of {021} in S, but enstatite does not have prominent crystal faces which make an angle of 55° with X_{en} or Y_{en}.

These considerations incited the author to look for another explanation of the observed fabric. The most appealing is the one which regards these rocks as S-tectonites. For olivine such an explanation is certainly acceptable. The plane in which translation gliding is to be expected {010} has a fixed orientation. The probable translation glide line [100] also shows strong orientation. According to Griggs, Heard and Turner (1960) the most probable translation glide plane in enstatite is {100}, while the translation glide line is [001]. Thus in the case of a fabric dominated by translation in S we might expect a parallel orientation of X_{ol} with Y_{en}, and Z_{ol} with Z_{en}. The latter of these conditions is much better fulfilled than the former. Consequently it is not yet possible to reach a definite conclusion regarding the validity of the interpretation of this rock type as an S-tectonite. It will however be clear that the subsidiary concentration of both X_{ol} and Y_{en} at 55° from the pole of S will be difficult to reconcile with such an interpretation. The occurrence of numerous translation lamellae in olivine does not prove that the rock is an S-tectonite. These translation lamellae have also been observed in rocks which suffered compression due to load (Brothers 1962).

There exists a close relation between crystal lattice and crystal habit. The longer diameter of a crystal mostly coincides with the direction of strongest bonding between the constituting ions. (Pyroxenes, amphiboles) (Hartman & Perdok, 1955). The direction of weakest bonding mostly coincides with the shorter axis of the crystals (Micas). Besides the structure s.s., the introduction of foreign elements in the lattice also affects the form. In this respect it is interesting to note that crystals from one locality mostly have a constant habit. The influence of the structure and chemical composition on the habit of crystals is well demonstrated in the group of sodium pyroxenes. The sodium ions occupy positions in between the silicon-oxygen chains. The introduction of these ions at the expense of calcium, weakens the bond between the chains, consequently the bond strength in these chains increases relatively. This fact is expressed by the habit of the crystals which are generally much more acicular than the calcium pyroxenes.

The above digression is intended to demonstrate that a relation between crystal structure and habit is likely to exist. This implies that if a crystal is free to grow, its shape as far as its short and long diameters are concerned, is more

or less predestined. This means that an orientation of crystals in which their lattice occupies a fixed orientation in relation to external forces, as for instance directed pressure, possibly determines a statistical dimensional orientation. On the other hand it means that if a preferred orientation is observed in which the lattice orientation is linked with a dimensional orientation, the latter is not necessarily to be interpreted as the cause of the former.

Numerous theories have been developed to predict the probable orientation of crystals growing in a given stress field. Several approaches of the problem are possible, of which a thermodynamical calculation is probably the most attractive. A summary of the results of these calculations will be given at the end of this paper, when other arguments have been advanced to demonstrate that the fabric of the nodulelike inclusions in lavas, is not governed by the crystal habit of olivine and enstatite.

CHAPTER III

A BANDED NODULE OF LHERZOLITIC COMPOSITION, FROM LE PUY, AUVERGNE, FRANCE

1. *Introduction*

The ultrabasic nodulelike inclusions in the basalts of the Chaîne des Puys in France have not the world-wide fame of those from the German localities. However the nodules are particularly abundant in the Villafranchian (Pleistocene) basalts of the "Plateau de Velay" near le Puy. The samples studied in this paper come from a quarry in this region [3]). There exists no recent detailed study dealing with the petrography of these rocks, thus we have to rely on the descriptions of Boule (1892) and Lacroix (1893) as far as the petrography is concerned. The ultrabasic inclusions do, however, not differ from those described from other localities, neither in shape nor in mineralogical composition and texture. The nodules range in size from a few centimetres up to several decimetres, they have the usual oval shape and often show a strongly banded structure. The mineralogical composition varies over a wide range just as that of the German samples. The composing crystals are usually rather coarse grained. Most samples are fresh and do not show the slightest alteration, but according to Boule amphibole sometimes occurs as an alteration product.

The composition of the three main minerals of sample A. 1. described in this chapter, has been determined by optical means as far as enstatite and diopside are concerned, and by means of X-ray powder diffraction in the case of olivine. For enstatite the following data have been obtained:

$N_x = 1.666$, $N_y = 1.669$, $N_z = 1.675$,
$2V_z = 84°—86°$ (five readings),

from which a composition in between $Mg_{89}Fe_{11}$ and $Mg_{92}Fe_8$ can be inferred.

The optical properties of the diopside are:

$N_x = 1.678$, $N_y = 1.683$, $N_z = 1.706$,
$Z/C = 40°—43°$ (five readings),
$2V_z = 57°—61°$ (five readings).

The estimated chemical composition is $Ca_{48}Mg_{44}Fe_8$ (Hess 1949).

Following the method of Yoder and Sahama for the determination of olivine a $d_{(130)}$ of 2.7705 Å is found which corresponds with a forsterite content of 93 percent, a value slightly above that inferred from the observed N_y of 1.672.

These data suggest that the chemical composition of the three main minerals of the nodular inclusions from le Puy does not differ from those generally found in ultrabasic inclusions in lavas.

[3]) The exact location of the quarry is: Hill no. 985, 1 km. NE. of Tarreyres near Solignac.

Chemically, the basalts of the "Plateau de Velay" belong to the alkali-olivine basalt suite. According to Brousse (1961) the chemical composition is the following:

TABLE I

SiO_2	42.50
Al_2O_3	14.35
Fe_2O_3	4.70
FeO	7.
MnO	0.25
MgO	9.50
CaO	10.50
Na_2O	3.25
K_2O	1.15
TiO_2	2.75
P_2O_5	1.25
H_2O+	2.
H_2O-	1.
	100.20

TABLE II

	Finkenberg		le Puy
	Total	Groundmass	
al	16.45	18.31	18
fm	59.12	53.71	50
c	15.49	17.27	24
alk	8.94	10.71	8
si	93.06	98.97	91
ti	4.39	3.73	4
k	0.13	0.16	0.2
mg	0.58	0.56	0.6

The corresponding Niggli values are listed in table II, together with the Niggli values of the Finkenberg basalt in Germany (Frechen 1948 a) in which also many ultrabasic inclusions occur. It is seen that the two basalts are much alike, although the French one is poorer in fm and richer in c. The in relation to the total basalt, lower fm and higher c content of the groundmass of the German basalt, suggests that the difference between the two basalts may be regarded as the extrapolated effect of the evolution of the Finkenberg magma.

2. *Description of the specimen*

The photograph of figure 2 represents the face, which will be referred to as the front face of the banded specimen (A. 1), the petrofabrics of which have been investigated in detail. The dark E.—W. bands on the photograph are picotite-rich layers, which alternate with much lighter picotite-poor bands. In thin sections it is seen that the dark bands are not only marked by a higher picotite content, both the clino- and orthopyroxene percentages in these layers are also higher than in the other parts of the rock. Consequently the banding can also be described as a rapid vertical change in the olivine content of the rock.

It is important to stress the fact that this lamination is not a feature visible in the front face only. The bands are really laminae i.e. planar not linear fabric components which intersect all faces of the sample, except the surface parallel to them. This is clearly seen in figure 3, a photograph of the top face of the sample. The intersection of the north direction of this face with the lamination is about fifteen degrees, consequently the lamination appears in the top face as a rather broad E.—W. lineation.

At first sight the lamination is the only macroscopically observable feature in the rock. A close observation of the photograph of the front face (fig. 2) however, reveals another important structural property [4]). Two sets of intersecting

[4]) The feature referred to is best seen if the photograph is observed under as acute an angle as possible.

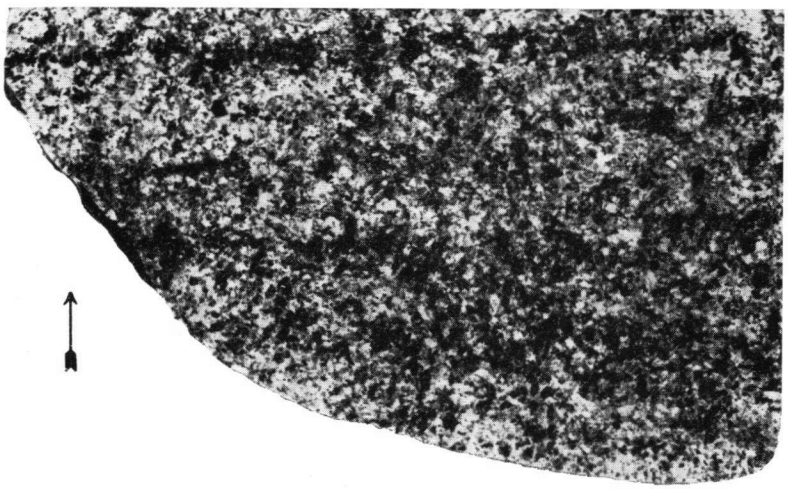

Figure 2.
Photograph of the front face of sample A. 1., a banded nodular inclusion in a lava of Auvergne. The dark horizontal bands are picotite-rich layers which are intersected by two sets of diagonal lineations. (× ¾).

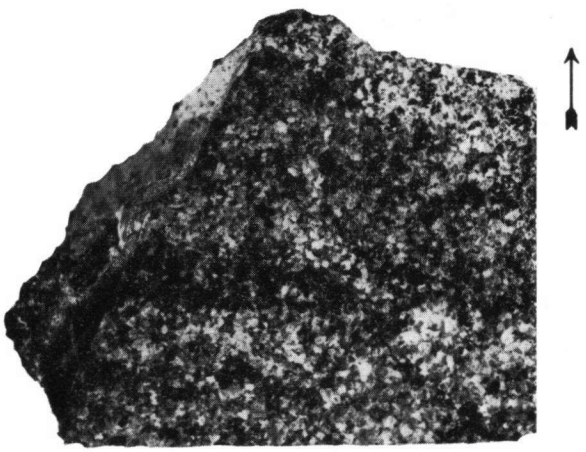

Figure 3.
Photograph of the top face of sample A. 1. The broad E.—W. trending bands are the intersection lines of the lamination and the top face. Several sets of intersecting lineations can be observed on the photograph. (Natural size.)

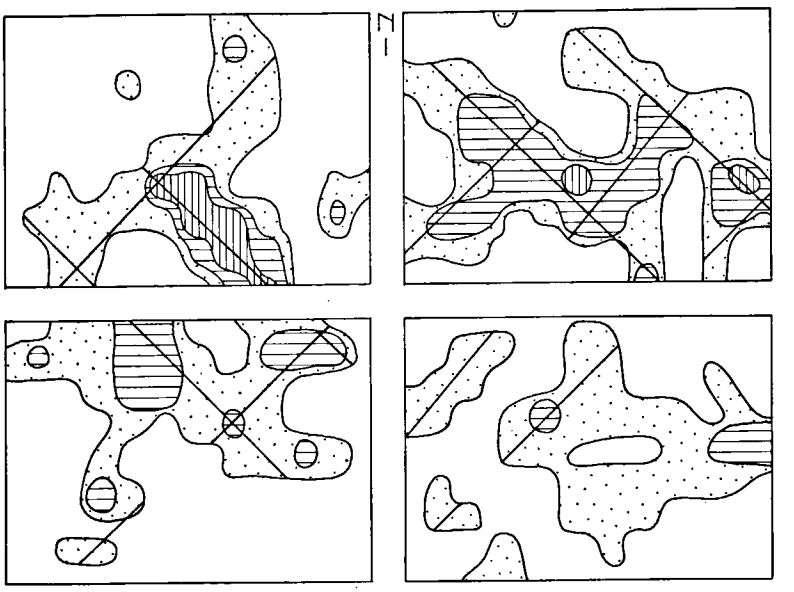

Figure 4.
Crystal distribution analysis of 423 enstatite crystals in the front face of sample A. 1. Contours 5—6, 7—9, 10—12 crystals per 1 % area. (× 2,5)

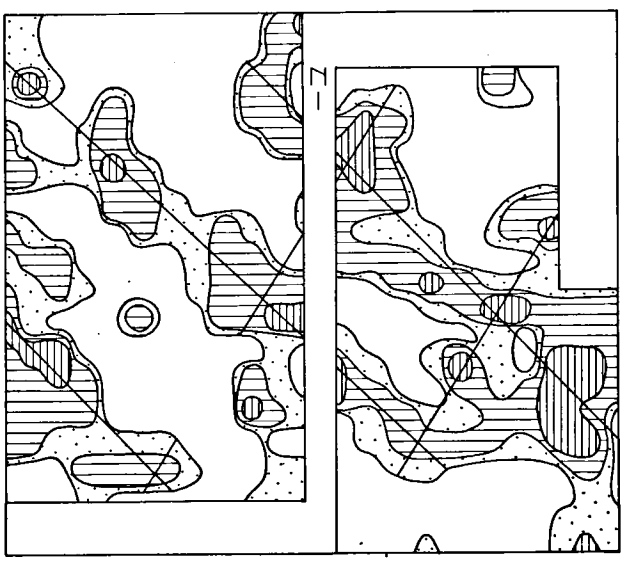

Figure 5.
C.D.A. of 531 enstatite crystals in the top face of sample A. 1.
Contours 6, 7—8, 9—10 crystals per 1 % area. (× 2)

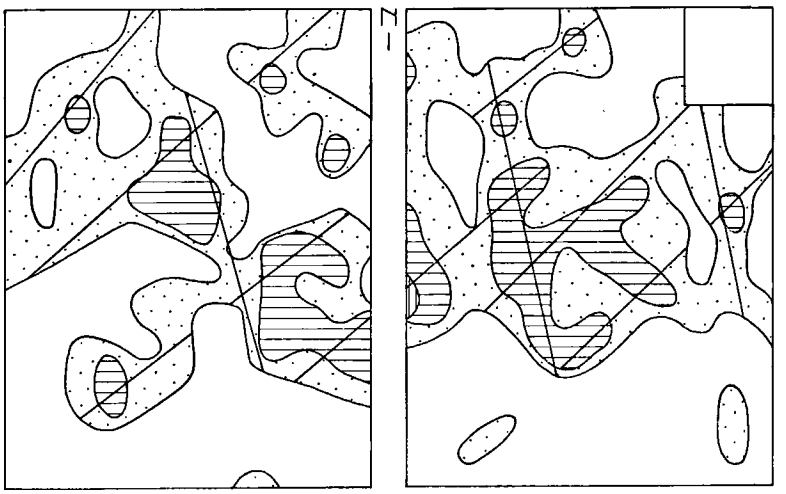

Figure 6.
C.D.A. of 411 enstatite crystals in the side face of sample A. 1.
Contours 5—6, 7—9, 10 crystals per 1 % area. (× 2)

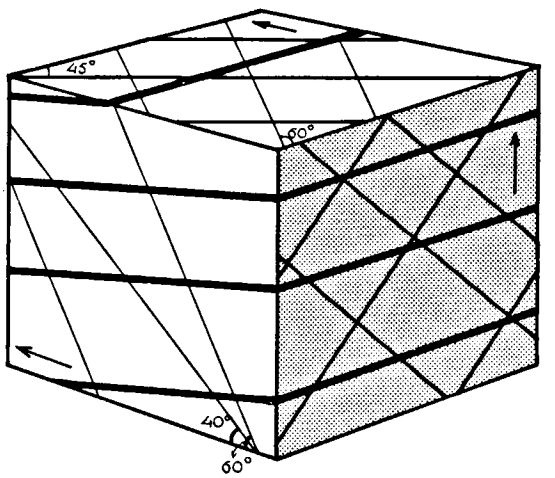

Figure 7.
Sample cube of specimen A. 1.
The sub-horizontal planes represent the lamination.
On each face of the cube the lineations which have been observed in the crystal distribution diagrams, are represented.

diagonal lines, along which offset of the banding occurs, are visible in the front face. The intersecting directions are definitely younger than the lamination, which is disturbed by them.

The top face also reveals intersecting lineations (fig. 3). The exact direction of these lineations can however not be estimated in the photograph. No photograph of the side face is given because, apart from the intersection lines of the lamination, no macroscopic linear features can be observed in the photograph of this plane.

Before starting to measure the orientation of the olivine and enstatite crystals in the sample, it is important to know whether the macroscopically observable directions in the photographs also occur on a microscopic scale in the thin sections. This is done by making Crystal Distribution Analyses (C. D. A.) in each of the three faces. Such a C. D. A. is made by plotting the centre of each crystal of one species on a photograph of the thin sections. Density contours are afterwards constructed on the basis of these points. The resulting density diagrams visualize the distribution of the crystals of one mineral species in the observed plane. In the photographs of the front and top face it can be seen that the lineations are characterized by a high concentration of crystals of one species. In order to visualize these lineations the distribution of the crystals of one mineral species in a rather big surface (about 6 cm^2) has to be represented. The construction of a C. D. A. of olivine would need the plotting and contouring of thousands of crystals. The enstatite content of the rock however, is such that in each face a reliable C. D. A. can be constructed, based on about 400 crystals.

Figure 4 refers to the C. D. A. of enstatite in the front face. The diagonal pattern which was observed in the photograph is even more clear in the C. D. A. of the front face. The already mentioned higher enstatite content of the banding is supported by the E.—W. direction in the enstatite distribution diagram.

The same procedure is followed in the top face. The result is represented in figure 5. The C. D. A. reveals a strong N. 45° W. direction. Other lineations are certainly less distinct, but an E.—W. direction, attributable to the lamination is probably also present. A lineation trending about N. 30° E. might be present. As the directions visible on the photograph are rather weak, apart from the lamination, it becomes difficult to co-ordinate the photograph and the C. D. A. of the top face.

Figure 6 refers to the enstatite distribution in the side face. Although the observed lineations are much less pronounced, two main linear trends of density maxima can be recognized of which the N. 15° W. direction is probably the intersection of the lamination with the side face. The direction of the second lineation must be in between N. 40° E. and N. 60° E.

As yet it is impossible to decide which of the lineations observed in the different faces of the rock are intersections of planar fabric components. In the block diagram of figure 7 all the observed lineations are represented without a further interpretation of their relation, with the exception of the lamination.

3. *The fabric diagrams of three perpendicular faces of the specimen*

The orientation of hundred olivine grains of the front face is represented in the diagrams 32, 33 and 34, which refer respectively to the X_{ol}, Y_{ol} and Z_{ol} axes (see plate I). The most striking feature of the orientation of the X_{ol}

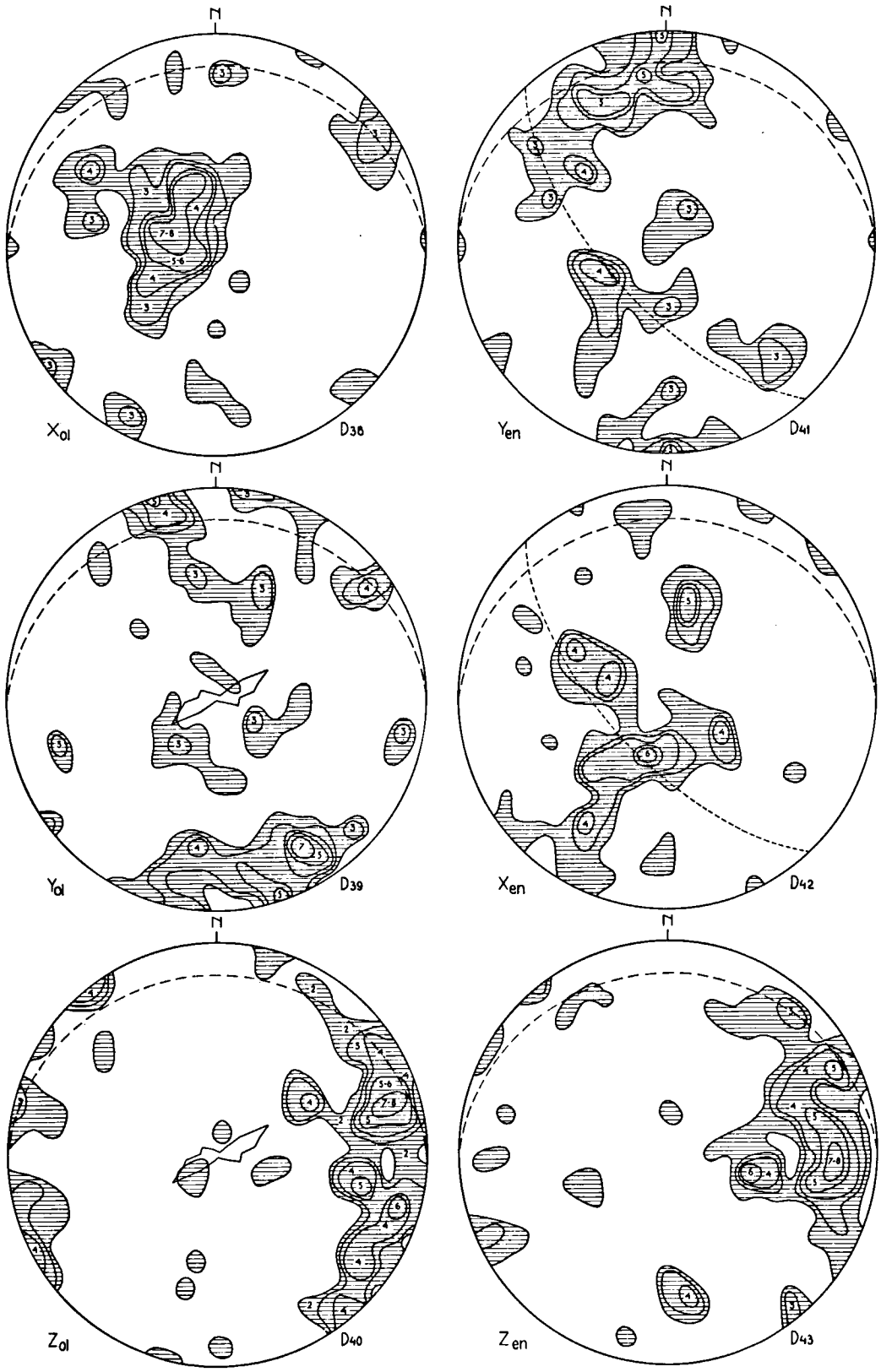

D. 38.: A. 1., 100 X_{ol}, top face.
D. 39.: A. 1., 100 Y_{ol}, top face.
D. 40.: A. 1., 100 Z_{ol}, top face.
D. 41.: A. 1., 100 Y_{en}, top face.
D. 42.: A. 1., 100 X_{en}, top face.
D. 43.: A. 1., 100 Z_{en}, top face.

axes is without doubt the fact that these axes are not oriented perpendicular to the banding, which is represented by an interrupted great circle, but are concentrated along two intersecting incomplete girdles, indicated by two solid great circles. The orientation of the Y_{ol} axes (D. 33) does not show a very regular pattern. Z_{ol} (D. 34) however shows a strong concentration in the NW. and SE. quadrants mainly along the great circle, which will be referred to as S_1, perpendicular to the intersection point of the two X_{ol} incomplete girdles. A tendency of spreading of the Z_{ol} axes towards the banding can also be observed.

The enstatite diagrams of the front face are D. 35 (Y_{en}), D. 36 (X_{en}), D. 37 (Z_{en}) (see plate I). The Y_{en} axes are concentrated in an almost complete girdle which is parallel to one of the incomplete X_{ol} girdles. The almost random orientation of X_{en} reminds one of the orientation of Y_{ol}. The orientation of the Z_{en} axes, which are represented in diagram 37, shows a close relationship with the Z_{ol} axes. The concentration of the Z_{en} axes, however, is stronger and the girdle-forming tendency weaker than for Z_{ol}. The Z_{en} axes show a clear spreading towards the banding. However neither the olivine nor the enstatite fabric shows any obvious relation with the banding such as could be expected. In anticipation of the interpretation of the microfabric, it may be said that the symmetry of the diagrams of both olivine and enstatite in the front face shows a close relation with the observed diagonal lineation pattern in the C. D. A. of the front face.

Fabric diagrams of both other faces of the sample have also been constructed. The diagrams 38, 39, 40 represent the X_{ol}, Y_{ol}, Z_{ol} orientations in the top face. The lamination is represented by an interrupted great circle in the diagrams. Although the comparison of diagrams of two different faces of one specimen needs a trained eye, it is obvious that the X_{ol} axes in diagram 38 do not show the same pattern of two intersecting incomplete girdles, as was observed in the front face (D. 32). However the main concentration of X_{ol} in diagram 38 is still not in the expected position, perpendicular to the banding. The Z_{ol} axes form an incomplete girdle, with its main concentration almost E.—W. near the intersection of the top face and the lamination (D. 40).

The orientation of enstatite in the top face is represented in the diagrams 41, 42, 43. The main concentration of Y_{en} is found nearly within the lamination, and only a subsidiary concentration of Y_{en} occurs approximately normal to it. There is little correspondence between the orientation of X_{ol} and Y_{en}. The concentration of the Z_{en} axes is strong, and shows some affinity with that of Z_{ol} although the tendency of Z_{en} to form a girdle is considerably weaker.

No obvious relationship exists between the observed lineations in the C. D. A. of the top face and the fabric diagrams of this face. A relation between the orientation of both Z_{ol} and Z_{en} and the lamination seems to be present, but the strong N. 45° W. lineation observed in the C. D. A. is certainly not clearly represented in the olivine diagrams. In the enstatite diagrams, however, one might infer the presence of an incomplete girdle formed by Y_{en} and X_{en} together, approaching this direction. A dotted line marks the orientation of the supposed girdle in the X_{en} and Y_{en} diagrams (D. 41, D. 42).

The olivine diagrams of the side face (D. 44, D. 45, D. 46) strongly resemble those of the top face. Diagram 44 is characterized by an X_{ol} concentration which does not consist of two intersecting girdles, but the main maximum of

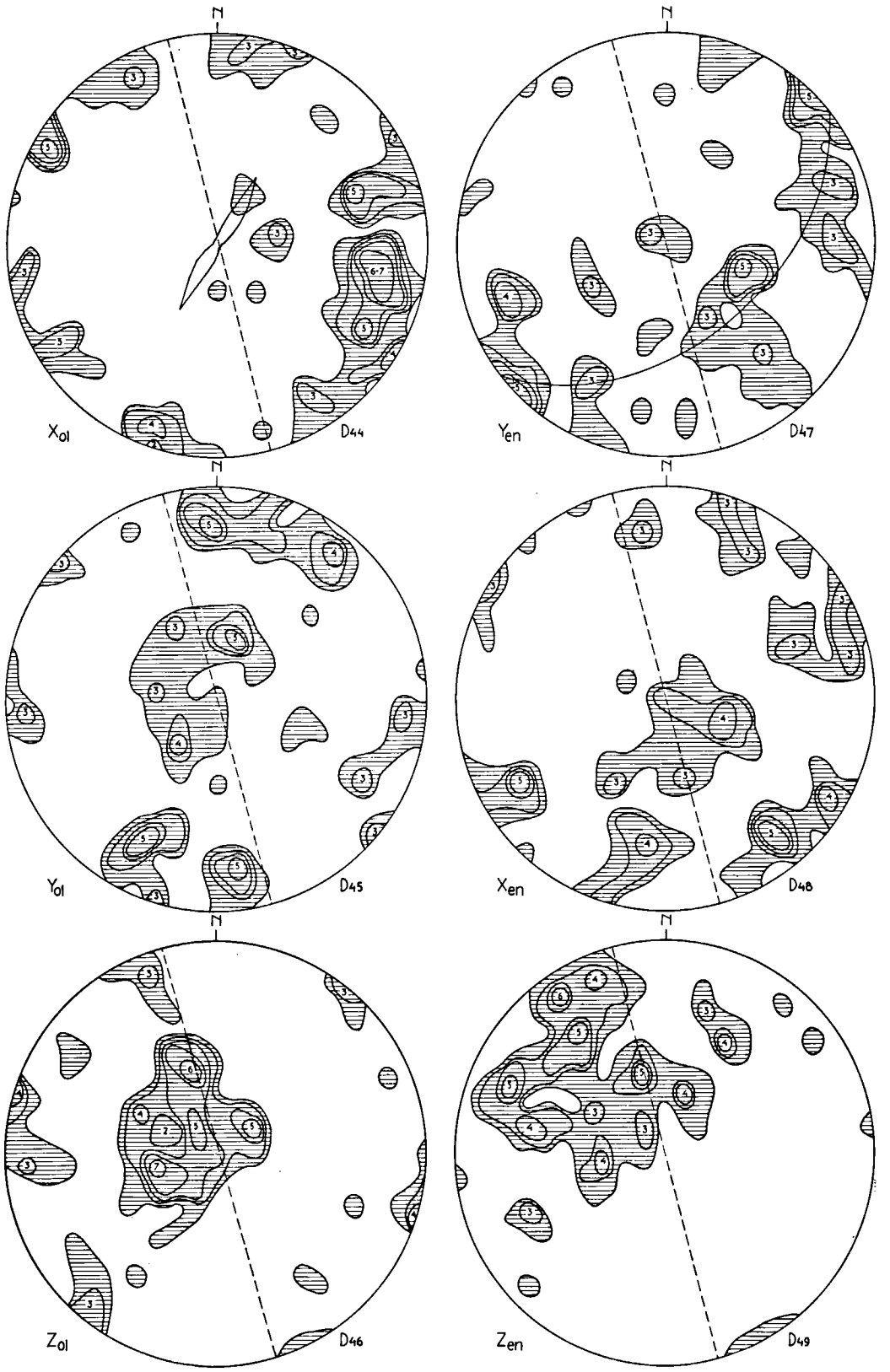

D. 44.: A. 1., 100 X_{ol}, side face.
D. 45.: A. 1., 100 Y_{ol}, side face.
D. 46.: A. 1., 100 Z_{ol}, side face.
D. 47.: A. 1., 100 Y_{en}, side face.
D. 48.: A. 1., 100 X_{en}, side face.
D. 49.: A. 1., 100 Z_{en}, side face.

which also clearly deviates from the position perpendicular to the lamination. The latter is represented by an interrupted line. Most of the Z_{ol} axes (D. 46) have a parallel orientation close to the lamination.

The enstatite fabric of the side face (D. 47, D. 48, D. 49) however, does not correspond with the olivine fabric. The Y_{en} axes show a tendency to form a girdle, which is represented in diagram 47 by a solid great circle. This girdle, which henceforth will be referred to as S_2, is also weakly present in the X_{en} diagram (D. 48). It represents a plane with the same orientation as the inferred X_{en}-Y_{en} girdle in the enstatite diagrams of the top face. (D. 41, D. 42). The Z_{en} axes cluster around the pole of S_2 and also show a spreading towards the lamination.

Apart from the lamination, there is no obvious relation between the C. D. A. of the side face and the observed orientation of the olivine crystals. The inferred N. 40°-60° E. lineation in the C. D. A. of the side face is probably the intersection of S_2 with this face. The strike of S_2 in the side face, as estimated from the Y_{en} diagram is N. 40° E. The difference between both values is explicable in view of the inaccuracy of the C. D. A. method.

It is now convenient to rotate all the diagrams of both the top and side face to the front face, in order to make a further comparison possible. The diagrams 50, 51, 52 and 53, 54, 55 (see plate I) are the X_{ol}, Y_{ol} and Z_{ol} diagrams of the top and side face respectively, rotated to the front face. A comparison of the diagrams of both faces reveals that they are very similar proving that the fabric is significantly anisotropic. The main X_{ol} concentration deviates clearly from a position normal to the banding. The bulk of the Z_{ol} axes are still found near to the banding, although a tendency to a more SE. position occurs particularly in the rotated diagram of the top face (D. 52). A comparison with the original diagrams of the front face (D. 32, D. 33, D. 34) leaves no doubt that the fabric is inhomogeneous. The two intersecting incomplete X_{ol} girdles of the front face do not occur in the other faces, while the tendency to a more SE. position observed in the Z_{ol} diagrams of the top and side face, is actually a fact in the Z_{ol} diagram of the front face.

The enstatite diagrams of the top and side face are also rotated to the front face. The rotation results in the diagrams 56, 57, 58 for the top face, and 59, 60, 61 for the side face (see plate I). It is now clearly seen that the enstatite diagrams of both these faces diverge strongly. The main trend of Y_{en} in diagram 56 corresponds roughly with the trend of the Y_{en} axes in the diagram of the front face (D. 35). The Z_{en} axes in diagram 58 are concentrated near the banding, but a spreading towards the SE. becomes noticeable. The main trend of the Y_{en} axes (D. 59) in the enstatite diagrams rotated from the side face to the front face, shows a weak girdle, S_2 which almost goes through the intersection point of the two X_{ol} girdles of the front face (D. 32). The SE. position of the Z_{en} axes in diagram 61 corresponds with that of the Z_{en} axes measured in the front face (D. 37), but the shape of the concentration is different.

This brief description leaves no doubt that the fabric of both olivine and enstatite is inhomogeneous. Depending on the face of the sample studied, the observed fabric may be quite different. In order to prove that the observed trend in the Y_{en} diagram of the side face (D. 47) really coincides with the weak X_{en}-Y_{en} trend in the enstatite diagrams of the top face (D. 41, D. 42),

and consequently with the observed N. 45° W. lineation in the C. D. A. of the top face, the enstatite diagrams of the side face have been rotated to the top face. The resulting diagrams are D. 62, D. 63, D. 64 (see plate I). The observed trend of Y_{en} in diagram 62 (S_2) proves to be the same as the one in diagram 41 and 42. The Z_{en} axes in diagram 64 show a particular distribution, which might be interpreted as two intersecting incomplete girdles. This phenomenon will be dealt with in the next paragraph.

4. *Interpretation*

An interpretation of the observed facts has to account for the inhomogeneity of the fabric and for the differences between the olivine and enstatite diagrams. Furthermore the linear and planar features observed in the C. D. A. have to be incorporated in any realistic interpretation.

From the literature it is known that the olivine fabric of banded peridotites is mostly characterized by a strong concentration of X_{ol} perpendicular to the banding. The Z_{ol} or Y_{ol} axes or both usually have a more or less fixed orientation in the plane of the banding. This characteristic fabric, which has been described in chapter II, is not observed in the banded lherzolite studied in this chapter.

The inhomogeneity of the fabric, taken in conjunction with the intersecting directions observable in the C. D. A., constitutes conclusive evidence for the rock to be a secondary tectonite. This implies that the rock was subject to deformation in the predominantly solid state. In such a deformed rock the observed fabric can be the result of a rotation of a pre-existing fabric. Relics of the initial pre-deformational fabric are then still likely to exist. In this paragraph it will be demonstrated that the observed fabric can be explained as the result of the rotation of a pre-deformational fabric of the type observed in the sample from Dreiser Weiher.

The fabric of olivine in the front face is the most characteristic, and its relation with the macroscopically and microscopically observable intersecting directions in the front face of the sample is obvious. Any interpretation should therefore commence with the olivine fabric observed in this face. The most conspicuous features of the olivine orientation in this face are the intersecting incomplete X_{ol} girdles, which are accompanied by a single incomplete Z_{ol} girdle (S_1) the axis of which coincides with the intersections of the two X_{ol} girdles. (D. 32, D. 34). If we accept the view of Chudoba and Frechen (1950) that {010} is the most probable translation glide plane in olivine, then it becomes probable that the orientation of olivine in relation to slip planes or directions in the rock is determined by the orientation of the X_{ol} axis to wards these planes or directions. This implies that the axis of rotation of the olivine crystals is the pole to the common plane of the old and the new orientation of the X_{ol} axes. In this concept the potential slip planes in the rock, are predestined by the new stress field. The old fabric is often not suitably disposed for translation or twinning to occur on these slip planes. Consequently, the crystals are rotated into a more favourable orientation. For olivine this new orientation is likely to be one in which the X_{ol} axis is perpendicular to a potential slip plane.

In order to locate the possible rotation axis (see figure 8), a plane is constructed through the observed main X_{ol} concentration and the probable pre-deformational X_{ol} concentration perpendicular to the banding. The pole of this plane, i.e. the rotation axis, is found in the intersection of the banding and

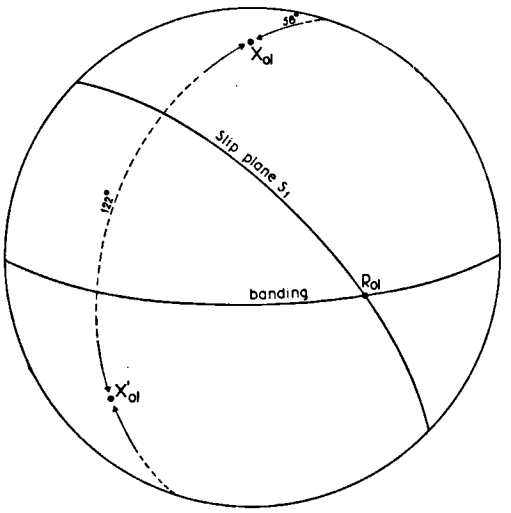

Figure 8. Construction of the rotation axis and rotation angles of olivine in the front face of sample A. 1.

X_{ol}: probable pre-deformational X_{ol} orientation in the pole of the banding.

X'_{ol}: observed post-deformational X_{ol} orientation in the intersection of two incomplete X_{ol} girdles. (D. 32).

R_{ol}: rotation axis of olivine in the pole of the great circle through X_{ol} and X'_{ol}. R_{ol} is the intersection of the banding and the potential slip plane S_1 normal to X'_{ol}.

The rotation angles are 58° in the dextral and 122° in the sinistral sense.

the Z_{ol} trend: S_1. The angle of rotation, which is he angular distance between the old and new X_{ol} concentrations is 58° or 122°, depending on the sense of the direction in which the angle is measured.

From the Dreiser Weiher sample we know that apart from the main concentration of the X_{ol} axes, in the pole of the great circle occupied by the Z_{ol} axes, a tendency of X_{ol} to form a girdle could be observed (D. 21). The axis of this girdle coincides with the main Z_{ol} and Z_{en} concentrations (D. 24, D. 30). We can now assume that the pre-deformational fabric of the sample studied in this chapter was of the same type. This implies that the pre-deformational X_{ol} orientation was not restricted to the pole of the lamination but extended in an incomplete girdle, normal to this plane. The axis of this girdle was the main pre-deformational Z_{ol} and Z_{en} orientation in the banding. Z_{ol} and Z_{en} axes in the banding, i.e. relics of the pre-deformational fabric, are mainly restricted to the fabric diagrams of the top and side face of the specimen. (D. 52, D. 55, D. 58, D. 61.) This is logical as far as the top face is concerned, because this face is sub-parallel to the banding plane. Relics of a fabric related with the banding, will have the best chance to be preserved in a section parallel to this plane. The fact that the fabric of the side face also shows relics of the pre-deformational fabric is less understandable, but it is well in accordance with the observation that in the C. D. A. of this face (fig. 6) the lineations resulting from the deformation are less distinct than in the other faces. The pre-deformational Z_{ol} and Z_{en} orientation in the banding can be estimated from the Z_{ol} diagrams D. 34, D. 52, D. 55, and the Z_{en} diagrams D. 37, D. 58, D. 61. It is clear that the exact orientation of this concentration is difficult to evaluate, but a point in the banding at 10° from the eastern margin seems to agree with the available data.

We have now all the elements needed for the reconstruction of the pre-deformational fabric. (See figure 9). The main concentration of Z_{ol} which coincides with Z_{en} is the pole of the incomplete X_{ol} girdle and the complete Y_{en} girdle. The main X_{ol} concentration on the other hand is the pole of the Z_{ol} and the less well developed Z_{en} girdle, which coincide with the banding.

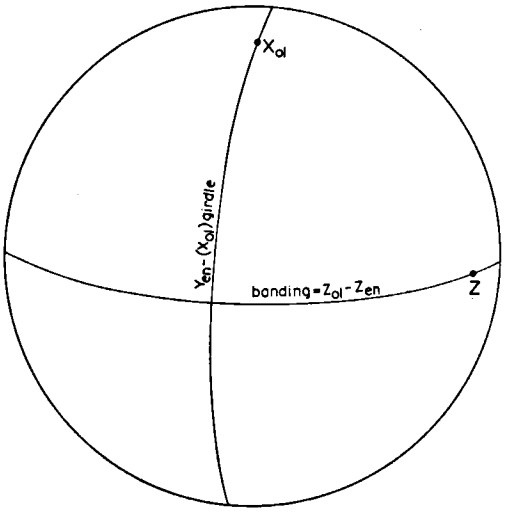

Figure 9. Reconstruction of the pre-deformational olivine and enstatite fabric, in the front face of sample A. 1.

X_{ol}: the main pre-deformational X_{ol} concentration in the pole of the banding.

Z: main pre-deformational coinciding Z_{ol} and Z_{en} concentrations.

Banding: plane marked by a complete girdle of pre-deformational Z_{ol} axes, and an incomplete girdle of Z_{en} axes.

Z is the pole of a complete pre-deformational Y_{en} girdle, which is parallel to an incomplete X_{ol} girdle.

It has been argued above that the X_{ol} axes could have been rotated over 58° or 122° around the rotation axis. This rotation can now be carried out. Figure 10 shows that the rotation of the incomplete pre-deformational X_{ol} girdle over angles of 58° and 122° respectively in opposite sense, yields two intersecting incomplete girdles, which almost coincide with the actually observed X_{ol} incomplete girdles in the front face [5]). (D. 32). The same result can be obtained by rotating the crystals in one sense but over angles of respectively 58° and 238°. The fabric diagrams do not reveal which of the two rotation patterns is preferable. However a rotation in one sense over the mentioned angles implies that part of the crystals

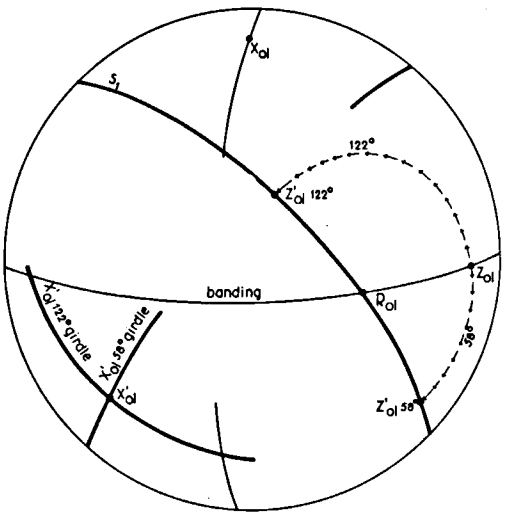

Figure 10. Transposition of olivine in the front face of sample A. 1.

The pre-deformational incomplete X_{ol} girdle is rotated around the rotation axis R_{ol} over 58° in the dextral and 122° in the sinistral sense. Instead of the X_{ol} girdle its pole: Z_{ol} is rotated. The resulting Z'_{ol} 58° and Z'_{ol} 122° concentrations are the poles of two intersecting X_{ol} girdles.

[5]) The easiest manner of rotating a plane, consists in rotating its pole. This method is followed in the text figures.

rotated through their apparent equilibrium position. It does not seem very likely that such a rotation took place. Therefore the interpretation which accounts for the deformation in terms of a rotation in opposite sense, over supplementary angles is preferred here and in the following chapters of this paper.

If however, the X_{ol} axes have been rotated in opposite sense around a rotation axis the same rotation must have affected the Z_{ol} axes. The pre-deformational position of Z_{ol} was restricted to the banding plane. In order to locate the new orientation of Z_{ol}, the banding plane has to be turned around the rotation axis. The fact that the rotation axis is parallel to the banding and that the opposite rotations are supplementary causes only one new orientation for the banding. This is clearly seen in figure 10. The rotation of the pole of the banding: X_{ol}, yields per definition only one new point: X'_{ol} which is the pole of S_1. The fact that the orientation of the pre-deformational Z_{ol} axes was almost restricted to a narrow zone in the banding, makes that the Z_{ol} axes, after rotation, will be concentrated in two maxima in S_1: $Z'_{ol}(58°)$ and $Z'_{ol}(122°)$, of which the former will be the stronger. See diagram 34. In that diagram there are only faint indications for the existence of the $Z'_{ol}(122°)$ concentration. This is probably due to a sampling error in the sense as has been described in chapter II. (The olivine crystals are elongate parallel to Z.) In the fabric diagram of the Z_{ol} axes made in a section parallel to S_1 (D. 73) the $Z'_{ol}(122°)$ concentration is anyway clearly represented.

If it is true that the olivine crystals have been rotated around an axis, over a specific angle, it is likely that the same should have happened to the enstatite crystals. However from the diagrams of the sample from Dreiser Weiher we know that the initial orientation of the Y_{en} axes may have been different from that of the X_{ol} axes. The former constitute a complete, rather broad girdle perpendicular to the banding plane. (D. 27). If this Y_{en} girdle is rotated in a similar manner, around the rotation axis that was deduced for olivine, it should normally yield two intersecting complete girdles, of which only one is observed: the girdle which results from a dextral [6]) rotation over 58°. Although the close correspondance of the observed Y_{en} girdle with the expected orientation is strong circumstantial evidence for the validity of the transposition theory, the absence of the other girdle corresponding to a sinistral rotation of 122°, needs an explanation. This may be found in the side face, where a Y_{en} girdle (D. 47) has been observed, the orientation of which is in accordance with the enstatite C. D. A. of the side and top faces. This girdle, S_2 when rotated to the front face, appears to go through the intersection point of S_1 and the pre-deformational $X_{ol} = Y_{en}$ trend. (D. 59, fig. 11).

The hypothesis on which the transposition theory of olivine is based, is the assumption that the rotation of olivine is determined by the orientation of the X_{ol} axes in relation to the potential slip planes in the rock. If olivine forms the bulk of the rock, the movements of other minerals such as enstatite will probably be determined largely by the rotation of the olivine crystals. However, the question arises how enstatite will orient itself if it is free to rotate independently. On theoretical grounds the most probable translation glide plane in the enstatite space lattice is {100} with glide direction [001]. (Griggs, Turner, Heard, 1960). Whether the Y_{en} or Z_{en} axis will pre-dominate in a tectonic orientation

[6]) The terms dextral and sinistral rotation used here refer to the sense of rotation in the stereographic net. The real rotations occur in the opposite sense for all the projections are lower hemisphere projections.

is not known, but the strong Z_{en} concentration observed in the probably tectonic fabric of the sample from Dreiser Weiher (D. 30) might indicate that the Z_{en} axis, [001], is the most important. If an explanation of the rotation of enstatite is based on the assumption that the Z axis is the most important, then many of the observed facts can be explained.

A close observation of the Z_{en} diagrams of the side face, especially diagram 64, reveals that the Z_{en} axes are mainly concentrated in a maximum that can be interpreted as the intersection of two incomplete girdles. If we accept the view that the orientation of enstatite is predominantly determined by the Z axis, then a similar reasoning as developed for olivine may be applied to enstatite. The transposed orientation of Z_{en} seems now to be governed by two conditions: an orientation of Z_{en} parallel to S_1 and normal to S_2. The fact that S_1 and S_2 are not absolutely perpendicular prevents the fulfilment of both these conditions.

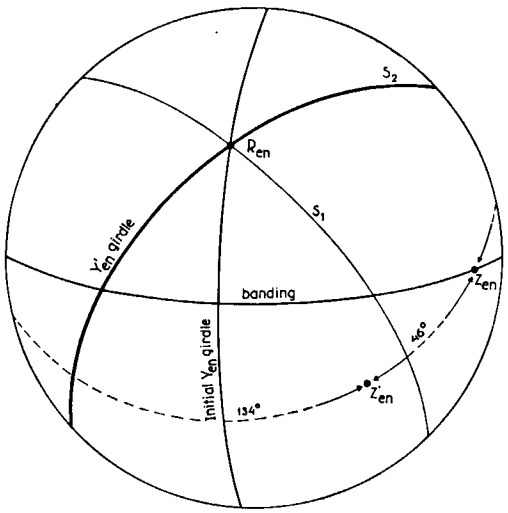

Figure 11. Construction of the rotation axis and rotation angles of enstatite in the front face of sample A. 1.

Z_{en}: probable main pre-deformational Z_{en} concentration.

Z'_{en}: observed post-deformational Z_{en} concentration in the intersection of two incomplete Z_{en} girdles. (D. 61, D. 64).

R_{en}: rotation axis of enstatite in the pole of the great circle through Z_{en} and Z'_{en}. R_{en} is the intersection of the pre-deformational Y_{en} girdle with S_2 and S_1.

S_2: potential slip plane marked by an almost complete Y_{en} girdle. (D. 59).

The rotation angles are 46° in the dextral and 134° in the sinistral sense.

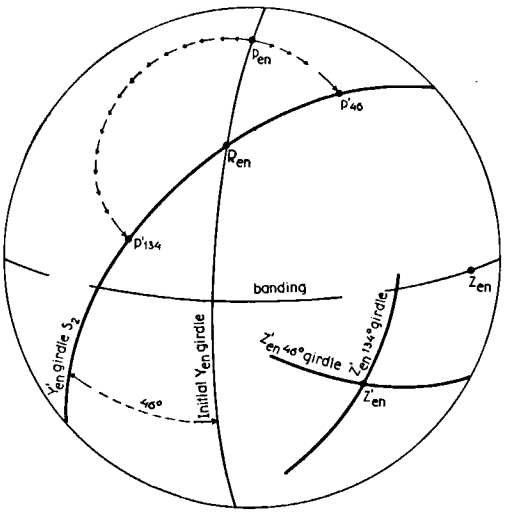

Figure 12. Transposition of enstatite in the front face of sample A. 1.

The pre-deformational incomplete Z_{en} girdle is rotated around the rotation axis R_{en} over 46° in the dextral and 134° in the sinistral sense.

Instead of the Z_{en} girdle its Pole P_{en} ($= X_{ol}$) is rotated. The resulting projections are the poles of two intersecting incomplete Z_{en} girdles.

The same rotation affects the pre-deformational complete Y_{en} girdles, which is transposed to its new orientation parallel to S_2.

The main Z_{en} concentration was ever again found to be a few degrees away from S_1 (see also chapter IV). The enstatite rotation may thus be deduced from the pre-existing and the transposed orientation of the Z axes. The pre-existing orientation of Z_{en} is the same as the initial Z_{ol} orientation. (See figure 9.) The intersecting incomplete girdles of the transposed Z_{en} axes are best expressed in the enstatite diagrams of the side face, especially the one which is rotated to the top face. (D. 64) The rotation axis of enstatite can now be found by constructing the plane common to the pre-existing and transposed orientations of Z_{en}. (See figure 11.) The axis of this great circle is found to be the intersection line of S_{11} and S_2 and the pre-deformational Y_{en} trend. The rotation angle appears to be 46° or 134°, depending on the sense in which the angle is measured.

The transposition of enstatite can now be carried out, and results in two intersecting incomplete Z_{en} girdles, the intersection of which is the axis of the great circle S_2 formed by the Y_{en} axes. (See figure 12, which has to be compared with the diagrams 59 and 61.)

So far we have seen that the transposition of olivine and enstatite is of the same type in as much as the rotation in opposite sense over supplementary angles is concerned. The orientation of the main rotation axis, however, is different for each mineral, as well as the actual rotation angles. The olivine transposition is mainly expressed in the front face, while the enstatite rotation can best be observed in the diagrams of the side face. The terms olivine rotation axis and enstatite rotation axis seem only to be right as a first approximation. In fact it is improbable that the rotation of the two minerals will be completely independent. This is clearly seen in the Y_{en} and Z_{en} diagrams of the front face. (D. 35, D. 37.) The orientation of the central Y_{en} girdle in diagram 35 coincides with the incomplete X_{ol} girdle (D. 32) which resulted from the dextral rotation of the initial X_{ol} trend, around the olivine rotation axis, over an angle of 58°. (See figure 10.) It has been demonstrated that the Z_{ol} orientation to match with this central X_{ol} girdle is at the SE. margin of the diagram. (Fig. 10.) From the construction of the enstatite transposition (Fig. 12) we know that the Z_{en} axes tend to rotate to the SE. margin of the diagrams of he front face. We may now conclude that the enstatite crystals followed the rotation of olivine (i.e. the rotation around the olivine rotation axis) only in so far as it gave rise to an orientation of Z_{en} favouring translation gliding of enstatite. If enstatite would also have been rotated in the sinistral sense, then the resulting Z_{en} concentration would have been in the centre of the diagram (fig. 10) an orientation which does apparently not favour the translation gliding of enstatite. The inhomogeneity of the fabric as far as enstatite is concerned appears now to be adequately explained.

As yet little has been said on the olivine fabric of the side and top face (D. 50—D. 55). If the Z_{ol} diagrams (D. 52, D. 55) are considered it is seen, that the bulk of these axes have an orientation sub-parallel to the banding plane, a feature which implies that the olivine crystals have hardly been affected by the rotation. This conclusion is confirmed by the observed X_{ol} orientations in these faces. The main concentration of these axes in the side face (D. 53) is found at 33° from the presumed pre-deformational X_{ol} concentration. In the top face (D. 50) this angle is even less: 25°. These observations leave little doubt that the olivine fabrics observed in the top and side face have to be interpreted as

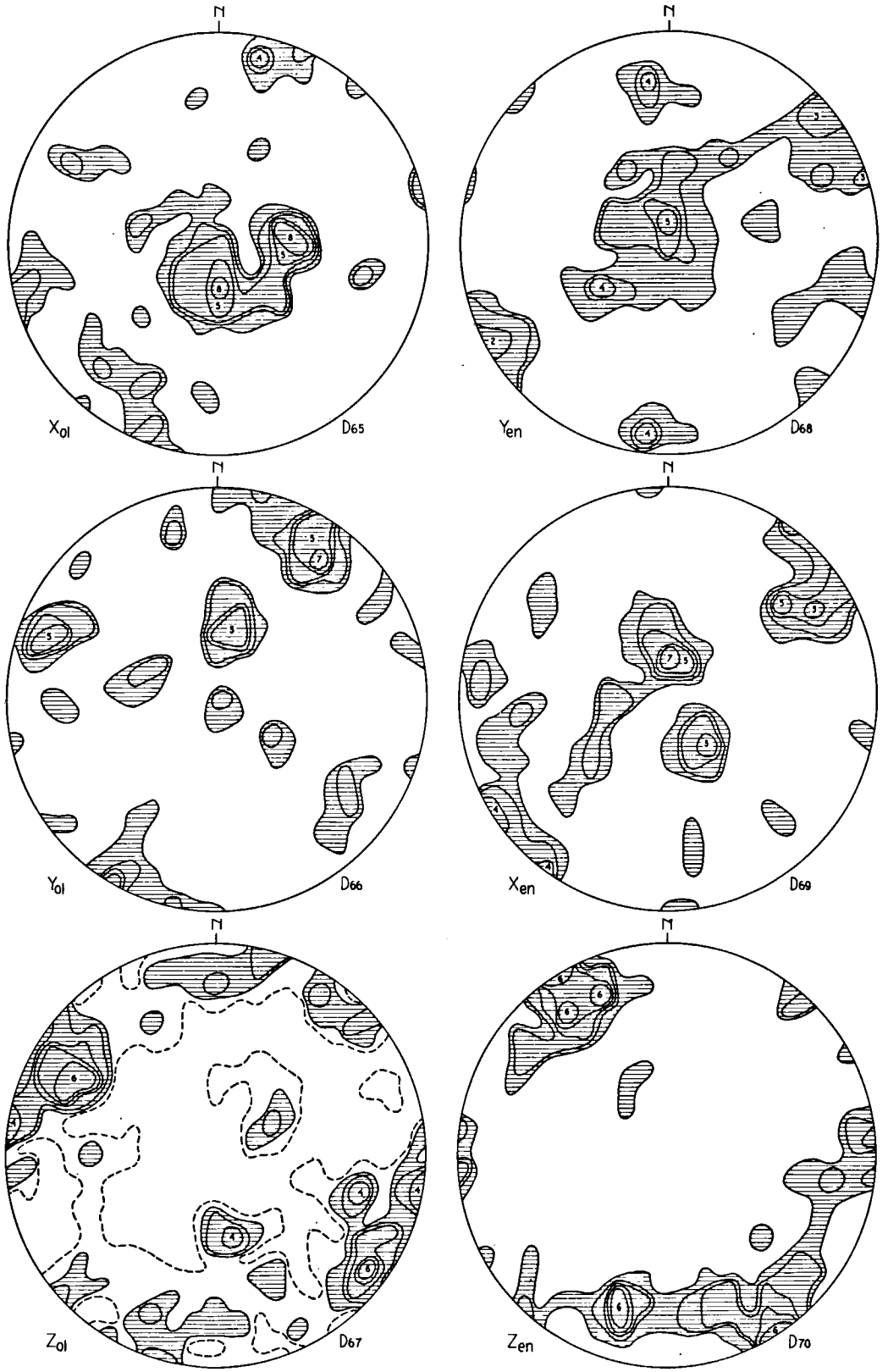

D. 65.: A. 1., 100 X_{ol}, slip plane S_1.
D. 66.: A. 1., 100 Y_{ol}, slip plane S_1.
D. 67.: A. 1., 100 Z_{ol}, slip plane S_1. Interrupted line is 1 % contour.

D. 68.: A. 1., 100 Y_{en}, slip plane S_1.
D. 69.: A. 1., 100 X_{en}, slip plane S_1.
D. 70.: A. 1., 100 Z_{en}, slip plane S_1.

intermediate stages between the pre- and post-deformational olivine fabric. This conclusion is important because it implies that rotation and not recrystallization has been the main agency in the deformation, for intermediate orientations are not likely to occur in a recrystallized fabric.

The "lineations" observed in the C. D. A. have now to be incorporated in the transposition theory. There is little doubt that the lamination is a vestige of the original fabric. In the interpretation of the other planes and directions we have to keep in mind that they refer to the enstatite and probably not to the olivine distribution.

The observed N. 45° W. direction in the top face can be correlated with the N. 40°-60° E. direction in the side face, both having S_2 (the Y_{en} trend in these faces), as a common plane. The intersection of this plane S_2 with the front face yields a N. 48° E. direction, which coincides with the lineation observed in the C. D. A. of the front face. These arguments leave little doubt that S_2 is actually a slip plane in this specimen.

The N. 45° W. direction observed in the C. D. A. of the front face undoubtedly refers to the orientation of the Z axes. The intersection of the supposed plane S_1, containing this direction, with the top face should yield a N. 28° E. "lineation" in the top face. This "lineation" is not very strong in the C. D. A. of this face. The fact that the C. D. A. refers to the enstatite and not to the olivine distribution possibly accounts for the suppression of this feature.

In order to collect further information on the postulated S_1 plane, a thin section sub-parallel to it was made and fabric diagrams of both olivine and enstatite were constructed. The diagrams 65 to 70 refer to this plane. Diagram 65 shows clearly that the main X_{ol} concentration is perpendicular to S_1. The Z_{ol} axes in diagram 67 are concentrated in a marginal girdle, with a well defined NW. trending maximum. The interrupted lines enclose the areas of one percent density. The enstatite diagrams (D. 68—D. 70) show a comparable pattern, with Y_{en} sub-normal to S_1 and Z_{en} within this plane mainly oriented NW. The diagrams 71 to 76 are the results of the rotation of these S_1 diagrams to the front face. The full lines indicate the orientation of the supposed S_1 plane, which is parallel to the actual observed Z_{ol} trend. Besides the expected Z_{ol} concentration near the SE. margin of diagram 73, a second concentration occurs, which has been predicted on theoretical grounds. (See page 37 and figure 10.) This central concentration is the result of a rotation of the pre-existing Z_{ol} orientation in the sinistral sense over 122°.

The main Y_{en} concentration in diagram 74 deviates slightly from the pole of S_1 and corresponds with the main Y_{en} concentration observed in the side face (D. 59). The greater part of the Y_{en} axes seems to have an orientation parallel to S_2.

From the foregoing it is obvious to conclude that S_1 is a slip plane for olivine.

The fact that even in a section parallel to S_1 the enstatite fabric is symmetric with S_2, combined with the information from the C. D. A., suggests that the S_2 plane is a slip plane for enstatite.

The two planes intersect at about 80°, they are probably not truly monomineralic slip planes. Otherwise the C. D. A. of enstatite in the front face would not show the strong N. 45° W. direction, corresponding with S_1. It is much more probable that they represent slip planes for both minerals, however with a certain preference of olivine for S_1 and of enstatite for S_2.

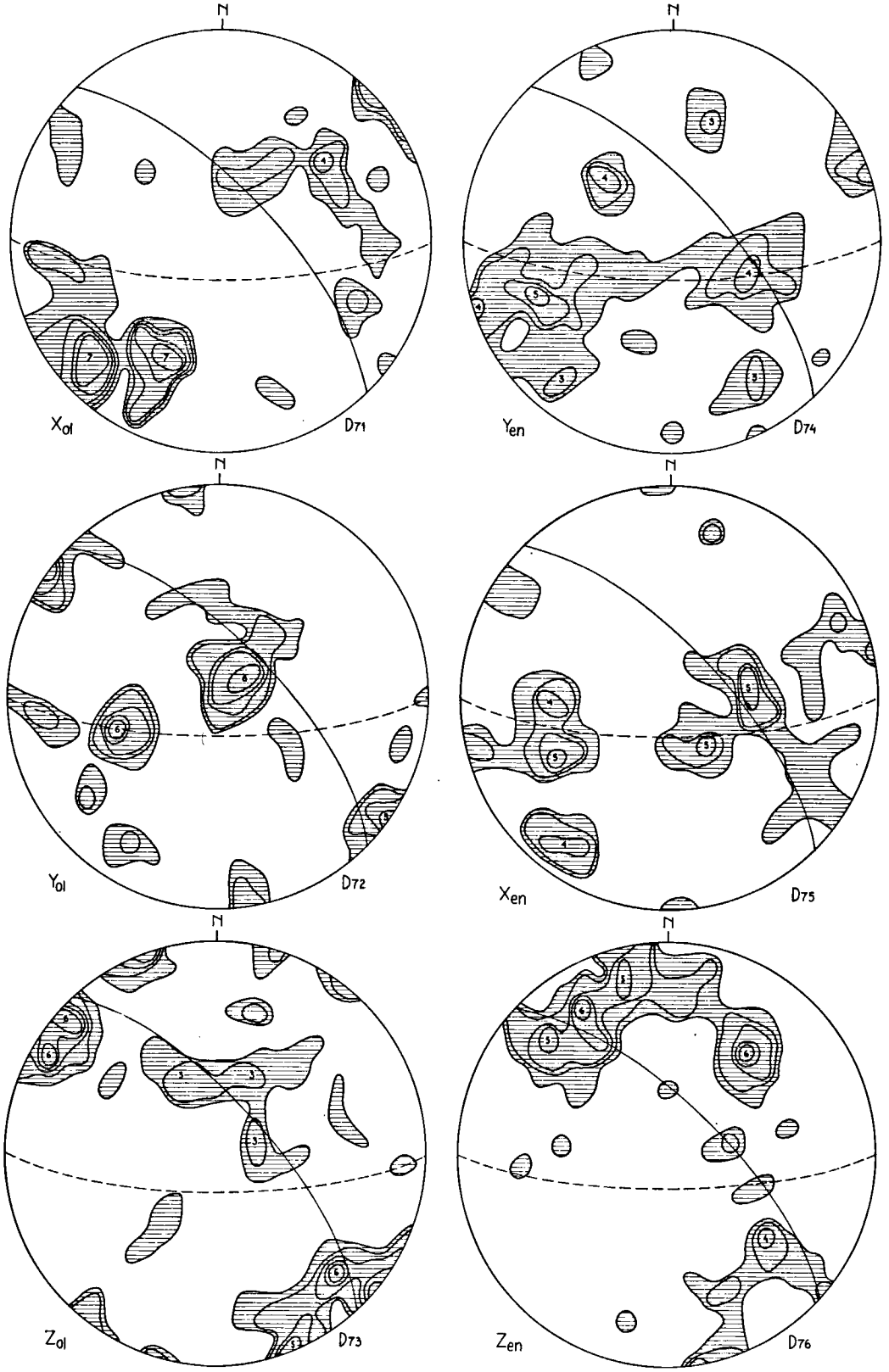

D. 71.: A. 1., 100 X_{ol}, S_1 rotated to front face.
D. 72.: A. 1., 100 Y_{ol}, S_1 rotated to front face.
D. 73.: A. 1., 100 Z_{ol}, S_1 rotated to front face.
D. 74.: A. 1., 100 Y_{en}, S_1 rotated to front face.
D. 75.: A. 1., 100 X_{en}, S_1 rotated to front face.
D. 76.: A. 1., 100 Z_{en}, S_1 rotated to front face.

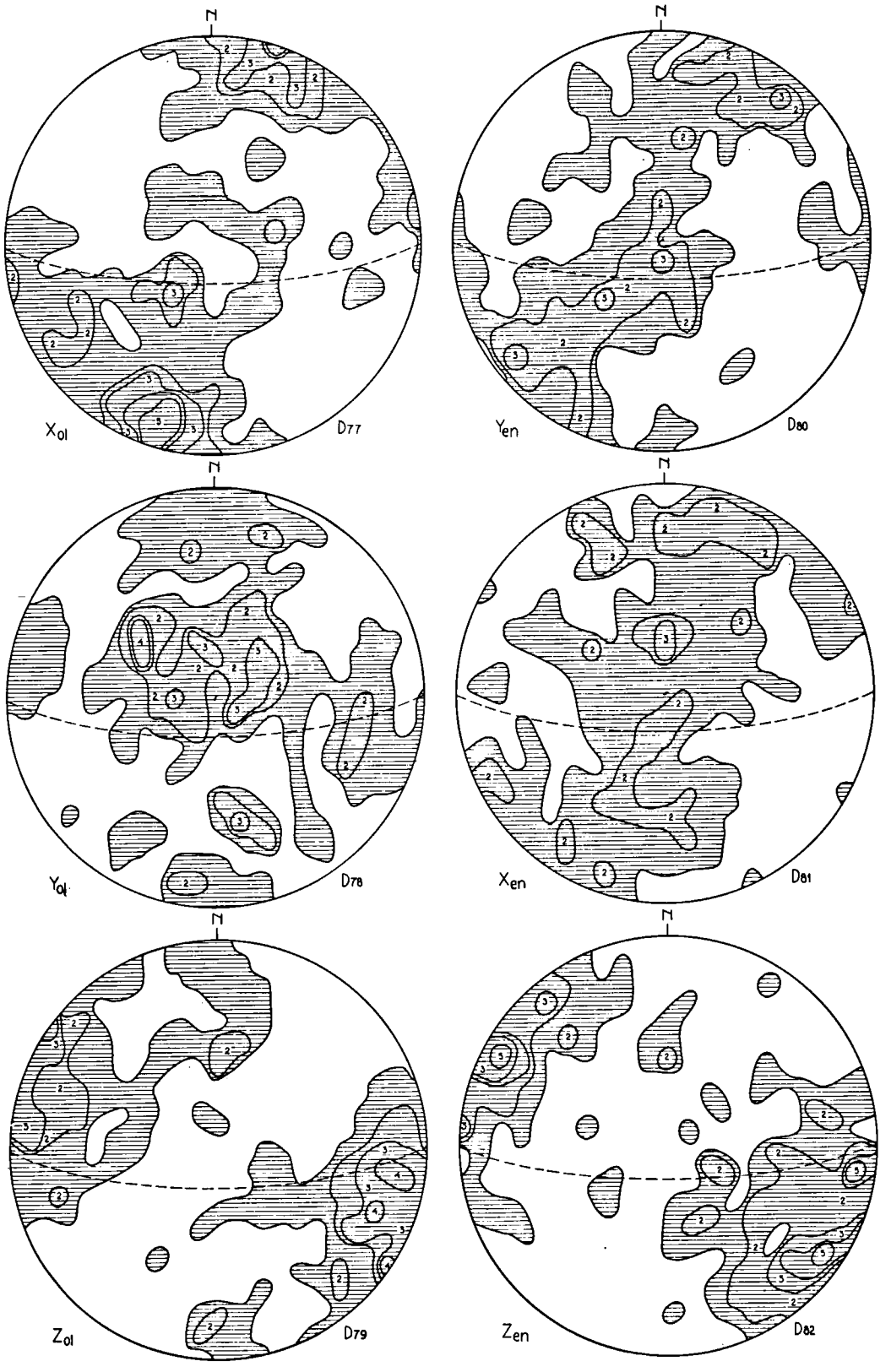

D. 77.: A. 1., 300 X_{ol}, collective diagram of front, top, and side face projected on front face.
D. 78.: A. 1., 300 Y_{ol}, collective diagram id.
D. 79.: A. 1., 300 Z_{ol}, collective diagram id.
D. 80.: A. 1., 300 Y_{en}, collective diagram id.
D. 81.: A. 1., 300 X_{en}, collective diagram id.
D. 82.: A. 1., 300 Z_{en}, collective diagram id.

TABLE III

	OLIVINE			ENSTATITE		
Pre-Deformational	X_{ol}	Maximum	**Pole of banding.**	Y_{en}	Maximum	—
		Girdle	incomplete, $\perp Z_{ol}$-Z_{en}.		Girdle	$\perp Z_{en}$-Z_{ol}.
	Z_{ol}	Maximum	// Z_{en}.	Z_{en}	Maximum	**Pole Y_{en}-X_{ol} girdle.**
		Girdle	// **Banding.**		Girdle	// Banding.
Transposed	X_{ol}	Maximum	Pole S_1.	Y_{en}	Maximum	—
		Girdle	**Two intersecting incomplete girdles.**		Girdle	// S_2.
	Z_{ol}	Maximum	**Poles of intersecting X_{ol} girdles.**	Z_{en}	Maximum	Pole S_2.
		Girdle	// S_1.		Girdle	**Two intersecting incomplete girdles.**
Rotation axis is intersection line of banding and S_1.				Rotation axis is intersection line of pre-deformational X_{ol}—Y_{en} girdle and S_2 and S_1.		
Rotation angles: 58°, 122°.				Rotation angles: 46°, 134°.		

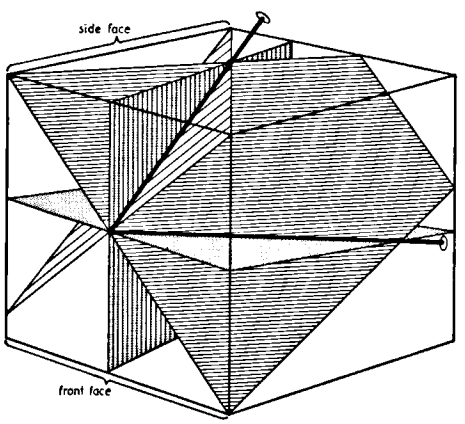

Figure 13. Block-diagram illustrating the relation between the two diagonal slip planes S_1 and S_2 and the pre-deformational fabric elements: the sub-horizontal banding plane and the plane normal to it characterized by a complete Y_{en} and incomplete X_{ol} girdle. The two axes are the rotation axes.

To summarize the geometry of the fabric, collective diagrams both for olivine and enstatite, based on the three faces of the specimen have been constructed. (D. 77—D. 82.) In these diagrams, which are oriented parallel to the front face both the pre-existing and transposed fabrics are present. Their value for interpretational purposes is limited, since we know that the constituting diagrams from different faces of the sample cube are in many respects very dissimilar.

Table III gives a summary of the main properties of the fabric described in this chapter. The block diagram of figure 13 visualizes the relation between the slip planes and the two pre-deformational fabric planes.

PLATE I

D. 32.: A. l., 100 X_{ol}, front face.
D. 33.: A. l., 100 Y_{ol}, front face.
D. 34.: A. l., 100 Z_{ol}, front face.

D. 35.: A. l., 100 Y_{en}, front face.
D. 36.: A. l., 100 X_{en}, front face.
D. 37.: A. l., 100 Z_{en}, front face.

D. 50.: A. l., 100 X_{ol}, top face rotated to front face.
D. 51.: A. l., 100 Y_{ol}, top face rotated to front face.
D. 52.: A. l., 100 Z_{ol}, top face rotated to front face.

D. 53.: A. l., 100 X_{ol}, side face rotated to front face.
D. 54.: A. l., 100 Y_{ol}, side face rotated to front face.
D. 55.: A. l., 100 Z_{ol}, side face rotated to front face.

D. 56.: A. l., 100 Y_{en}, top face rotated to front face.
D. 57.: A. l., 100 X_{en}, top face rotated to front face.
D. 58.: A. l., 100 Z_{en}, top face rotated to front face.

D. 59.: A. l., 100 Y_{en}, side face rotated to front face.
D. 60.: A. l., 100 X_{en}, side face rotated to front face.
D. 61.: A. l., 100 Z_{en}, side face rotated to front face.

D. 62.: A. l., 100 Y_{en}, side face rotated to top face.
D. 63.: A. l., 100 X_{en}, side face rotated to top face.
D. 64.: A. l., 100 Z_{en}, side face rotated to top face,

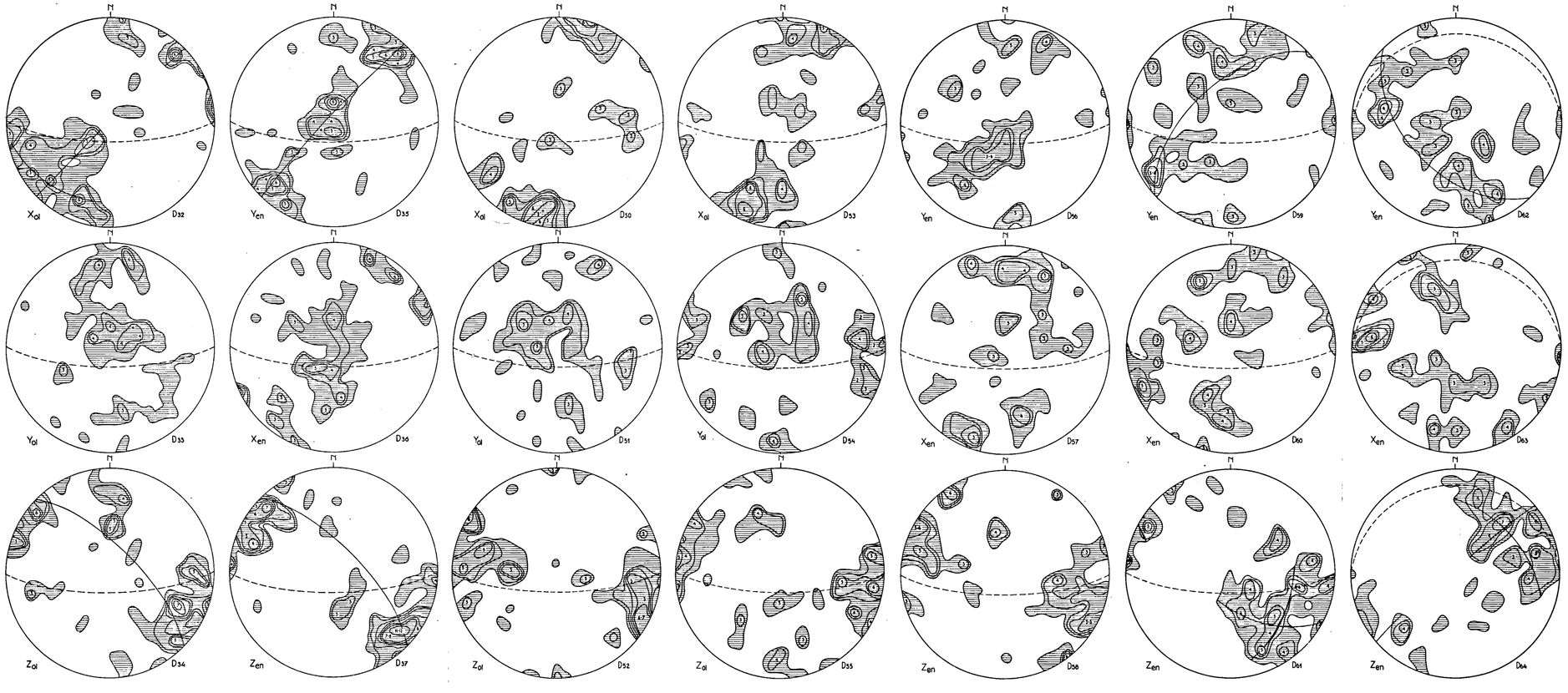

CHAPTER IV

THE AXIAL DISTRIBUTION ANALYSIS (A. D. A.)

1. *Introduction*

The purpose of making an A. D. A. consists of establishing a relation between the preferred orientations of crystals and their locations in the rock sample. In the case of a homogeneous fabric such a relation does not exist, but if the fabric is inhomogeneous, i.e. if the crystals in different parts of the rock have a different preferred orientation, it may happen that there exists a specific relation between the orientation and the location of various groups of crystals.

The study of the sample described in the foregoing chapter, has revealed that the fabric diagrams of different planes in the rock, differ strongly. The existence of potential slip planes has been proved. The crystal distribution analyses of enstatite showed that this mineral is inhomogeneously distributed, and concentrated in the slip planes of the rock. For olivine however, such a distribution of the crystals has not been established, although the inhomogeneity of its distribution is beyond doubt.

The fact that the construction of a significant A. D. A. requires the measuring of a great many, possibly over a thousand crystals, practically excludes the possibility of making Axial Distribution Analyses of several planes in one sample, as would be required to draw up a true picture of the structural units of the rock. The sample described in the foregoing chapter has two sorts of planes which are of particular interest for making an A. D. A.

1. Planes in which apart from the banding two intersecting directions are seen, which are probably the intersection lines of slip planes sub-perpendicular to the plane of observation.

2. The slip planes, in which a possible relationship between slip directions in the rock and translation directions of the crystals might yield a linear pattern. To test this possibility a C. D. A. of enstatite in the plane S_1 of the sample described in chapter III has been made. The very faint linear pattern observed in this C. D. A. did not encourage the writer to construct an A. D. A. in a plane of this type.

Consequently the A. D. A. has been made in a plane, comparable with the front face of the former sample. For the purpose of making an A. D. A. a rock specimen is needed of which olivine is by far the most important constituent, and the crystals of which are not too coarse grained. The sample of chapter III did not meet these requirements. Furthermore it seemed advantageous to use a specimen which does not show any macroscopic lineations. Another advantage of studying a different sample is the fact that the deformation theory, evolved in the foregoing chapter, will be corroborated if it can be applied to the fabric of a second sample.

2. Preparation of the thin sections.

There are several technical problems related to the construction of an A.D.A. The fact that the lherzolitic nodules are rather coarse grained, makes it necessary to study a

large surface of the rock in order to attain the required number of crystals. The rock in question contains about eighty percent olivine, with an average cross-sectional surface of 0.7 mm^2. If 1500 olivine crystals have to be measured, the thin section has to cover a surface of 13 cm^2. The maximum range of the conventional universal stage, however, does not exceed 3.75 cm^2. Consequently several thin sections had to be made, the mutual position of which had to be known accurately. To achieve this purpose, the following method has been applied. A slice one centimetre thick and of the required size is sawed and carefully polished. With a pencil a rectangle is drawn on this polished surface. Next a photograph of this surface is made with incident light. The slice is then cut in four pieces, with a thin-blade saw. The polished surface of each of the four pieces is subsequently mounted on a glass plate. The preparations are then brought to the required thickness. Great care has to be taken to avoid holes, which easily arise from the fact that the rock in question is brittle. The four thin sections, on which the previously mentioned pencil lines are still visible, are then photographed with transmitted light. The mutual position of these photographs, and consequently of the thin sections, can then be reconstructed with the aid of the previously made photograph of the whole slice.

3. *Construction of the fabric diagrams*

The orientation of all the olivine crystals, present in the four thin sections has to be measured and represented in a diagram. Each crystal is given a number which is recorded on the photograph of the thin section. It is not recommendable to draw the outline of each crystal on the photograph. This proves to be very time consuming and is of no use, unless a coloured picture of the axial distribution is to be made. If not, it is sufficient to mark each measured crystal with a point in its centre.

The four partial diagrams are then added up to obtain a collective diagram. The diagrams of olivine (see plate II) are based on 1512 crystals. Diagram 83 refers to the orientation of the X_{ol} axes, which form two intersecting incomplete girdles, the same pattern as has been described in the front face of the former sample. The stronger girdle is almost parallel to the plane of the section, the weaker one is normal to this plane. The large number of measurements excludes every possibility of the observed pattern to be fortuitous. Diagram 84 refers to the orientation of the Y_{ol} axes. The density contours are drawn between 1—1.5—2—2.5 percent. The axes are concentrated in an almost complete girdle perpendicular to the main X_{ol} concentration. The distribution of the axes shows a spreading along the northern and southern margins of the diagram. Diagram 85 refers to the orientation of the Z_{ol} axes. The density contours are drawn between 1—1.5—2—2.5—3 percent. The incomplete girdle, which is the counterpart of the Y_{ol} girdle, has three well defined maxima.

The corresponding enstatite diagrams are 86(Y_{en}), 87(X_{en}), 88(Z_{en}) (see plate II). They are based on two hundred readings each, and come up to the expectations derived from the previous specimen. The Z_{en} axes are concentrated in two incomplete intersecting girdles. Their main concentration almost coincides with one of the Z_{ol} maxima. The Y_{en} axes form a girdle which does not altogether coincide with one of the X_{ol} intersecting girdles. X_{en} hardly has any preferred orientation.

4. *Subdivision of the fabric diagrams in petrotectonic units*

It has been stated before that the purpose of the investigation is to look for a relation between the orientation of the crystals and their location in the plane of the sample. The fact that the full orientation of biaxial crystals depends on the direction of two of the three crystallographic axes, makes their represen-

tation in an axial distribution diagram problematic. But from the descriptions in the foregoing chapters and from a thorough scrutiny of the diagrams it will become clear that in olivine the X and Z axes are the ones most likely to have a tectonic significance. If one has to make groups of crystals with an analogous orientation, it is obviously best to base such a division on the observed maxima. These are: for X_{o1} the two intersecting incomplete girdles, and for Z_{o1} the three point maxima which together form the almost complete girdle. On this basis one may make two major groups, depending on the position of X_{o1} in girdle I or II. Each major group will then comprise three sub-groups, depending upon the orientation of Z_{o1} in one of the three maxima in the Z_{o1} girdle. In such a way six sub-groups of different orientation can be recognized. However this method, which appears most appropriate on theoretical grounds, is impracticable, because each sub-group will not even comprise two hundred crystals. This is due to the fact that the X_{o1} axes which lie in or near the intersection point of the two X_{o1} girdles I and II cannot be incorporated in one of the two major groups, because it is not sure to which they belong. Furthermore all the crystals with a more or less random orientation of either X_{o1} or Z_{o1} reduce the number of crystals in each group. As reliable density contours cannot be based on the distribution of two hundred crystals, the setting up of six independent and structurally different groups of crystals had to be abandoned

A more convenient way of dealing with the problem under discussion consists in treating the X_{o1} and Z_{o1} axes separately. By doing so, one gets three groups of X_{o1} orientations. The first contains all the olivine crystals with X axes lying in the sub-marginal girdle I, the second comprises those with X axes in the sub-diametrical girdle II. A third group is formed by the olivine crystals the X axes of which lie near or on the intersection of the two girdles. In order to attain a sufficient number of grains, this group was made to overlap the other X_{o1} groups to some extent. In the same way three Z_{o1} groups were made, each referring to one of the three Z_{o1} maxima in the Z_{o1} girdle.

From the distribution of these crystal groups over the sample studied, it will become clear whether the two X_{o1} girdles have a different tectonic significance. It will also be possible to draw conclusions regarding the role of the orientation of the Z_{o1} axes in respect of potential slip directions in the rock.

5. *The representation of the axial distribution*

The best way of visualizing a relation between the orientation of crystals and their location in the sample, consists in colouring a picture of the thin section, in such a way that each group of crystals of a specific orientation recieves a characteristic colour. In almost monomineralic rocks of constant grain size, such a method gives good results, if the relation between orientation and location of the crystals is strong. If the investigated mineral, however, forms only about eighty percent of the rock and if the grain size is variable, this way of representation fails to bring out the expected relationship. In such a case a better procedure consists of marking a point in the centre of each crystal belonging to one orientation-group, and drawing density contours around these points in the same way as is done in fabric diagrams. But this method does not acount for variations in grain size of the crystals. A big crystal with a certain orientation will yield only one point; if a similar surface elsewhere is covered by five crystals of which only two have the same orientation, these two will show up in the density contours as a concentration twice as high. A second error is introduced by not accounting

Figure 14.

Axial distribution diagram. ($\times$ 3.5)

The distribution of 677 (44.7 %) olivine crystals with **X** axes // to the marginal X_{ol} girdle (D. 83), is represented.

Relative contours:	hatched background	50—61 %
		62—73 %
		$>$ 73 %
	white background	40—49 %
	dotted background	20—27 %
		14—27 %
		$<$ 14 %

Figure 15.

Axial distribution diagram. ($\times$ 3.5)

The distribution of 554 (36.6 %) olivine crystals with **X** axes // to the diametrical X_{ol} girdle (D. 83), is represented.

Relative contours:	hatched background	42—53 %
		54—65 %
		$>$ 65 %
	white background	32—41 %
	dotted background	21—31 %
		11—20 %
		$<$ 11 %

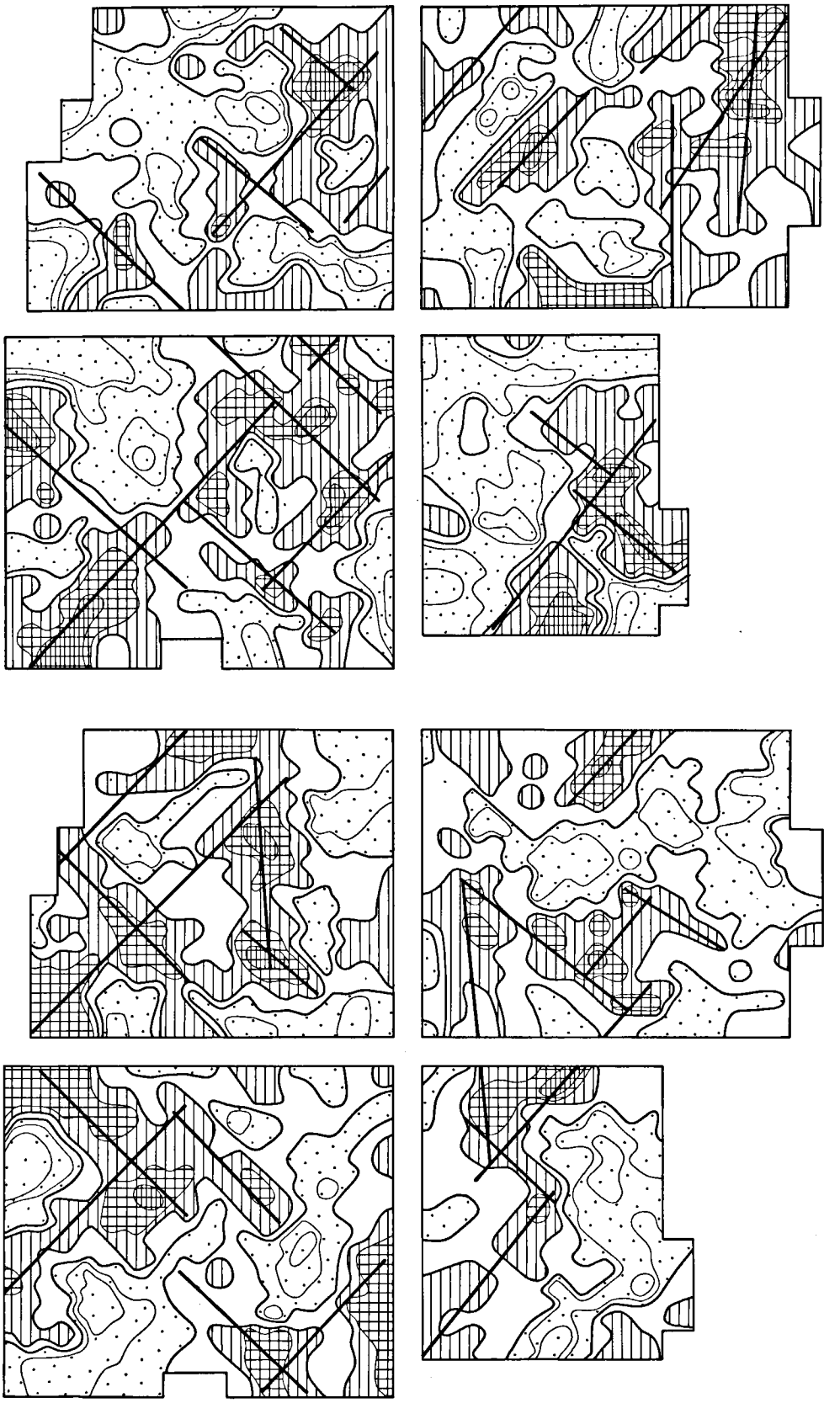

Figure 16.

Axial distribution diagram. ($\times$ 3,5)

The distribution of 354 (23.4 %) olivine crystals with X axes // to the intersection of the two X_{ol} girdles (D. 83), is represented.

Relative contours:	hatched background	28—40 %
		40—53 %
		$>$ 53 %
	white background	20—27 %
	dotted background	10—19 %
		$<$ 10 %

Figure 17.

Axial distribution diagram. ($\times$ 3,5)

The distribution of 504 (33.3 %) olivine crystals with Z axes // to the NE concentration of diagram 85, is represented.

Relative contours:	hatched background	38—49 %
		50—61 %
		$>$ 61 %
	white background	29—37 %
	dotted background	19—28 %
		9—18 %
		$<$ 9 %

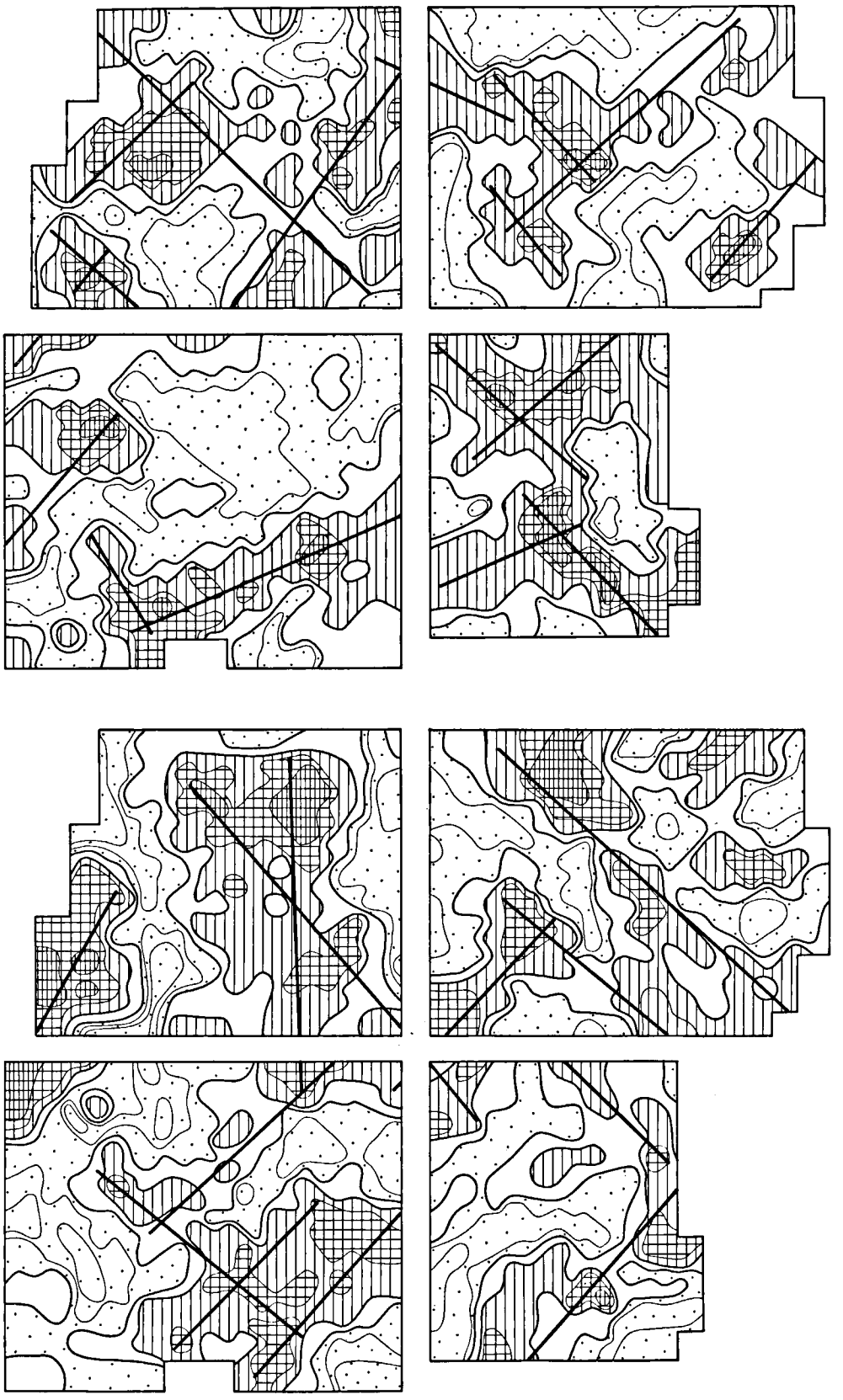

Figure 18.

Axial distribution diagram. (× 3.5)

The distribution of 523 (34.6 %) olivine crystals with Z axes // to the central concentration in diagram 85, is represented.

Relative contours:	hatched background	39—50 %
		51—62 %
		> 62 %
	white background	30—38 %
	dotted background	20—29 %
		10—19 %
		< 10 %

Figuur 19.

Axial distribution diagram. (× 3.5)

The distribution of 314 (20.7 %) olivine crystals with Z axes // to the SE. concentration of diagram 85, is represented.

Relative contours:	hatched background	26—38 %
		39—51 %
		> 51 %
	white background	17—25 %
	dotted background	9—16 %
		< 9 %

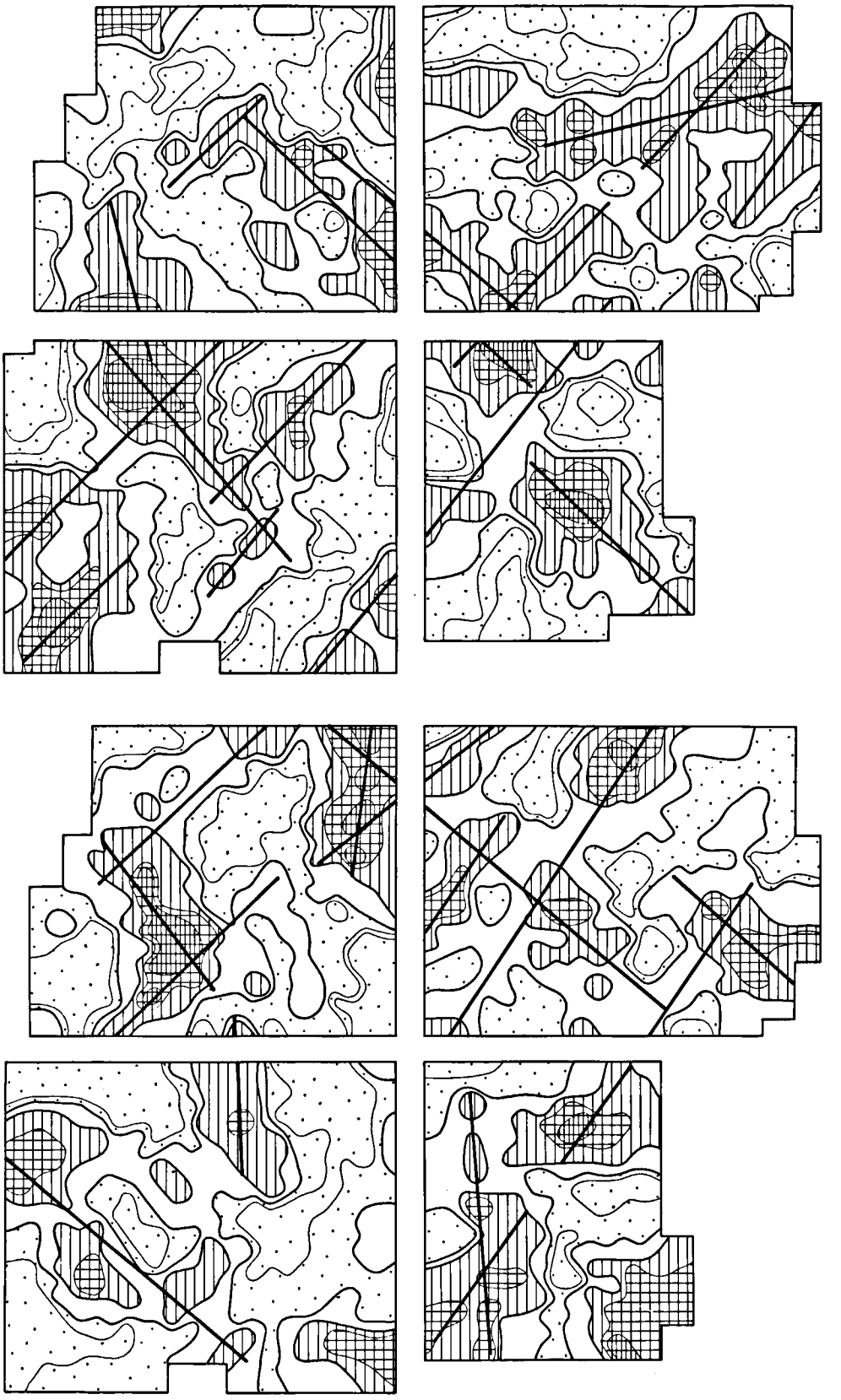

Figure 20.

Collective diagram of the directions inferred in the three X_{ol} distribution diagrams. (fig. 14, 15, 16.) (× 3,5)
The full lines refer to fig. 14.
The interrupted lines refer to fig. 15.
The dotted lines refer to fig. 16.

Figure 21.

Collective diagram of the directions inferred in the three Z_{ol} distribution diagrams. (fig. 17, 18, 19.) (× 3,5)
The full lines refer to fig. 17.
The interrupted lines refer to fig. 18.
The dotted lines refer to fig. 19.

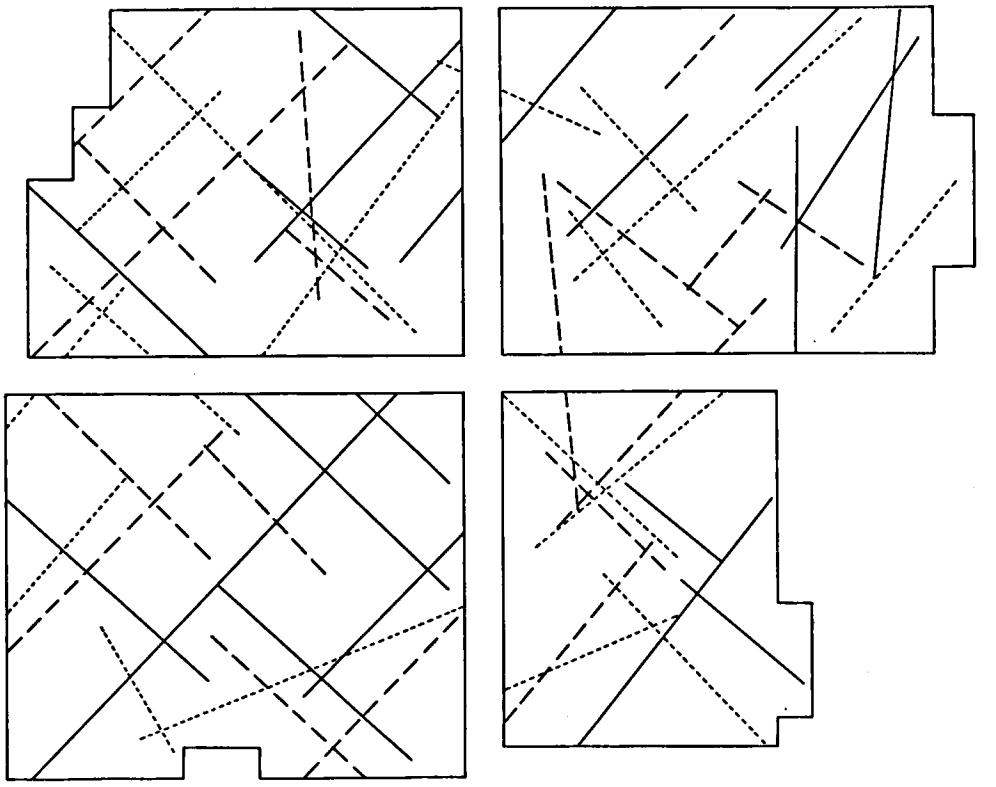

for the fact that the rock is polymineralic. In the sample described in the foregoing chapter the enstatite crystals in the front face are concentrated in two intersecting directions, while the banding plane of the rock is marked by a high concentration of picotite. Such distributions do not fail to affect the position of the other minerals. If an independent representation of the distribution of olivine is wanted, the method of representation has to exclude the influence of other minerals in the sample.

To meet both these requirements, the usual way of representation has been modified. The basic idea of the method consists of representing in the distribution diagrams the relative instead of the absolute densities. Once the group of similarly oriented crystals is delimited, the percentage of olivine crystals with this orientation in relation to the total amount of olivine crystals in each unit area, is calculated and noted. In such a manner a grid of percentage numbers is obtained which can be contoured. The size of the unit squares has to be chosen so as to contain the centres of at least ten olivine crystals. The unit squares overlap each other in a similar way as the grids used for the preparation of density contours in conventional fabric diagrams. If the group of crystals the distribution of which in the sample has to be represented, forms for instance thirty percent of the total amount of olivine crystals, the lowest positive density contour will have to be chosen a little above thirty percent, which value represents the expected average. The interval between the different density contours can then be chosen freely. An additional advantage of this method is the fact that not only positive concentrations, i.e. concentrations which exceed the expected average, but also negative concentrations can be represented.

6. *The axial distribution diagrams*

The figures 14—19 refer to the distribution of the crystals belonging to each of the six different crystal groups. The contours in the figures are divided into three units, which are marked by a different background. The hatched areas refer to positive concentrations, i.e. to those areas where the accumulation of crystals with a specific orientation is greater than the calculated average. The dotted areas stand for negative concentrations. The white areas in between group the concentrations which are close to the average. Density contours further subdivide the positive and negative areas.

The fabric diagrams 89—94 (see plate II) show the boundaries of the crystal groups involved, and the orientation of the corresponding Z_{ol} or X_{ol} axes.

The purpose of the figures is now to scan them for preferred directions among the positive concentrations. There is no doubt that these directions, if they exist at all, are not very pronounced. Strongly preferred directions, however, are not to be expected in a rock which does not show any macroscopically visible lineations or S planes. The very reason of this investigation was to see whether the conclusions reached in the foregoing chapter, where a direct relation between the micro fabric and visible structures could be established, are also applicable in the case of a sample in which such macroscopic features do not exist. Therefore the figures should be examined in the light of the conclusions reached before.

In the opinion of the writer, the lines drawn in the figures fit in best with the observed pattern of contour directions. Difference of opinion on several of these lines may ensue, but the general trend of directions appears to be rather definite. The three figures (14, 15, 16) which refer to the three X_{ol} groups

each show two perpendicular directions: N. 45° E. and N. 45° W. respectively. A subsidiary system trending more or less N.—S. and E.—W. seems also to be present. The directions observed in each of the three figures separately have been added up and represented in figure 20.

The same procedure is followed for the figures which refer to the three Z_{ol} groups. Here, the same phenomenon is observed namely that each of the figures shows the same pattern of intersecting diagonal directions. Figure 21 is the collective diagram of the directions observed in the three partial diagrams. The comparison of figure 20 and 21 reveals that the directions for the X_{ol} and Z_{ol} groups are the same.

The obvious conclusion from the six figures is that each group of crystals shows the same directional pattern although minor differences of strength of the pattern may occur. In other words the two X_{ol} girdles do not seem to have a structural significance in such a way that either of them is related with one of the two potential slip planes in the rock. The same holds for the three Z_{ol} maxima. It is not likely that any of them has a relation with only one of the potential slip planes in the rock.

7. *Interpretation*

In the light of the conclusion reached in chapter III, in which the deformation pattern of one of the nodular inclusions from Auvergne has been investigated in detail, one may attempt to establish an analogous reasoning for the sample of which the axial distribution analysis has been made. The fabric observed in the present sample has many features in common with that of the banded sample described in the foregoing chapter: intersecting incomplete X_{ol} girdles, the intersection of which is the projection of the axis of the Z_{ol} girdle: S_1; intersecting incomplete Z_{en} girdles, the intersection line of which is sub-parallel to S_1, and forms the axis of a complete Y_{en} girdle: S_2. In the light of these analogies it is obvious to base an interpretation on the assumption that the deformation of both specimens has been of the same type. In other words: it is probable that the same kind of rotation as was found in the former sample, affected the olivine and enstatite crystals in the present sample, and rotated them from an initial orientation into their present orientation. In the previous sample, both the fabric and the major structural features such as the banding, made an assumption of the pre-deformational fabric possible. But in the present case no remnants of an initial fabric nor any macroscopic structural features indicate the existence of such a pre-existing fabric.

It has been demonstrated in chapter III that intersecting girdles can be explained as the result of a rotation in opposite sense of a single initial girdle, over supplementary angles. In such a case the projection of the rotation axis in the diagrams was found to be the intersection of the bisectrix of the acute angle of the intersecting girdles with the plane S, which is perpendicular to the intersection point of the incomplete girdles. If this is a rule it enables us to construct the projections of the rotation axes of olivine and enstatite in the present sample. (See figure 22.)

From the foregoing chapter we know that the main difference between the transposition of olivine and enstatite is the fact that the rotation axis of the former is perpendicular to the X_{ol} rotation plane, while the rotation axis of the latter is perpendicular to the Z_{en} rotation plane. This implies that the main initial Z_{en} concentration is to be expected in the plane of which the rotation

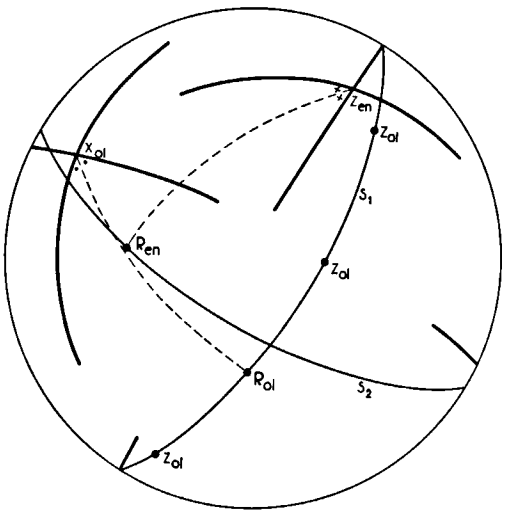

Figure 22. Construction of the rotation axes of olivine and enstatite in sample A. 2.

S_1 is marked by three Z_{ol} concentrations (D. 85), which form an almost complete girdle, the pole of which is the intersection of the two incomplete X_{ol} girdles. (D. 83). The rotation axis of olivine is the intersection of S_1 and the bisexctrix of the acute angle of the two incomplete X_{ol} girdles.

S_2 is marked by a complete Y_{en} girdle (D. 86), the pole of which is the intersection of the two incomplete Z_{en} girdles (D. 88). The rotation axis of enstatite is the intersection of S_2 and the bisectrix of the acute angle of the two incomplete Z_{en} girdles.

axis of enstatite is the pole. On the other hand we know that the olivine crystals rotated around the olivine rotation axis. This rotation resulted in two intersecting incomplete X_{ol} girdles and two point maxima of Z_{ol} in the poles of these girdles. As yet the angle of rotation of the olivine crystals is not known, but from the available data: the orientation of the rotation axis of olivine and the transposed orientation of the Z_{ol} axes, the path of the rotation of the Z_{ol} axes can be reconstructed. (See figure 23.) The conical section which results from this construction, intersects the plane in which the initial Z_{en} concentration has to be found in two points. As we know that the initial Z_{en} and Z_{ol} concentrations coincided, (see chapter II) we may now conclude that one of these points is the projection of the main initial $Z_{ol} = Z_{en}$ concentration.

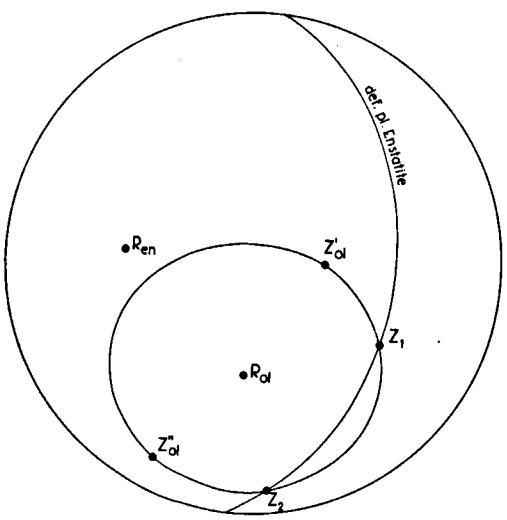

Figure 23. Reconstruction of the main pre-deformational $Z_{ol} = Z_{en}$ concentration in sample A. 2.

The conical section on which the observed Z_{ol} concentrations Z'_{ol} and Z''_{ol} lie, and of which R_{ol} is the axis, is the common place of all the possible pre-deformational Z_{ol} concentrations.

The common place of all the possible pre-deformational Z_{en} concentrations is the great circle the pole of which is the rotation axis of enstatite: R_{en}.

As the pre-deformational Z_{ol} and Z_{en} concentrations coincided, the intersections: Z_1 and Z_2 of the conical section and the great circle are the possible pre-deformational $Z_{ol} = Z_{en}$ concentrations.

It has now to be decided which one of the two possible Z axes orientations is the real pre-existing Z orientation. From diagram 83 we know that the marginal X_{ol} girdle is the stronger of the two intersecting X_{ol} girdles. It has been argued before that the stronger girdle probably resulted from the rotation over the smaller of the supplementary angles. The rotated Z_{ol} concentration to match with the marginal X_{ol} girdle is the observed central Z_{ol} concentration of diagram 85. This concentration must therefore result from a rotation over the smaller rotation angle. This leads to the conclusion that in figure 23, Z_1 and not Z_2 is the main initial $Z_{ol} = Z_{en}$ concentration.

There are now enough data available to attempt a reconstruction of the pre-existing olivine and enstatite fabric. (See figure 24.) From chapter III we

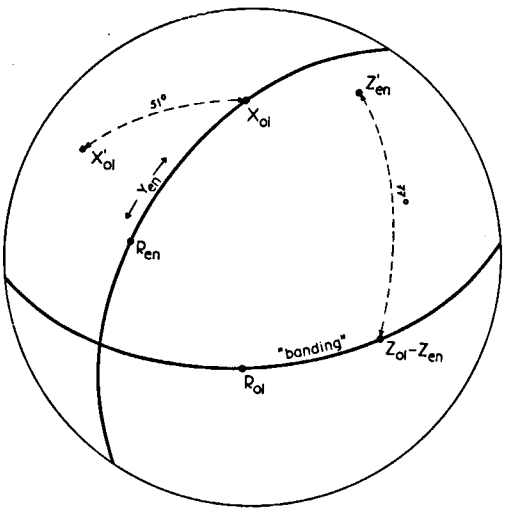

Figure 24. Reconstruction of the pre-deformational olivine and enstatite fabric in sample A. 2.

Z_{ol}—Z_{en} is the main pre-deformational concentration of the Z axes of both minerals, but these axes form also a girdle: "the banding" which is parallel to the rotation axis of olivine.

The great circle normal to Z_{ol}—Z_{en}, is the pre-deformational Y_{en} trend.

The main pre-deformational X_{ol} concentration is parallel to this great circle and normal to the "banding".

The rotation angles of olivine are 51° and 129°, and those of enstatite 77° and 103°.

know that the "banding" plane contains both the rotation axis of olivine and the initial $Z_{ol} = Z_{en}$ concentration. Thus the assumed "banding" can now be constructed. Furthermore it is known that the initial X_{ol}—Y_{en} trend is a girdle of which Z_{en}—Z_{ol} is the axis. This girdle is parallel to the rotation axis of enstatite. The main X_{ol} concentration is found 90° away from the intersection of the "banding" and the Y_{en}—X_{ol} girdle.

The rotation angles of olivine and enstatite can now be evaluated. For olivine this is done by measuring the angle between the initial X_{ol} concentration and the intersection of the two observed incomplete X_{ol} girdles. The rotation angles of olivine appear then to be 51° or 129°, depending on the sense in which the angle is measured. If the same is done for the Z_{en} axes in the plane perpendicular to the rotation axis of enstatite, angles of 77° and 103° respectively are found.

The practical interest of this so far purely theoretical reconstruction of the pre-existing fabric can now be tested. In figure 25 the transposition of olivine is visualized. The rotation over 51° or 129° brings the initial X_{ol} concentration to the intersection point of the two incomplete X_{ol} girdles. In order to rotate the initial incomplete X_{ol} girdle, its pole Z_{ol} is rotated. This rotation results in

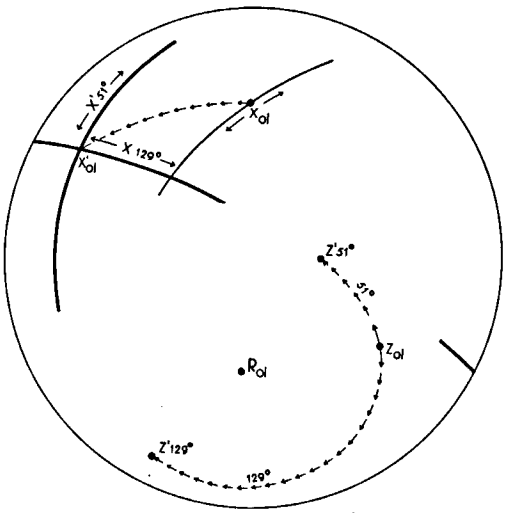

Figure 25. Transposition of olivine in sample A. 2.

The pre-deformational incomplete X_{ol} girdle is rotated around the rotation axis of olivine: R_{ol}. The rotation angles are 51° in the sinistral, and 129° in the dextral sense. Instead of the incomplete X_{ol} girdle its pole: Z_{ol} is rotated. The resulting $Z'_{51°}$ and $Z'_{129°}$ concentrations are the poles of two intersecting incomplete X'_{ol} girdles.

The results of the rotations have to be compared with the diagrams 83 and 85.

two maxima: Z'_{51} from a rotation over 51° in the sinistral sense, and Z'_{129} from a rotation over 129° in the dextral sense. These two maxima are the poles of the observed incomplete X_{ol} girdles. The fact that the result of the rotation agrees with the observed fabric (D. 83, D. 85) does, however, not prove the validity of the transposition theory, because this result was the assumption on which the theory has been based.

This is not the case for the enstatite transposition. (See figure 26.) A rotation of the initial Z_{en} concentration around the enstatite rotation axis, over 77° in the sinistral or 103° in the dextral sense brings the main initial Z_{en} concentration in the expected orientation: the intersection of the two incomplete Z_{en} girdles. The transposed Z_{en} orientation will, however, not be a point maximum, it will consist of two intersecting incomplete girdles, because the initial Z_{en} orientation showed a spreading in the "banding". These intersecting girdles

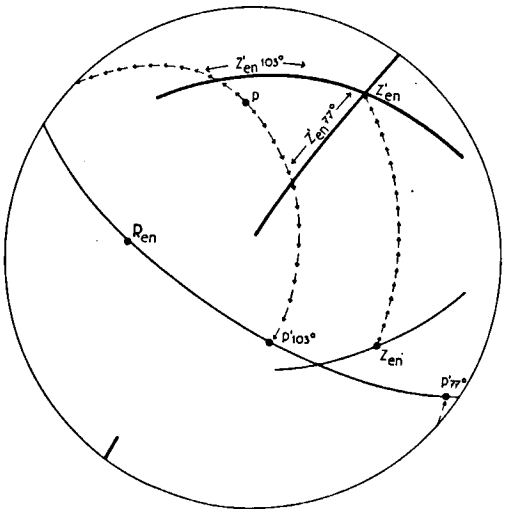

Figure 26. Transposition of enstatite in sample A. 2.

The pre-deformational incomplete Z_{en} girdle is rotated around the rotation axis of enstatite R_{en}, over 77° in the sinistral and 103° in the dextral sense. Instead of the incomplete Z_{en} girdle its pole: P is rotated. The resulting projections $P'_{77°}$ and $P'_{103°}$ are the poles of two intersecting incomplete Z'_{en} girdles. Z'_{en} is the pole of a complete Y'_{en} girdle which is parallel to R_{en}, $P'_{103°}$ and $P'_{77°}$.

The results of the rotations have to be compared with the diagrams 86 and 88.

can now be constructed by rotating the pole of the "banding" — the initial X_{ol} concentration — around the enstatite rotation axis. This rotation yields two new points, which are the poles of the intersecting Z_{en} girdles. If these constructed incomplete Z_{en} girdles are compared with the observed girdles of diagram 88, it is seen that they almost coincide. In contrast with the rotation of olivine, this good agreement between the observed and the theoretically predicted enstatite orientation constitutes strong evidence in proof of the validity of the deformation theory. For the angle between the two intersecting Z_{en} girdles depends on the orientation of the axes of these girdles. For a given rotation axis, this orientation is determined by the rotation angle and the initial orientation of the "banding". As both these data did not form part of the assumptions on which the deformation theory of this sample, has been based, the good agreement between the theoretically expected Z_{en} orientation and the observed Z_{en} fabric is strong evidence in favour of the theory.

So far nothing has been said to account for the third Z_{ol} concentration in S_1, in the NE. quadrant of diagram 85. However any realistic deformation theory has to explain this concentration. The assumption that the initial Z_{ol} orientation in the "banding" was restricted to a single direction is a simplification which probably does not correspond with reality. The sample from Dreiser Weiher, described in chapter II, shows a rather strong spreading of Z_{ol} within the "banding" plane. (D. 24.) The mechanism of rotation around a rotation axis in opposite sense yields two new directions for each initial direction, the orientation of which does not make an angle of 0° or 90° with the rotation axis. For the latter two orientations the rotation results in only one new direction, which consequently has a double strength. This fact can partly account for the observed Z_{ol} concentration in S_1 in the NE. quadrant of diagram 85, 90° away from the rotation axis of olivine. The corresponding X_{ol} orientation will then mainly be restricted to a short marginal girdle. However this explanation can probably not account for the strength (about 500 crystals) of the NE. concentration. In chapter III we have seen that the transposition of olivine and enstatite is

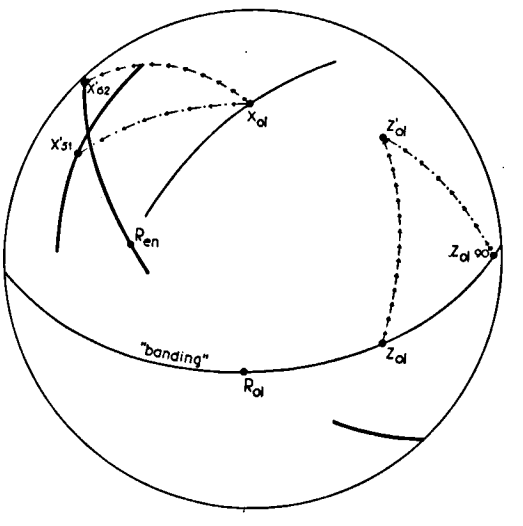

Figure 27. Interpretation of the Z_{ol} concentration in the NE. quadrant of diagram 85.

1. Part of the Z'_{ol} axes results from a rotation of the Z_{ol} axes with a pre-deformational orientation 90° away from the rotation axis of olivine. The corresponding X_{ol} transposition results in a short marginal girdle through X'_{51}.

2. The major part of the NE. Z'_{ol} axes results from a rotation of olivine around the rotation axis of enstatite: R_{en}. The rotation angle is 62°. The corresponding rotation of the incomplete X_{ol} girdle results in a new incomplete X'_{ol} girdle parallel to X'_{62} and R_{en}.

The two intersecting X'_{ol} girdles have to be compared with those in diagram 92.

probably not restricted to a rotation around their "proper" rotation axis. This observation can now be used to account for the NE Z_{o1} concentration. The great circle, perpendicular to the projection point of the enstatite rotation axis, goes through this Z_{o1} concentration. We can now assume that part of the olivine crystals have rotated around the enstatite rotation axis, so far as to bring the Z_{o1} axes parallel to S_1. Such a rotation of the Z_{o1} axes over an angle of 62°, has to be expressed in the orientation of the X_{o1} axes. In figure 27 the incomplete X_{o1} girdle (X'_{62}—R_{en}) which will result from such a rotation is constructed. The short marginal X_{o1} girdle resulting from the rotation around the olivine rotation axis is also constructed in this figure. If the NE. Z_{o1} concentration is the result of two different rotations as has been discussed above, the corresponding X_{o1} axes can be expected to form two intersecting girdles, as is demonstrated in figure 27. Diagram 92 clearly demonstrates that the X_{o1} axes which refer to the NE. Z_{o1} concentration are really concentrated in these two trends.

The foregoing discussion leaves little doubt that the deformation theory can account for the main properties as well as for the details of the observed fabric. According to the writer, the interpretation given above is the only one which can explain all the aspects of the fabric. This statement is based on an accurate study[7]) of other possible interpretations, which for instance can be based on a different orientation of the rotation axes, or on different rotation angles, but each of these interpretations failed in explaining at least one of the aspects of the fabric.

The theory that has been evolved to explain the deformation of the nodular inclusions from Auvergne, has been based on the assumption that the mechanism of the transposition of olivine is dominated by the orientation of the X_{o1} axis in relation to the possible slip planes in the rock. It has been demonstrated that this olivine rotation occurred in opposite sense. The resulting intersecting X_{o1} girdles are coupled with Z_{o1} concentrations in their poles. This rotation mechanism implies that the intersecting X_{o1} girdles do not have a different structural significance, both are an adaption of the fabric to the same set of probable slip planes. The rotated orientation of the Z_{o1} axes is entirely dominated by the initial Z_{o1} orientation and the rotation of the X_{o1} axes. Consequently there is no reason to assume that each of the Z_{o1} concentrations has a different structural significance. The NE. concentration of the Z_{o1} axes however, is at least partly caused by a rotation of the Z_{o1} axes along a great circle. The orientation of these Z_{o1} axes in S_1 and sub-normal to S_2 together with the concentration of the corresponding X_{o1} axes normal to S_1 and sub-parallel to S_2, favours the conclusion that this orientation too is an adaption to both S_1 and S_2. Summarizing it can be said that the deformation theory favours the conclusion that the axial distribution diagrams of each of the three X_{o1} groups as well as the three Z_{o1} maxima should show the same pattern of intersecting directions, corresponding with the intersection lines of the slip planes with the plane of observation. The conclusions reached in paragraph six of this chapter, where the axial distribution diagrams have been discussed are in good agreement with these expectations.

The directions observed in the distribution diagrams however, show a small departure from the expected directions. The fabric diagrams of olivine and enstatite do suggest a direction N. 30° E., the strike of the S_1 plane, and N. 60° W.

[7]) An all inclusive treatment of this subject should need the publication of at least a dozen other text-figures, which have been omitted for reasons of surveyability.

PLATE II

D. 83.: A. 2., 1512 X_{ol}, contours 1—2—3—4—5 %.
D. 84.: A. 2., 1512 Y_{ol}, contours 1—1.5—2—2.5 %.
D. 85.: A. 2., 1512 Z_{ol}, contours 1—1.5—2—2.5—3 %.

D. 86.: A. 2., 200 Y_{en}, lowest contour 1 %.
D. 87.: A. 2., 200 X_{en}, id.
D. 88.: A. 2., 200 Z_{en}, id.

D. 89.: A. 2., 677 Z_{ol} corresponding with marginal X_{ol} girdle.
D. 90.: A. 2., 554 Z_{ol} corresponding with diametrical X_{ol} girdle.
D. 91.: A. 2., 354 Z_{ol} corresponding with X_{ol} axes parallel to the intersection of the incomplete girdles.

D. 92.: A. 2., 504 X_{ol} corresponding with NE. Z_{ol} concentration.
D. 93.: A. 2., 520 X_{ol} corresponding with central Z_{ol} concentration.
D. 94.: A. 2., 315 X_{ol} corresponding with SW. Z_{ol} concentration.

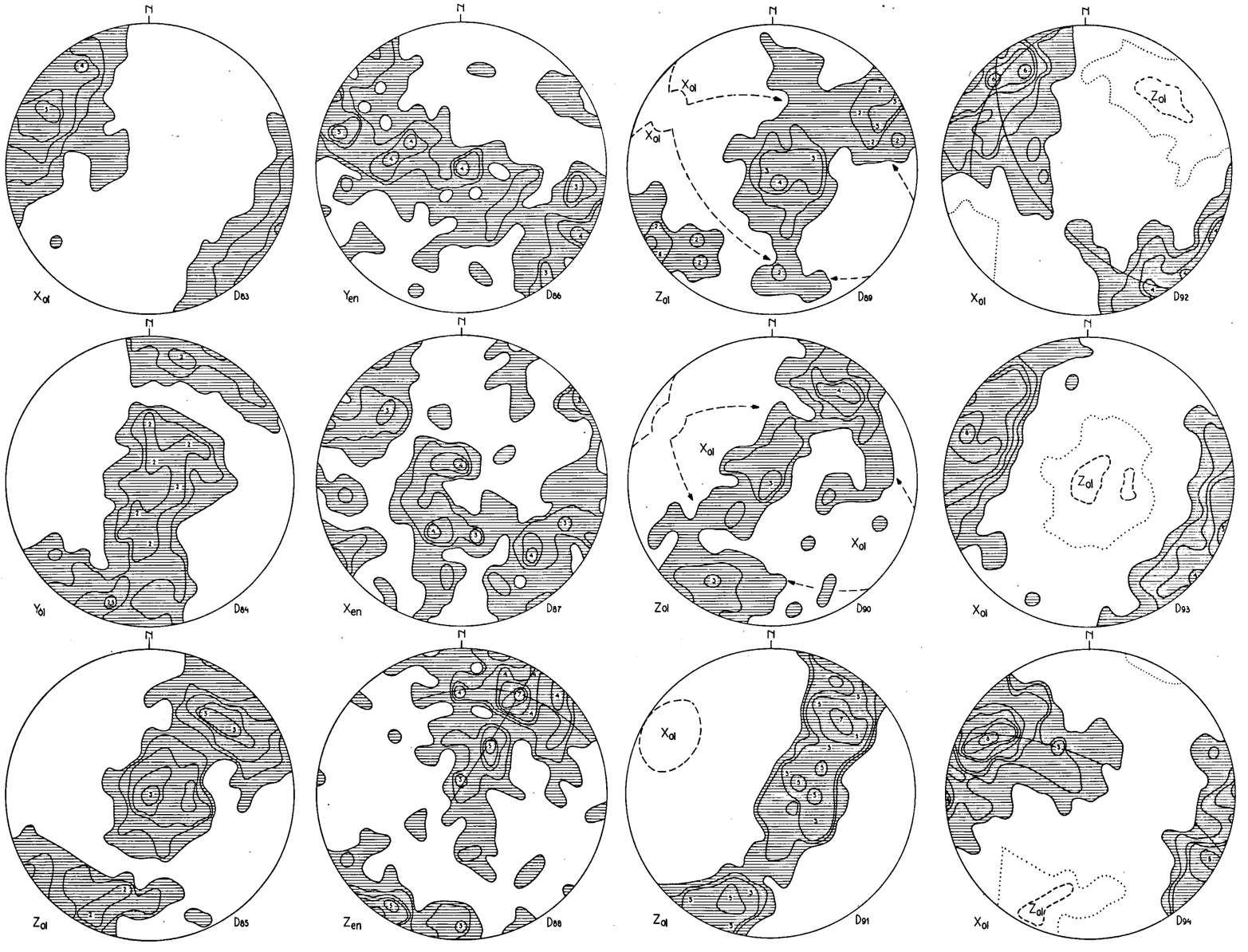

the strike of the S_2 plane. In the distribution diagrams, however, the observed directions are N. 45° E. and N. 45° W. This is probably due to the fact that the construction of the density diagrams has been based on a grid with fixed observation points. The use of an asymmetrical net is practically beyond realization if relative concentrations have to be represented. The observed pattern, however, is of the same type as the one in the front face of the sample in chapter III. Consequently there seems to be little doubt, that the observed directions in reality are parallel to the strike of the two S_2 planes.

In chapter III of this paper a deformation theory has been evolved which could be based on the simultaneous occurrence of an old and new fabric in the same sample. In the present chapter it has been demonstrated that the theory can also be applied to account for the fabric of a nodule which does not show any relics of an initial fabric. In spite of minor differences, as for instance the rotation angles of enstatite, the basic idea of the deformation of both samples is the same. An important advantage of the interpretation applied in this paper is the fact that the observed tectonic fabrics can be reduced to a kind of fabric that, both from personal observation (see chapter II) as well as from the literature is known to be a common fabric of ultrabasic rocks.

8. *The grain shape of olivine*

The great number of crystals of which the orientation has been measured, makes it possible to carry out a qualitative analysis of the grain shape of olivine. All crystals with one axis perpendicular to the plane of the thin sections are apt to give us information on the length ratio of both the other axes. The Z_{01} axis of 132 crystals deviates less than 15° from the perpendicular orientation. A deviation of less than 20° is found for the Y_{01} axis of 112 crystals. The length ratio of both the other axes of these crystals has been measured, and the results are listed in figure 28. Although the number of readings is probably too small to make the observed ratios absolutely reliable, it is clear that the olivine crystals tend to be equidimensional.

These results will now be compared with the rose figures of the olivine diagrams in the top and side face of the sample described in chapter III. (D. 39, D. 40, D. 44.) In these diagrams which represent the initial hardly rotated olivine fabric, the rose figures indicate that olivine is elongate in the Z direction. These observations suggest that the grain shape of olivine has been altered during the deformation in such a way as to make the formerly elongate crystals equidimensional.

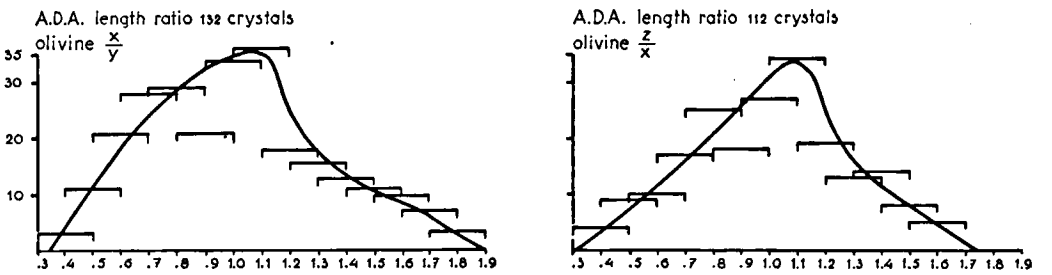

Figure 28.
The grain shape of olivine in sample A. 2.

CHAPTER V

FURTHER ASPECTS OF THE FABRIC AND PETROLOGY OF THE NODULAR INCLUSIONS IN THE LAVAS OF AUVERGNE

1. *The fabrics of other samples from the same locality*

In order to fathom the secrets of the fabrics of the two samples described in chapter III and IV, a rather elaborate investigation has been necessary. As long as one cannot apply techniques such as X-rays, which enable a more rapid approach of the problem, it will be practically impossible for an individual investigator to test the validity of the theory on samples of various other localities. In order to rule out the possibility that the observed fabric, described in the foregoing chapters is fortuitous, the fabrics of four other samples from the same locality have been investigated. As far as can be judged from diagrams of one randomly oriented section, the fabric of these nodules is of the same type as the one described so far in this paper. The diagrams of two of these samples are published here. The diagrams 95 and 96 refer to the X_{ol} and Z_{ol} orientations, the diagrams 97 and 98 represent the Y_{en} and Z_{en} axes of sample A. 3. The importance of these diagrams is found in the fact that the Y_{en} axes form a clear girdle which bisects the two intersecting trends formed by the projections of the X_{ol} axes. In the theory, as it has been developed in the foregoing chapters, this intersecting single Y_{en} girdle (S_2) plays an important role. However, sample A. 1 in chapter III has a rather weak Y_{en} girdle in S_2. Therefore it seemed important to publish a fabric diagram from the same type of rock, in which this Y_{en} girdle is fully developed. Another important feature of these diagrams is the fact that the Z_{en} axes show a stronger concentration (D. 98) than the Z_{ol} axes (D. 96). This stronger Z_{en} concentration is in accordance with the deformation theory, which claims that the transposition of enstatite is governed by the orientation of the Z_{en} axes in relation to the slip planes in the rock, in contrast with olivine where the orientation of the X_{ol} axes predominates.

The samples which have been treated so far, all contain over fifty percent olivine. The fabric of these samples is undoubtedly dominated by the reaction of the olivine crystals to the deformation. There are, however, strong indications that enstatite tends to react independently upon the deformation. This implies that the fabric of deformed ultrabasic inclusions in which olivine does not form the bulk of the composing minerals, will probably be different. The solution of this problem would call for an analogous investigation of enstatite-rich rocks. The starting point should have to be a sample of the Dreiser Weiher type, but mainly composed of enstatite. The fabric of such a rock could then be compared with the fabric of a more highly deformed rock rich in enstatite. Such an investigation would certainly be interesting, but a major practical problem is that pure enstatite rocks are rare, and that if they occur, they tend to be coarse grained, a feature which prevents petrofabric work on a sound statistical basis. The Auvergne collection at my disposal did not contain pure enstatite

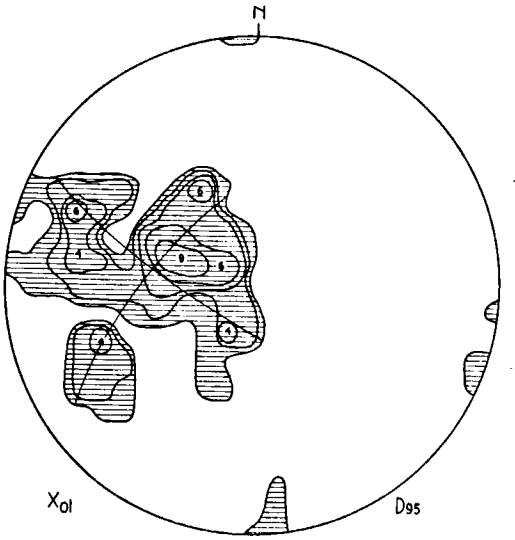

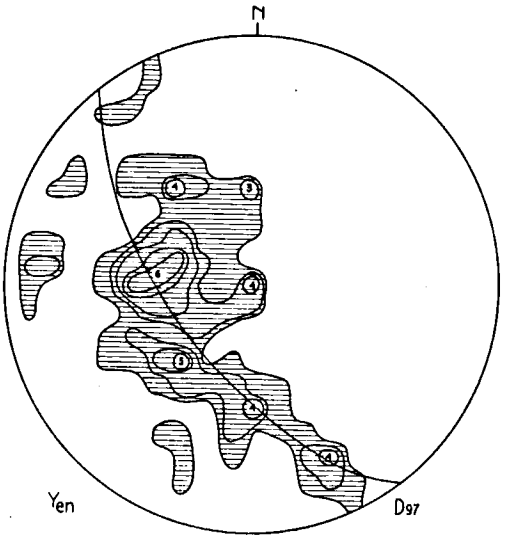

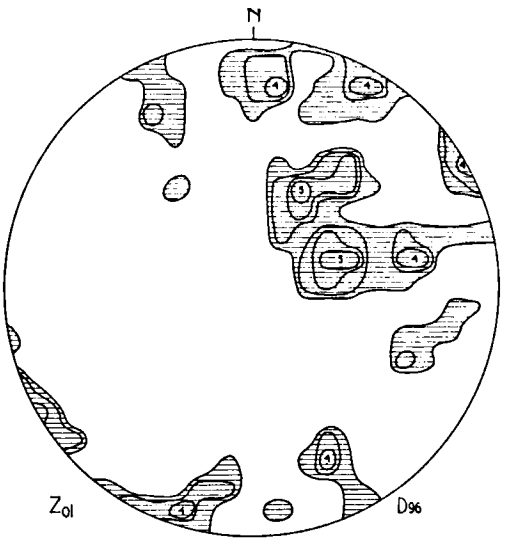

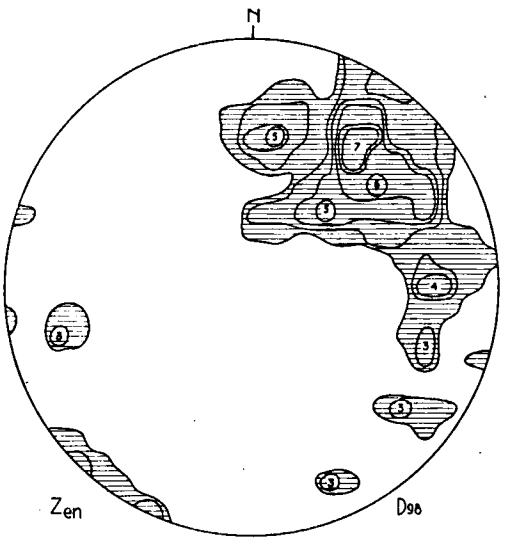

D. 95.: A. 3., 100 X_{ol}.
D. 96.: A. 3., 100 Z_{ol}.
D. 97.: A. 3., 100 Y_{en}.
D. 98.: A. 3., 100 Z_{en}.

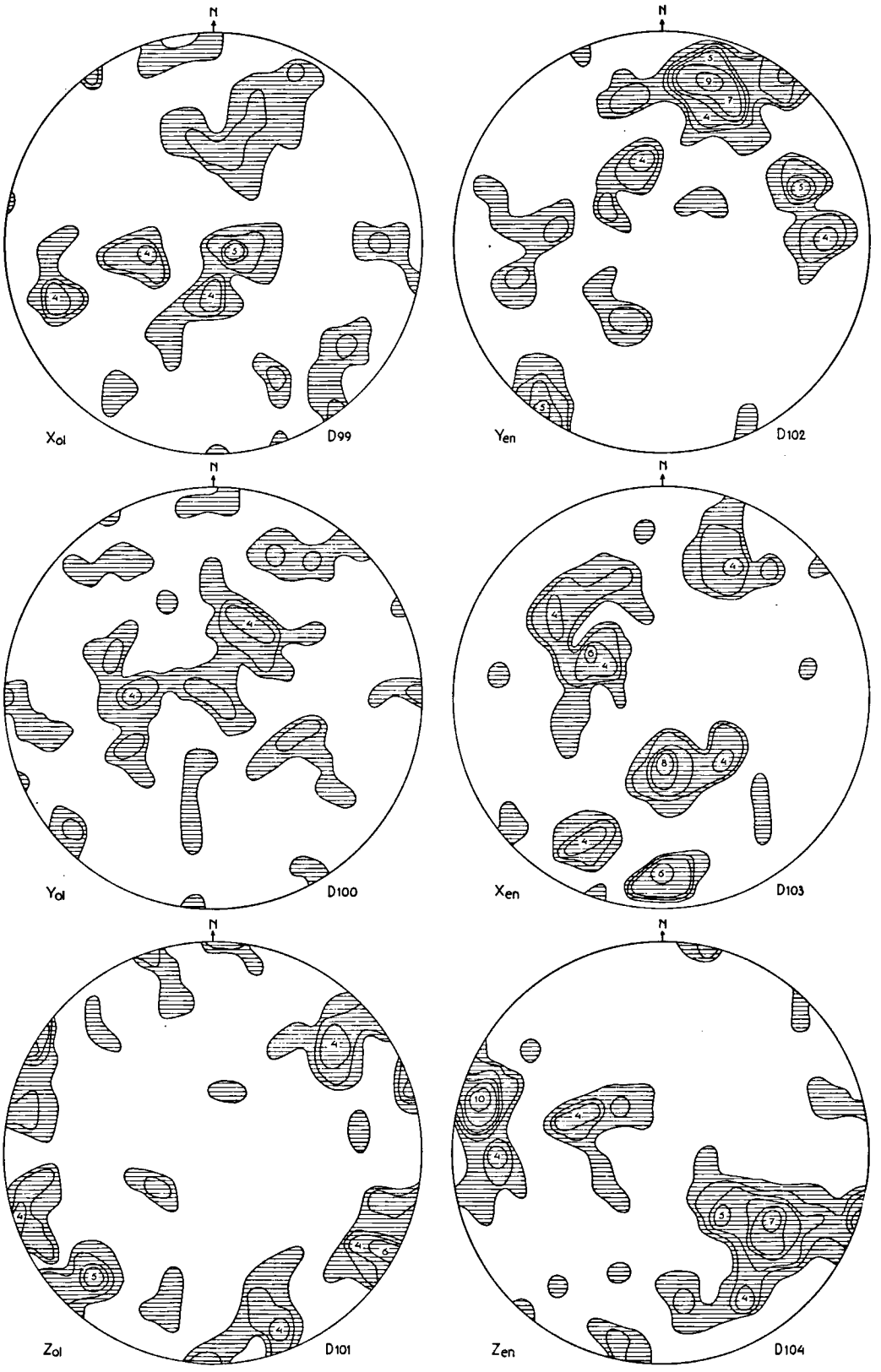

D. 99.: A. 4., 100 X_{ol}.
D. 100.: A. 4., 100 Y_{ol}.
D. 101.: A. 4., 100 Z_{ol}.
D. 102.: A. 4., 100 Y_{en}.
D. 103.: A. 4., 100 X_{en}.
D. 104.: A. 4., 100 Z_{en}.

rocks. One sample however showed an olivine percentage of only about forty-five percent. If the suggested hypothesis regarding the different type of componental movement of olivine and enstatite in response to deformation should be correct, we might expect that in this sample the fabric is no longer dominated by the olivine orientation. The diagrams 99 to 104 refer to the fabric of this sample. There is little doubt that the fabric is actually dominated by the enstatite orientation. The preferred orientation of olivine (D. 99—D. 101) is rather weak, and its relation with the enstatite fabric obscure. The enstatite crystals, especially their Y (D. 102) and Z (D. 104) axes show a very strong preferred orientation. For lack of any sign of macroscopically visible structures or of a pre-deformational fabric, it is impossible to infer the manner in which the rock has been deformed. However the importance of these diagrams lies in the fact that they prove the fabric to be dominated by the orientation of the enstatite crystals as predicted by our hypothesis.

A further proof of the fact that the preferred orientation of olivine increases with increasing olivine content can be found in the graph of figure 29. Here the degree of preferred orientation of the X_{ol} axes is plotted against the olivine content of the samples. No universally accepted method exists for the representation of the degree of preferred orientation in diagrams containing more than one maximum. The following method will be used here: Over each X_{ol} diagram a grid has been thrown, containing three hundred overlapping hexagonal cells, each covering one percent of the total surface [8]). The number of axes occurring in each of these cells is counted and marked. As the X_{ol} diagrams are based on hundred grains and each grain is counted in three different cells, the total of these figures attains three hundred. For each sample the number of cells which do not contain any axis is counted, the same is done for the cells with one or two axes, and with three or four axes. The number of cells with more than four axes forms a fourth group. For each sample the total cell-content of these groups attains three hundred. The stronger the preferred orientation, the higher the number of cells with more than four axes will be, at the same time the number of cells containing no axes will increase. The number of hexagons with only one or two axes will be correspondingly less as the preferred orientation increases. As the samples are rather coarse grained, the quantative mineralogical composition is difficult to evaluate exactly with a point counter. For each sample the olivine content consequently will not be a point but an interval on the abcissa of the graph.

Although this method of representation is certainly not very accurate, the trend of the graph, indicating increasing preferred orientation of the X_{ol} axes, with increasing olivine content is clear.

2. *Critical review of the deformation theory*

The petrofabric data provided in this paper leave no doubt that the nodular inclusions from this French locality are secondary tectonites of a complex nature. The macroscopically visible intersecting lineations, taken together with the inhomogeneity of the fabric, as well as the ubiquitous intersecting incomplete

[8]) The grid in question has been designed by F. Kalsbeek and will be published elswhere.

girdles of the X axes of olivine, put the tectonic origin of the fabric of these nodules beyond any doubt.

The interpretation of the observed fabric however, may not meet with general approval. In the preceding chapters the deformation of the nodular

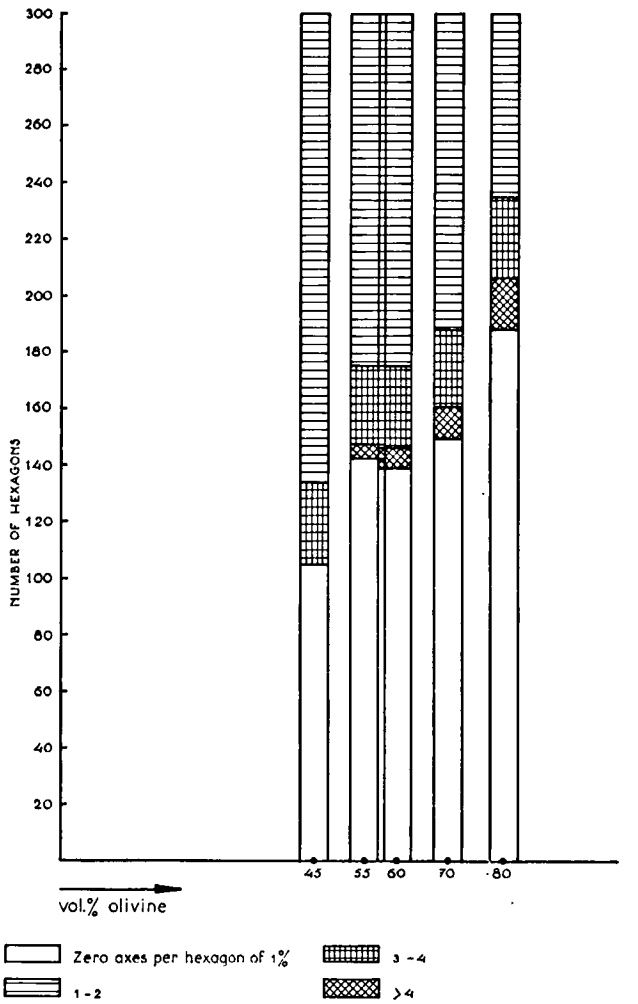

Figure 29.

The graph illustrates the relation between the strength of the preferred orientation of the X axes of olivine and the volume percentage of olivine in five nodular inclusions in the lavas of Auvergne.

inclusions has been described in terms of a mechanical rotation of the olivine and enstatite crystals. It has been argued in paragraph four of chapter III that this rotation is only a preliminary movement to bring the crystals into such an orientation in relation to the potential slip planes in the rock, as to favour the intra-crystalline movements such as translation gliding or twinning.

The author realizes that in explaining the re-orientation of the composing crystals of these nodules predominantly in terms of a mechanical rotation of the crystals, too little allowance has been made for recrystallization which probably attended the deformation. Although purely mechanical rotation of rigid grains is accepted by most authors as a means of deformation, it is still difficult to imagine how such a mechanism could act in an almost monomineralic rock composed of inequidimensional grains, without leaving any traces of crushing of the crystals. In this respect it is important to note that the crystals in these samples show many signs of strongly interlocking textures. That recrystallization played its part in the deformation is furthermore likely because the olivine crystals of the thoroughly deformed sample, described in chapter IV, are equidimensional, while the hardly rotated olivine crystals in the side and top face of the banded sample from the same locality, described in chapter III, are elongate in the Z direction. (D. 40, D. 44.) However in the opinion of the writer, the conclusive argument that rotation must have been the main mechanism in the re-orientation of the crystals is found in the fact that the top and side face of the banded sample, described in chapter III, show intermediate stages between the pre- and post-deformational orientation of the crystals, a feature not likely to be found in fabrics resulting from recrystallization. Furthermore the collective diagrams of chapter III (D. 77—D. 82), clearly show the trend of the rotation, especially for the Z axes of both olivine and enstatite. Once the view is accepted that rotation has been the main mechanism of re-orientation of the crystals the evaluation of the direction of the rotation axis and the sense and angle of rotation becomes a purely geometrical problem.

Intersecting girdles such as have been observed in quartz fabrics, have sometimes been explained as the result of two successive rotations, the first causing the main girdle in S_1, the second around an axis located in the pole of the S_2 plane giving rise to the intersecting girdle. If this interpretation is applied to biaxial minerals, the resulting orientation should consist of two intersecting X_{ol} girdles, with maxima of Z_{ol} in the poles of these girdles. However three Z_{ol} concentrations such as have been observed in the specimen described in chapter IV, cannot be explained from the point of view of that deformation theory. A further complication arises from the fact that two intersecting X_{ol} girdles should have a different structural significance according to the quoted theory, each one being connected with a specific slip plane. That this is not the case, has been revealed by the results of the axial distribution analysis of chapter IV. If the intersecting girdles cannot be the result of two successive rotations, then the only plausible explanation for their existence is to be found in a rotation of the crystals in opposite sense and over supplementary angles. The idea of such a supplementary rotation, as a movement preliminary to translation gliding or twinning, is not yet widely accepted. Rotation of crystals in opposite sense has only been proved for garnets which lack planes and directions suitable for translation and twinning. (Collette 1959, Peacy 1961.) It is important to stress the fact that the girdle resulting from the rotation over the larger angle is always the weaker, a feature that implies that most of the crystals rotated over the smaller angle. The diagrams of chapter III and IV further suggest that the weaker X_{ol} girdle is probably to some extent also the result of a rotation of olivine around the rotation axis of enstatite. The same probably holds, mutatis mutandis, for the weaker Z_{en} girdle.

This brings us to another uncommon aspect of the interpretation of the

diagrams: the assumption that the major part of the olivine and enstatite crystals did not rotate around the same axis. Apart from the purely geometrical considerations which lead to this conclusion, the main argument for this hypothesis is to be found in the fact that the degree of orientation of olivine depends on the olivine content of the rock. In the opinion of the writer this observation can only support the conclusion that the rotation of olivine is hampered by the apparently different reaction of the other constituents, in this case enstatite.

The axial distribution analysis described in chapter IV leaves little doubt that the olivine crystals are concentrated in the intersecting slip planes of the rock. This implies that inter-granular movement was not restricted to a mechanical rotation of the crystals, which only affects the orientation and leaves the location of the crystals in the sample unchanged, but was attended by differential movements of the crystals such as are effected by inter-granular slip. In the foregoing chapters little attention has been paid to this movement because it is not expressed in the fabric diagrams. The reason why the re-orientation mechanism of the crystals has in the foregoing been resolved into a mechanical rotation and an inter-granular slip movement, is that the former is expressed in the fabric diagrams and the latter in the crystal and axial distribution diagrams. In practice, however, both components act together and cause a rolling movement of the crystals, which brings them into both a position and an orientation favouring further deformation in the potential slip planes of the rock. This further deformation can best be described in terms of intragranular movements such as translation gliding.

3. *Tie-lines*

The practice of connecting in a Ca-Fe-Mg diagram the two points which represent the chemical composition of co-existing pyroxenes, has first been applied by Hess (1941) who noticed that the joints intersect the Ca-Mg limb of the triangle at a point close to $Ca_{75}\,Mg_{25}$. Ever since, various authors have dealt with the problem of the value of tie-lines and the conclusions which can be based on their intersection point with the limbs of the Ca-Fe-Mg triangle. At first sight the controversy between the adherents and opponents of the value of tie-lines seems fundamental, a closer inspection however reveals that their disagreement is only apparent.

A few authors among whom Wilson (1960) do believe that the intersection points of tie-lines with the limbs of the triangle might be different for co-existing pyroxenes of metamorphic as against magmatic origin. A paper by G. Brown (1961) leaves little doubt that, even if such a distinction between both groups could be made on theoretical grounds, the spreading of the intersection points within each group causes appreciable overlap. In other words it seems practically impossible to decide on the strength of the intersection point of one particular pair of co-existing pyroxenes whether they are of igneous or metamorphic origin. Under metamorphic pyroxenes in this context are understood the pyroxenes of the high pressure eclogite and the granulite facies.

A completely different approach to the problem has been made by Kretz (1961). His thermodynamical derivation leads to the conclusion that the distribution coëfficient $K_d = \frac{X_o}{1-X_o} \cdot \frac{1-X_c}{X_c}$ where $X_o = \frac{Mg}{Mg + Fe^{++}}$ in the orthopyroxene

and $X_c = \frac{Mg}{Mg + Fe^{++}}$ in the clinopyroxene depends primarly on the temperature and pressure of formation of pairs of pyroxenes of the same bulk chemical composition. This should have the result that igneous and metamorphic co-existing pyroxenes may have a different K_d value. This assumption seems to be confirmed in practice. A calculation of several chemically analyzed pairs of co-existing pyroxenes, proved that the K_d value of igneous pyroxenes is about 0.73, and for metamorphic pyroxenes about 0.54.

Bartholomé (1961) has treated the same subject. According to this author the chemical equilibrium between calcium-rich and calcium-poor pyroxenes may be written af follows: $CaFeSi_2O_6 + MgSiO_3 \rightleftharpoons CaMgSi_2O_6 + FeSiO_3$ the condition of equilibrium if the minerals are ideal solid solutions being $\left[\frac{Mg}{Fe^{++}}\right]_c \cdot \left[\frac{Fe^{++}}{Mg}\right]_o = K_t$. This K_t value proved to be 1.4 for igneous and 1.8 for the metamorphic pyroxenes. The conclusion of Bartholomé is essentially the same as the one reached by Kretz, for the formula for the calculation of K_d can be written as follows:

$$K_d = \left[\frac{\frac{Mg}{Mg + Fe^{++}}}{\frac{Mg + Fe^{++} - Mg}{Mg + Fe^{++}}}\right]_o \cdot \left[\frac{\frac{Mg + Fe^{++} - Mg}{Mg + Fe^{++}}}{\frac{Mg}{Mg + Fe^{++}}}\right]_c = \left[\frac{Mg}{Fe^{++}}\right]_o \cdot \left[\frac{Fe^{++}}{Mg}\right]_c$$

$$1/K_d = \left[\frac{Fe^{++}}{Mg}\right]_o \cdot \left[\frac{Mg}{Fe^{++}}\right]_c \quad = 1/0.73 = 1.4 \text{ for igneous pyroxenes.}$$
$$= 1/0.54 = 1.8 \text{ for metamorphic pyroxenes.}$$

The conclusions of Bartholomé and Kretz therefore seem to agree.

As has already been pointed out by Bartholomé the K_t values represent tie-lines in a Ca-Mg-Fe diagram. For each composition of the orthopyroxenes, the

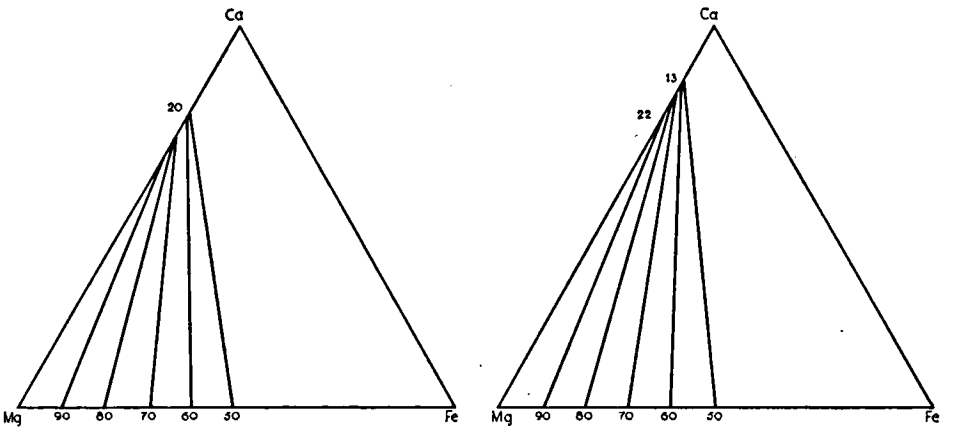

Figure 30.

30a: Tie-lines for co-existing pyroxenes of metamorphic origin, based on the assumption $K_t = 1.8$. After Bartholomé.

30b: Tie-lines for co-existing pyroxenes of igneous origin, based on the assumption $K_t = 1.4$. After Bartholomé.

corresponding Mg/Fe^{++} ratio of the clinopyroxenes can be calculated, for igneous rocks on the basis of $K_t = 1.4$ and for metamorphic rocks on the basis of a K_t value of 1.8. This results in tie-lines as they are represented in figure 30. Only the tie-lines of pyroxenes with a Mg/Fe^{++} ratio higher than one are represented. It is seen that for these pyroxenes the areas of intersection with the Ca-Mg limb differ only slightly. In practice the differences will be too slight to enable conclusions on the origin of co-existing pyroxenes to be drawn from intersection points only. Summarizing it can be said that a distinction between pyroxenes of metamorphic and magmatic origin can better be based on the calculation of the Mg/Fe^{++} distribution than on the intersection point of their projected tie-lines with the limbs of the Ca-Mg-Fe triangle.

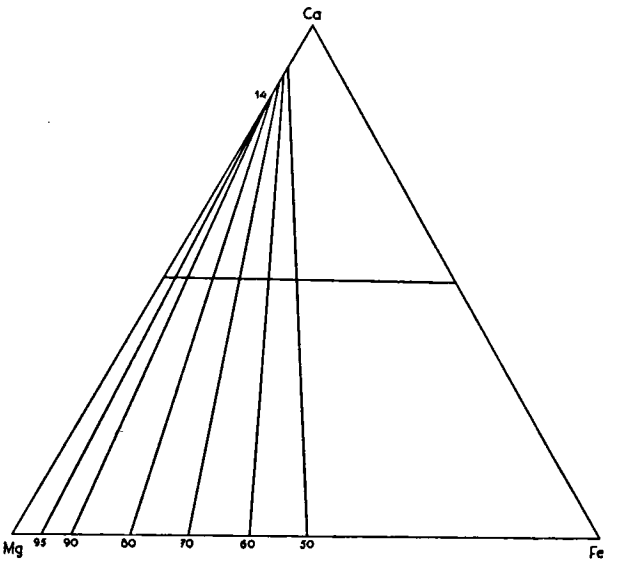

Figure 31.
Tie-lines of co-existing pyroxenes from ultrabasic nodular inclusions in lavas, based on the assumption $K_t = 1.2$.

This introduction to the theory of tie-lines of co-existing pyroxenes has been necessary to demonstrate the striking difference between the tie-lines of the above mentioned pyroxenes and those of pyroxenes from nodular inclusions in lavas. Ross, Foster, and Myers have published eight analyses of co-existing pyroxenes from such nodular inclusions. The K_t values obtained from these co-existing pyroxenes are the following: S. 1: 1.4 S. 2: 1.3 S. 3: 1.2 S. 4: 1.2 S. 5: 1.1 S. 7: 1.3 S. 8: 0.96 S. 9: 0.96. The average of these K_t values is 1.2. Most of these values show a significant departure from the values of magmatic and metamorphic pyroxenes. As the K_t value decreases with increasing temperature and pressure, the lower K_t value of most of the co-existing pyroxenes points to a higher temperature, or pressure, or both than those required for the co-stability of magmatic pyroxenes of the same bulk chemical composition. The tie-lines to be expected from a K_t value of 1.2 can be constructed. This is done in figure 31. It is seen that all the intersection points lie above the point

$Ca_{86}\,Mg_{14}$, i.e. above the intersection point of the tie-lines of magmatic pyroxenes. As we know that the K_t value of 1.2 is an average, we might expect that the difference between the intersection points of the tie-lines of magmatic pyroxenes and those of the nodular inclusions should be too slight to make the projection of these lines a useful operation, but this expectation is contradicted by the facts.

G. Brown (1961) has projected the tie-lines of the co-existing pyroxenes analyzed by Ross, Foster and Myers. The fact that the projection points of the chemical compositions, used by Brown are not based on the Mg/Fe^{++} ratio only, as is the case for the tie-lines based on the K_t values, but also on the other composing ions, notably Fe^{+++}, makes the projection points of the monoclinic pyroxenes shift to the right, and consequently also the intersection points. All the intersection points were found to lie on the Wo.-Fs. limb of the Wo.-En.-Fs. triangle. (N.B. The only exception mentioned by Brown, analysis 13 of the paper of Ross, is actually a peridotite of alpine type and not a nodular inclusion from a lava.) Thus it is seen that the tie-lines of co-existing pyroxenes from nodular inclusions in lavas differ strongly from those of magmatic assemblages. In contrast with the magmatic and metamorphic pairs of pyroxenes, the distinction of which could not be based on the intersection points of their tie-lines, the high temperature and pressure assemblages of the nodular inclusions can be readily distinguished from the magmatic assemblages, on the base of the intersection points of the tie-lines of the former on the Wo.-Fs. limb of the Wo.-En.-Fs. triangle.

No chemical analyses of the composing minerals of the rocks, described so far in this paper are available. The optical determination of the clino-pyroxene has been based on the diagrams of Hess (see chapter III), and are probably accurate enough to be used for the projection of a tie-line. On the basis of a Wo.-En.-Fs distribution of 48-44-8 in the clino-pyroxene, and a Mg/Fe ratio in the orthopyroxene of 92-89/8-11, a tie-line can be projected which intersects the Wo.-Fs. limb of the Wo.-En.-Fs triangle in between $Wo_{95}\,Fs_5$ and $Wo_{92}\,Fs_8$. This result is in good agreement with the data given by G. Brown (1961).

The Mg/Fe distribution in co-existing olivine and orthopyroxene has been used by Bartholomé (1960) as a means of estimating the crystallization temperature of these minerals. According to this author the equilibrium condition for the reaction:

$$(Mg_2SiO_4)_{Fo} + 2(FeSiO_3)_{Of} \rightleftharpoons (Fe_2SiO_4)_{Fa} + 2(MgSiO_3)_{En}$$

can be written $\left[\frac{Fa.}{Fo.}\right] \cdot \left[\frac{En.}{Of.}\right]^2 = K(T)$.

The application of the concentration constant of Guldberg and Waage on the equilibrium of these crystals is, however, contestable for the derivation holds only in the case of an equilibrium between molecules and it is therefore improbable that it may be applied to these crystals. Furthermore the construction of the curve which represents the change of K(T) with temperature has been based by Bartholomé on the assumption and the K(T) values observed in the nodular inclusions in lavas represent temperatures well above those of magmatic assemblages i.e. temperatures of the earth's mantle. This makes that apart from the theoretical objections mentioned above, the application of the K(T) value is useless as evidence for the high temperature of crystallization of the nodular inclusions in lavas.

4. *General conclusions*

The various attempts which have been made in the past to prove the tectonic nature of the nodular inclusions in lavas, have never resulted in an irrefutable conclusion. The present study however, leaves no doubt that the ultrabasic nodular inclusions in the lavas of Auvergne are tectonites of a complex nature. It is important to stress the fact that this conclusion is independent of the deformation theory evolved in the preceding pages. The inhomogeneity of the fabric taken together with the intersecting lineations, as well as the intersecting X_{ol} and Z_{en} girdles are decisive arguments to conclude that the studied samples are secondary tectonites.

The interpretation of the observed fabric has the important advantage to connect the fabric of these nodules with that, commonly observed in peridotites. In other words, it is probable that the fabric of the nodular inclusions in the lavas of Auvergne is the result of a deformation, and that the pre-deformational fabric was of the same type as the one observed in the nodular inclusions in the lavas of the Eifel and many other occurrences. The conclusions reached in chapter III and IV of this paper further demonstrate that the deformation of two different nodules can be interpreted as the result of analogous processes. This is a strong argument in favour of the opinion that both these specimens once formed part of one and the same secondary tectonite. The details of the deformation theory are only of interest for our insight into the process of rock deformation, they will not affect the conclusions regarding the origin of the nodular inclusions, except that the good agreement between the theoretically expected, and the observed crystal orientations favours the conclusion that the deformative stresses must have been uniform and constant for quite some time.

It has been argued in the preceding paragraph that the chemical composition of the composing minerals favours the conclusion that the rocks in question have crystallized at temperatures which exceed those of magmatic crystal assemblages. This observation inevitably leads to the conclusion that the rocks in question are also products of high pressure, for it is known that the melting temperature of anydrous basic rocks increases with increasing pressure.

Geophysical studies of the Hawaiian volcanoes (Eaton and Murata 1960) have resulted in the conclusion that the mantle of the earth is the probable source of basaltic lavas. Although the primary cause that starts the differential melting process is not known, it is clear that it must either be sought in a local elevation of the temperature or in a decrease of the prevailing pressure. The latter hypothesis is probably the more attractive in the first place because it is known that volcanoes are commonly linked with regions of instability of the earth's crust, in the second place because such a hypothesis could perhaps account for the as yet unsolved problem of the origin of the ascensive force of the lavas.

The problem whether the lavas accumulate in a primary, deep seated chamber is a highly theoretical one. Gorshkov (1957) has observed a shadow of transverse S waves which he attributed to a liquid-filled magma chamber at a depth of 50 to 60 kilometres. Evidence collected both from the Hawaiian volcanoes and from the Vesuvius, however, suggests that the actual eruption takes place from a "shallow" magma chamber at depth of about 5 kilometres.

The current views regarding the origin of the ultrabasic nodulelike inclusions have been reviewed in the first chapter of this paper. They have been said to split up into two theories, the endogenous which regard the nodules as

genetically related with the basalts in which they occur, and the exogenous theories which regard them as pieces of the earth's peridotite mantle, brought to the surface by the eruptive action of the lavas in which they occur. If the nodular inclusions are regarded as endogenous products of the lavas, their origin has to be sought in the shallow magma chambers, where a crystallization of magnesium-rich minerals is likely to occur.

The theory of the endogenous origin of the nodulelike inclusions has found its most powerful adherent in Frechen (1948a). His arguments can be summarized as follows: The crystallization sequence of the composing minerals and their alteration products is in accordance with the supposed path of magmatic differentation. The form of the nodules as well as their layered aspect, which often goes together with a changing grain size, is thought to be the result of crystal settling around a nucleus. The dimensional orientation of the composing crystals is the result of flow of the crystals in the magma.

The conclusions of the present paper can be summarized as follows:

1. The nodular inclusions of the basalts of Auvergne are secondary tectonites, the pre-deformational fabric of which was of the same type as the one commonly observed in the inclusions found in the basalts of the Eifel.

2. The two studied nodules are likely to be fragments of one secondary tectonite rather than accumulation products around two different nuclei.

3. The chemical composition of the composing minerals points to a very high crystallization temperature and consequently also to a high pressure.

Each of these conclusions by itself is difficult to reconcile with the theory of an endogenous origin of these rocks, their combination practically excludes the nodules from being endogenous products of the basalts in which they are found, for the strong deformation which must have acted in order to form the observed slip planes is not likely to occur in crystal accumulations which are still in contact with the liquid phase from which they precipitated. Neither the high temperatures and certainly not the high pressure can be expected in shallow magma chambers.

On the other hand the conclusions reached in the present paper can easily be incorporated in an exogenous theory which postulates that the nodules are fragments of the peridotite layer of the earth. It has already been mentioned that this theory has found a sound basis in the chemical work of Ross, Foster and Myers, and is further supported, among others by the petrographical work of Wilshire and Binns (1961) on the ultrabasic inclusions in the lavas of New South-Wales. A tectonic nature, resulting from a slowly acting and uniform deformation process, of fragments of the mantle is in accordance with current concepts such as convection currents, which tend to shift to the deeper parts of the earth the cause of the orogenic processes affecting the crust. Apart from these general considerations, however, shear is likely to occur at those places in the mantle where basalts are formed through differential melting of the peridotite layer. The observation that two fragments show an analogous, though not identical, deformation pattern is in good agreement with the supposed derivation of these nodules from the mantle. The assumed high temperature and pressure of formation of the rocks in question fits also in the exogenous theory, for a temperature of 1300° C is about the temperature at which according to Verhoogen, basaltic rocks will become completely molten at pressures prevailing at a depth of about forty kilometres.

Although ultrabasic nodular inclusions are not restricted to alkali-olivine basalts, they are much less frequent in tholeiitic basalts. This observation which has been verified by many authors has been used as an argument for the endogenous nature of the inclusions, for some investigators believe that alkali-olivine basalts originate from a tholeiitic parent magma through the fractional crystallization of pyroxene. (Murata 1960.) As forsterite is a normal early crystallization product of either basaltic magma it may be expected that, if alkali-olivine basalts develop from tholeiitic magmas, the former may contain inclusions consisting of accumulated olivine and pyroxene crystals. However such an interpretation is open to serious doubts, for the affinity between the two magma types is highly hypothetical.

Recent experiments on enstatite have demonstrated that the incongruent melting of this mineral, which takes place under pressures of one atmosphere, disappears certainly under 15 Kb. and probably already under 6 Kb. pressure. (Boyd, England 1961.) Previously Kushiro (1960) had already advanced the hypothesis that the mantle cannot be the source of tholeiitic magma in continental regions, if the incongruent melting of enstatite is restricted to a pressure interval below 10 Kb. The fundamental idea of this theory is that the incongruent melting of enstatite is the only possible manner in which a liquid oversaturated in silica can originate from a peridotite. As the earth's mantle is supposed to consist mainly of peridotite, and as the upper limit of this peridotite shell below the continents is thought to coincide with or to be lower than the 10 Kb. isobar, the earth's mantle cannot be the source of the continental tholeiitic magma. Recent geophysical evidence leaves little doubt that between the Conred and the Moho discontinuity a layer of rocks with a density comparable to that of basalts exists. Fusion of this layer could then provide the tholeiitic magma in the continental regions. Although some unsolved problems remain as for instance the origin of the heat required to attain 1200° C, the fusion temperature of basaltic rocks; as well as the occurrence of tholeiitic basalts outside the continents, the idea of a different origin rather than a genetic relationship of tholeiitic and alkali-olivine basalts seems attractive. If this idea proves to be right, then it becomes clear that the tholeiitic basalts on the continents will not contain exogenous ultrabasic inclusions, whereas alkali-olivine basalts which originate in the earth's peridotite shell may carry fragments of the earth's mantle to the surface.

CHAPTER VI

THE PYRENEAN LHERZOLITE

1. *Introduction*

The literature on the lherzolite type-locality in the French Pyrenees is one of the oldest in geological science. Already at the end of the eighteenth century attention has been paid to these rocks. However long standing, the problem of its genesis has never been solved conclusively. The lherzolites occur, sometimes together with gabbroic rocks, in a large number of mostly lenticular bodies along the north Pyrenean fault zone. The locality which gave its name to the lherzolite is the Etang de Lhers between Vicdessos, Aulus les Bains and Massat, in the Department Ariège.

The present analysis of the fabric of the Pyrenean lherzolite has been inserted in a study which mainly deals with the structural petrology of nodular inclusions in lavas in order to enlarge the information on the relation between the fabric of ultrabasic rocks and their tectonic environment. The fact that the Pyrenean lherzolite occurs in an area of which the tectonic structure is rather well known, was thought to facilitate the solving of the problem of the relation between the geometry of the fabric and the tectonic stress field. Although only a superficial relationship exists between the mineral orientation observed in the nodular inclusions and the fabric of the Pyrenean lherzolite, the results of this investigation are interesting enough to be incorporated as a quasi-independent subject in this paper.

During the summer of 1960, the writer had the opportunity to spend a few days in the French Pyrenees. This enabled him to take a dozen oriented samples from the lherzolite occurrence at the Etang de Lhers. The ultrabasic rocks there occur in a lenticular body, the long diameter of which (in the order of 1.5 kilometre) is parallel to the regional strike of the country rock while the short diameter, normal to it, does not exceed 700 metres. The country rock is a limestone of Aptian-Albian age folded into a pre-Cenomanian syncline, known as the syncline of Vicdessos, in the northern limb of which the ultrabasic body occurs. Further to the east several smaller ultrabasic bodies occur in the same syncline. South of this syncline runs the north Pyrenean fault which separates the axial zone of the Pyrenees, mainly consisting of Palaeozoic rocks, to the south from the Mesozoic rocks to the north. Although the north Pyrenean fault has been active both during the Hercynian and Alpine orogenies, its main activity is supposed to be Alpine. The movement along the fault in Alpine times has probably been restricted to a vertical displacement, together with a tilting to the north of the block north of the fault.

At present the ancient theory which considered the lherzolites as unaltered sediments does not find many supporters. However the controversy between the magmatic and metamorphic interpretations is still alive. The magmatic theory however, has further split up into two hypotheses: one extrusive and

the other intrusive It is beyond the scope of this paper to go deeply into the problem of the origin of the lherzolite. An extensive investigation in the field, should have to be combined with a thorough study of the literature in order to reach a conclusive solution of the problem. The knowledge that several investigators are working on this subject, incited the author to restrict his study to the fabric of a few samples from one locality, and to the publication and discussion of chemical analyses of the three main minerals of the lherzolite.

2. *Rock description*

As the picture of figure 32 shows clearly, the lherzolite has a layered aspect in the field. This structural feature has a strike of N. 40°—60° E. and a dip of about 40° SE. The monomineralic bands, composed of pyroxene or olivine, which vary in thickness from one centimetre to several decimetres, have this orientation. In some of the handspecimens, even if they are strongly altered into serpentine, faint lineations can be observed, which together constitute planes of the above mentioned orientation. The whole feature reminds one strongly of the banding observed in the nodular inclusions in lavas, and the banding described from many major peridotite bodies. The alteration of olivine and pyroxene into serpentine is in places remarkably weak. The thin sections of almost every handspecimen give the same picture of a thin network of very fine grained olivine and sometimes serpentine, in which coarse highly strained crystals of olivine, ortho- and clinopyroxene occur. The exact percentage by volume of olivine, enstatite and diopside could not be evaluated, however. All three minerals show signs of strong deformation, which in olivine crystals is expressed by numerous translation lamellae, while the pyroxenes have been strongly bent, resulting in undulose extinction which in one crystal provokes differences in extinction angle of more than twenty degrees. The overall impression is that the rock has been strongly deformed in a more or less plastic manner.

Figure 32.
The lherzolite at the Etang de Lhers in the French Pyrenees.

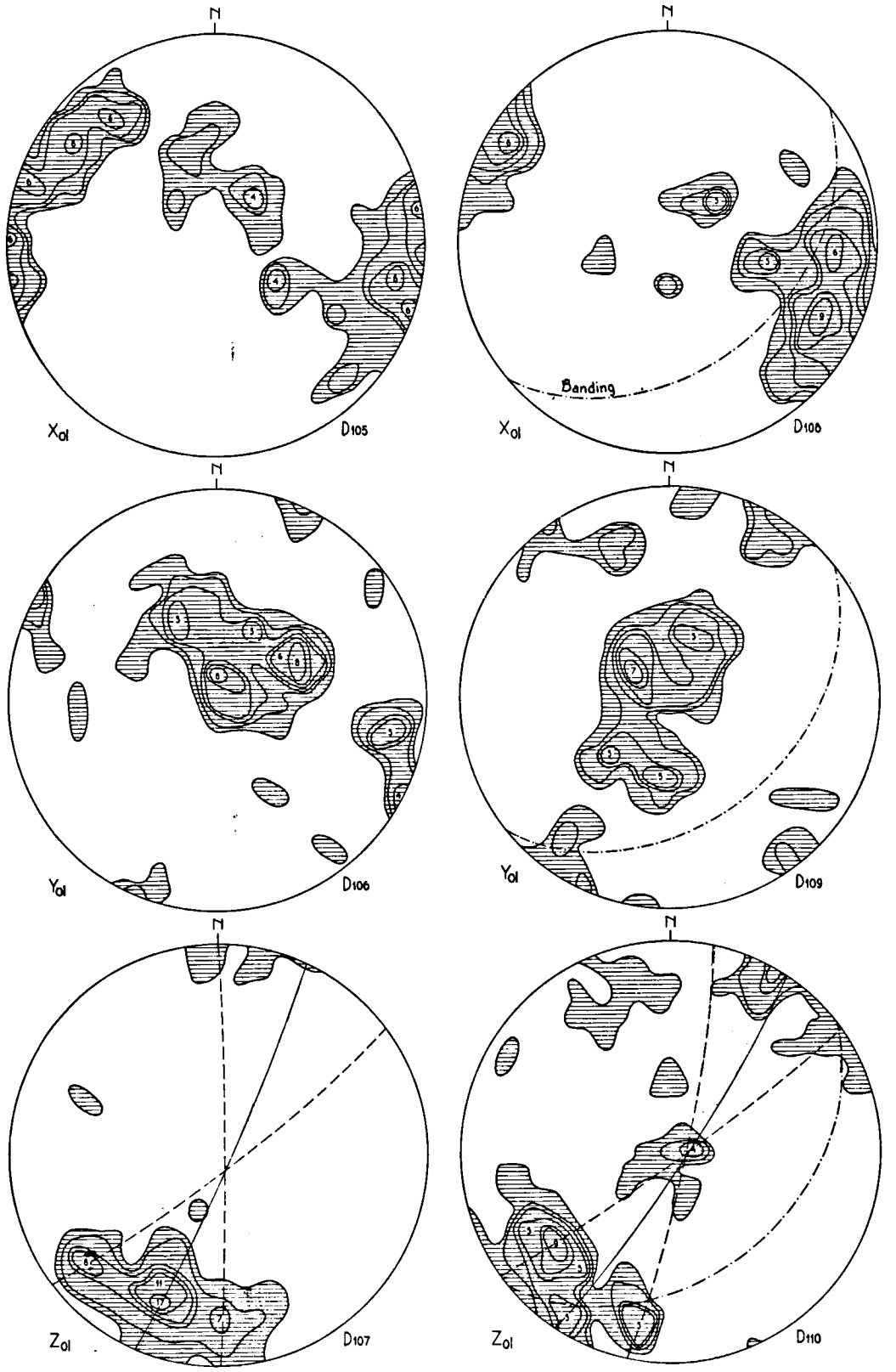

D. 105.: P. 1., 100 X_{o1}.
D. 106.: P. 1., 100 Y_{o1}.
D. 107.: P. 1., 100 Z_{o1}.

D. 108.: P. 2., 100 X_{o1}.
D. 109.: P. 2., 100 Y_{o1}.
D. 110.: P. 2., 100 Z_{o1}.

3. *The fabric diagrams*

From the samples which have been collected, three have been investigated as far as their fabric is concerned. The diagrams 105—116 refer to these samples. They represent projections on a horizontal plane which is oriented with respect to the North. The diagrams refer to the coarse grained olivine and enstatite crystals only, for the fine grained fraction was not amenable to measuring. All the olivine diagrams are dominated by a very strong Z_{ol} concentration reaching seventeen percent, a rather uncommon feature in olivine fabrics. The X_{ol} and Y_{ol} axes show a weaker preferred orientation, but the X_{ol} axes are mainly concentrated along the eastern and western margins of the diagrams, while most of the Y_{ol} axes occupy central positions in the diagrams. The perfect agreement of the olivine orientation in the three samples, which have been taken several hundred metres apart, is strong evidence for the observed fabric to be anisotropic within the body concerned.

The mineralogical composition and the coarse grained texture of the rocks prevented the measuring of sufficient enstatite crystals in two of the three samples, but the observed enstatite orientation in the third sample proved to be in accordance with the olivine fabric. The spreading of the Z_{en} axes (D. 116) is probably stronger than that of the Z_{ol} axes. Both the other axes X_{en} and Y_{en} are restricted to the border and centre of the diagrams as are the corresponding olivine axes.

4. *Interpretation*

From the local structural trend of the Pyrenees, expressed in the orientation of the fold axes and the strike of the north Pyrenean fault, a general direction N. 65° W.—S. 65° E. can be inferred, normal to which: (N. 25° E.—S. 25° W.) the main compressive force may be assumed to have acted. The diagrams 107, 110, 113 leave no doubt that the main concentrations of Z_{ol} are parallel to this assumed major axis of the stress deviator. The nearly vertical orientations of the axial planes of the mostly concentrically folded calcareous country rock, further indicate that two of the axes of the stress deviator were about horizontal and the third axis vertical. Consequently it may be concluded that the observed fabric is consistent with the geometry of the Alpine stress field.

A second important factor concerning the interpretation is the fact that the relation between the banding described above and the micro fabric is not of the type usually reported from ultrabasic rocks, i.e. a strong concentration of the X_{ol} axes normal to this plane and an orientation of Y_{ol} and Z_{ol} parallel to the banding plane. In the diagrams 108, 109, 110 of sample P. 2. in which the orientation of the banding plane could be evaluated, it is seen that only the Z_{ol} axes tend to have the expected orientation in the banding plane. Both the other axes X_{ol} and Y_{ol} diverge from their expected orientation, respectively normal to the banding plane and parallel to it. The intersection of the banding plane with the horizontal plane is expressed in some thin sections by a parallel — N. 60° E. — orientation of elongate picotite grains. The lower part of the photograph of figure 33 visualizes this feature. The upper part however, shows a parallel orientation of the opaque grains in a much steeper direction trending N. 25° E. parallel to the observed orientation of the Z_{ol} axes. This observation leads to the conclusion that the observed fabric is secondary i.e. that it resulted from a re-orientation of the composing minerals, which formerly tended to be arranged parallel to the banding plane.

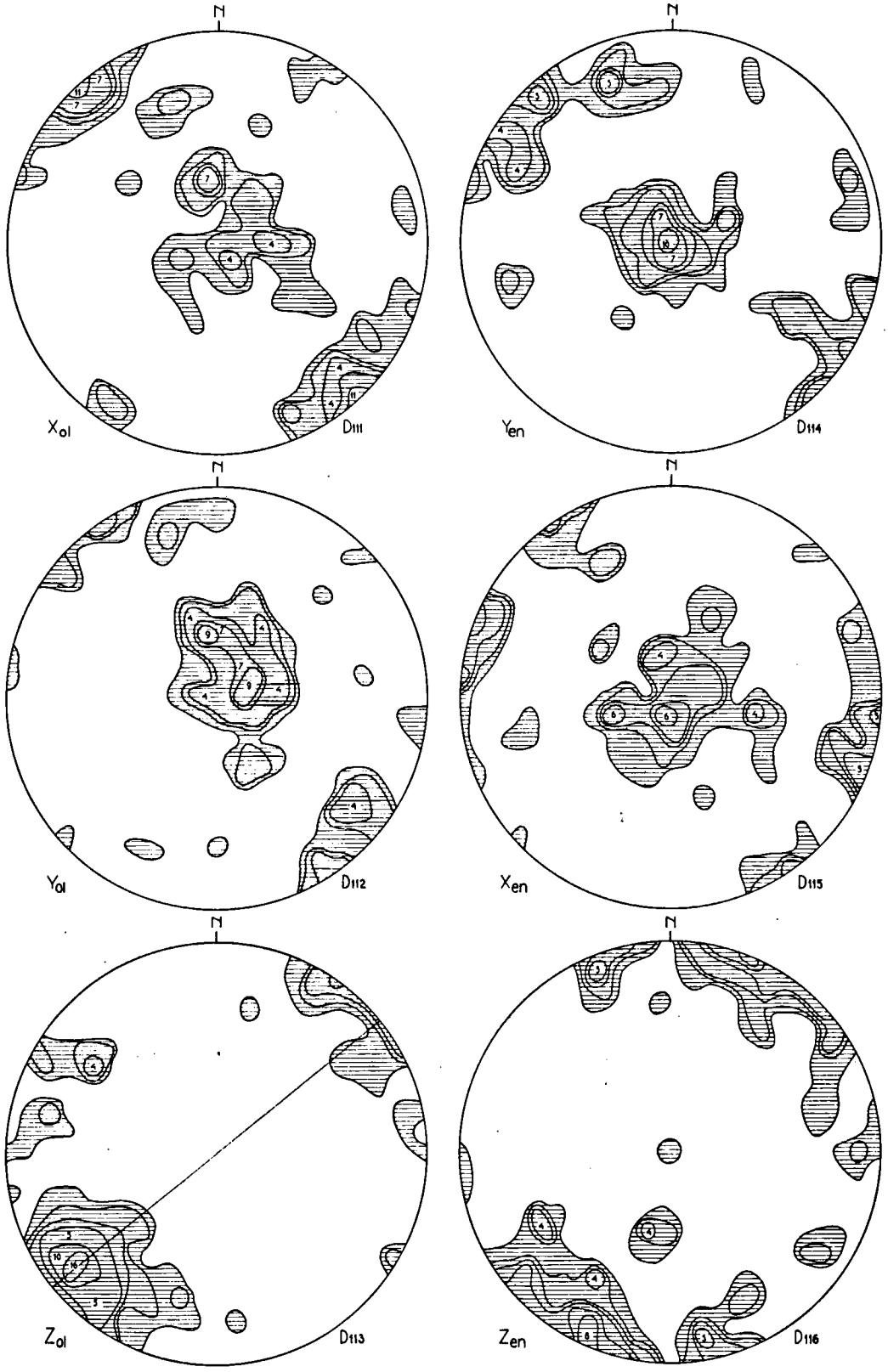

D. 111.: P. 3., 100 X_{ol}.
D. 112.: P. 3., 100 Y_{ol}.
D. 113.: P. 3., 100 Z_{ol}.
D. 114.: P. 3., 100 Y_{en}.
D. 115.: P. 3., 100 X_{en}.
D. 116.: P. 3., 100 Z_{en}.

From the foregoing it becomes clear that an interpretation of the observed fabric should be based on the secondary nature of the fabric and its consistency with the regional stress field. Now there are two processes which can result in a secondary fabric: 1st deformation and 2nd recrystallization of a primary fabric; but of course a combination of both factors is equally possible.

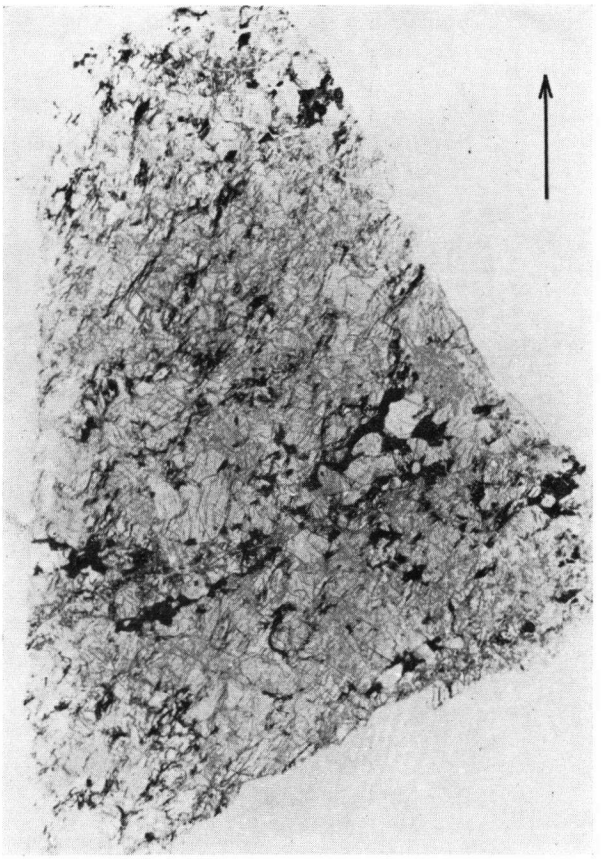

Figure 33.
Micro photograph of Pyrenean lherzolite. For explanation see text. (× 4)

The attraction of an interpretation of the observed fabric in terms of recrystallization lies in the fact that a Z_{ol} concentration parallel to the compressive stress axis is in accordance with the results of a thermodynamical calculation of the preferred orientation of olivine to be expected from a recrystallization under non-hydrostatic stress, in a solid environment, based on the theory of Kamp (1959). However in paragraph two of this chapter it has been mentioned that the Pyrenean lherzolite shows signs of strong plastic

deformation. This feature excludes the possibility that recrystallization was the only factor which caused the observed fabric, a subsequent deformation must also have affected the rocks.

The experiments of Bautsch (1960) who heated a pure forsterite rock, and observed that its recrystallization resulted in a lattice orientation of olivine in relation to the temperature gradient, have demonstrated that a recrysallization of olivine-rich rocks in the predominantly solid state can occur, but also that the temperature required is about 800° C. In order to decide whether the observed fabric can be the result of recrystallization, an estimate of the degree of metamorphism of the Cretaceous rocks in which the lherzolite occurs, is of the utmost importance.

The problem of the metamorphism of the Mesozoic rocks of the Pyrenees has been treated by Ravier (1959) in an extensive paper. It will be clear that the almost pure carbonate rocks, which form the major part of the country rock, can be of little interest for the determination of the degree of metamorphism. Half-way between the lherzolite and the north Pyrenean fault however, a small outcrop of a rock occurs, described by Ravier as a fine grained hornfels. The rock is composed of quartz, feldspar, biotite and probably pyroxene. The constituent equidimensional grains are strongly interlocking and show no signs of any preferred orientation. According to Ravier, who uses his own classification consisting of three degrees of metamorphism, this rock type belongs to the highest degree of metamorphism among those observed in the Mesozoic rocks of the Pyrenees. This third degree of metamorphism is characterized by the growth of green hornblende, diopside, garnet, biotite, sphene, large crystals of tourmaline, the plagioclase is recrystallized and some microcline occurs. It corresponds probably with the high-grade portion of the amphibolite facies.

The fact that this metamorphism resulted in the formation of completely unoriented rocks is also discussed by Ravier and he concludes that the metamorphism did not coincide with the pre-Cenomanian orogenetic phase. From the observation that the Cenomanian is non-metamorphic and that the pre-Cenomanian orogenetic phase must have acted at the end of Albian time, Ravier then concludes that the metamorphism must have preceded the deformation. Such a view, however, cannot account for the undeformed aspect of the hornfelses, which do not show any sign of deformation. It seems more likely that the crystallization outlasted the deformation (de Sitter and Zwart 1959). This conclusion is important because it implies that even if the degree of metamorphism is supposed to be high enough to enable a recrystallization of the ultrabasic rock, the recrystallization would probably not result in a strong lattice orientation of the minerals involved with the Z_{ol} axes parallel to the axis of compression, for the metamorphism was mainly thermal and static.

It has been argued in the foregoing chapter that the chemical composition of the composing minerals of ultrabasic rocks can give us information on the crystallization temperature of these rocks. Therefore chemical analyses have been made of the three principal constituents of the lherzolite. The results of the chemical analyses are listed in table IV.

TABLE IV

	Olivine	Enstatite	Diopside
SiO_2	40.42	54.48	51.94
Al_2O_3	0.77	2.39	3.17
Fe_2O_3	0.90	0.49	0.20
FeO	6.97	4.85	1.78
Cr_2O_3	—	—	1.30
MnO	0.14	0.09	0.08
MgO	48.86	34.52	17.55
CaO	0.19	0.95	20.65
Na_2O	tr	tr	1.10
K_2O	tr	tr	tr
H_2O	0.69	1.21	1.36
TiO_2	0.06	0.05	0.23
P_2O_5	0.02	0.05	0.10
	99.02	99.08	99.46

Analyst: Miss H. M. I. Bik.

For each mineral the cationic proportions are calculated, and from these the molecular composition of the mixed crystals can then be evaluated as follows:

TABEL V

Olivine

	Total.	Olivine.	Rest.
Si	100	96	4
Al	2	1	1
Fe_3	1	1	
Fe_2	14	14	
Mg	179	179	
	296	291	5

$$\text{Fo.}\frac{179}{1.94} - \text{Fa.}\frac{15}{1.94} = \text{Fo. } 92.3 - \text{Fa. } 7.7$$

Enstatite

	Total.	Enstatite.	Diopside.	Rest.
Si	96	92	4	
Al	4	4		
Al	1	1		
Fe_3	1	1		
Fe_2	7	7		
Mg	91	87	2	2
Ca	2		2	
	202	192	8	2

En. 91.9 — Fs. 8.1
Wo.-En.-Fs. = 2-90-8.

Diopside

	Total.	Diopside.	Jadeite.	Enstatite.	Rest.
Si	192	160	16	16	
Al	8	4	2↓	2	
Al	6		6 + 2		
Cr	4	4			
Fe_2	6	6			
Mg	97	72		18	7
Ca	82	82			
Na	8		8		
	403	328	32	36	7

Di.-Jad.-En. 83-8-9

Wo.-En.-Fs., $\frac{82+8}{2.03}$ — $\frac{97+5}{2.03}$ — $\frac{6+5}{2.03}$ = 44-50-6.

In chapter V the various calculation methods used for the estimation of the crystallization temperature of co-existing pyroxenes have been discussed. The K_t value of the co-existing pyroxenes in the Pyrenean lherzolite is $\frac{7}{91} \cdot \frac{97}{6} = 1.2$. As has been demonstrated in the foregoing chapter this value, which is the same as the average value of co-existing pyroxenes in volcanic nodules, points to a high crystallization temperature.

If the tie-line of the co-existing pyroxenes is projected on the basis of the Wo.-En.-Fs. distribution as mentioned before, an intersection point on the Wo.-Fs. limb of the composition triangle at $Wo._{97}\ Fs._3$ is found, a feature which also points to a high crystallization temperature.

The problem of the value of calculations based on the Mg/Fe distribution in olivine and enstatite has been discussed in the foregoing chapter. In spite of the negative conclusion reached there, the above mentioned similarity between the chemical composition of the composing minerals in the Pyrenean lherzolite and in the nodulelike inclusions in lavas finds further confirmation in the observed Mg/Fe distribution in the analyzed olivine and enstatite. Actually the high Mg content as well as the Mg/Fe ratio, which is about the same in both minerals, are similar to the values found in the nodular inclusions in basalts. This fact may be regarded as additional evidence for the conclusion that the Pyrenean lherzolite is not a product of recrystallization at moderate temperatures.

From the foregoing it may be concluded that the chemical composition of the principal constituents of the Pyrenean lherzolite does not favour the conclusion that these minerals have been (re)crystallized at the temperatures prevailing in the regional metamorphism of the Mesozoic of the Pyrenees. On the other hand the symmetry of the fabric is consistent with the geometry of the regional stress field as it can be inferred from the main structural features in the region concerned. Therefore it should be possible to base a structural interpretation of the microfabric on the local stress field. In this respect it is important to note that the observed strong Z_{ol} concentrations are parallel to the inferred tectonic axis of compression.

The deformation of olivine, resulting in the often observed translation lamellae, which are particularly abundant in the Pyrenean lherzolite, has been described

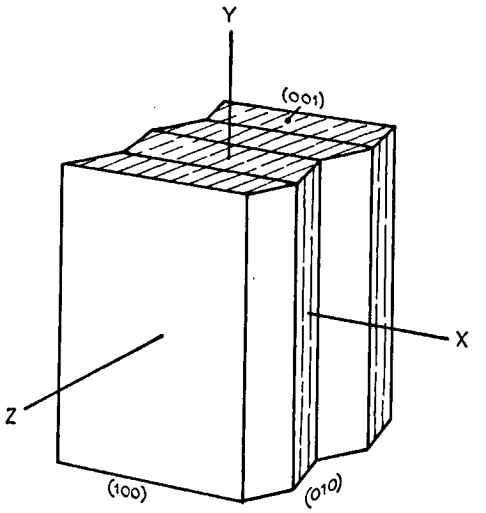

Figure 34.
The deformation of olivine. After Chudoba and Frechen.

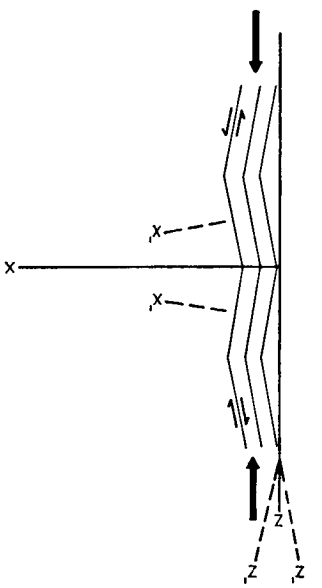

Figure 35.
The plane { 001 } of olivine. Deformation by pure shear.

by Chudoba and Frechen. (1950.) The interpretation which these authors give for the lamellae is a translation in the plane {010} with [100] as the most probable translation direction. The translation goes together with a kinking around the [001] axis, the symmetry plane of kinking is then {100}. Figure 34 visualizes the result of such a deformation. The correctness of this picture may be checked in thin sections where it can often be observed that the plane {010} is wrinkled.

This deformation pattern of olivine can also be interpreted as the result of pure shear on intersecting planes. (See figure 35.) If the olivine crystals are compressed in a direction sub-parallel to [100], shear can occur on {010}, the result may be a kinking around [001], while the boundaries between the translation lamellae will be parallel to [001]. The resultant distortion of the lattice will be expressed by a shift of [010] and [100], while [001] keeps its original orientation, a feature already mentioned by Frechen and Chudoba. These authors have also measured the angles of kinking in olivine in different ultrabasic rocks. Their study has resulted in the conclusion that in the group of ultrabasic rocks to which the Pyrenean lherzolite belongs, the angles do not exceed seven degrees. Above this limit rupture of the grains occurs [9]).

The problem now arises whether this deformation mechanism of olivine can be applied to the olivine fabric observed in the Pyrenean lherzolite. It has been mentioned before that the Z_{ol} axes are oriented parallel to the axis of compression. If the said deformation of olivine is the prime cause of the observed fabric, then the pairs of Z_{ol} axes, [100], should be parallel to the intersecting shear planes, the bisectrix of which is the axis of compression. As the maximum angle between the shear planes is only seven degrees, not only the mean but also the main concentration of Z_{ol} should indeed be practically parallel to the axis of compression.

The X_{ol} orientation to match with this Z_{ol} orientation can in principle be twofold: either horizontal i. e. normal to vertical slip planes, or vertical i. e. normal to horizontal slip planes. The elliptical form of the horizontal section through the ultrabasic body might indicate that the deformation is of the type known as flattening, but cannot inform us whether the deformation plane *ac* is horizontal or vertical. Neither can the regional almost horizontal direction of the fold axes be taken as a definite proof that the deformation plane has a vertical orientation in the ultrabasic body; for the difference in competency between the lherzolite and the calcareous country rock as well as the original form of the ultrabasic body may have affected the geometry of the local stress field and the related form ellipsoid.

If the X_{ol} diagrams are considered (D. 105, D. 108, D. 111) it becomes clear that the bulk of these axes are concentrated along the eastern and western margins of the diagrams, thus indicating that the major sets of slip planes tend to be vertical. The subsidiary central concentrations of X_{ol} may then indicate that secondary sets of slip planes have subhorizontal orientations. From these observations we may conclude that the maximum shortening of the body occurred in the N. 25° E.—S. 25° W. direction, while the dilatation mainly

[9]) In contrast the angles in olivine nodules from lavas reach eleven degrees. As it is known that the upper limit of plastic deformation rises with increasing temperature and confining pressure, this result agrees with the earlier reached conclusion that these nodules have been deformed at higher temperatures and pressures than those normally prevailing in the earth's crust.

acted along a sub-horizontal axis trending N. 65° W.—S. 65° E., and to a minor extent also in an almost vertical direction.

This interpretation does, however, not account for all aspects of the observed olivine fabric. The Z_{o1} axes in diagram 107 for instance show to well-defined secondary concentrations on either side of the main concentration. This feature has to be incorporated in the interpretation. It has often been inferred, and occasionally observed, that during a flattening process the initial slip planes tend to rotate around their intersection line, from their initial orientation in such a sense as to enlarge their originally acute angle with the compressive force. Such a rotation of the vertical slip planes has probably occurred in the studied samples, for the X_{o1} and Z_{o1} axes in the diagrams 105 and 107 are not only

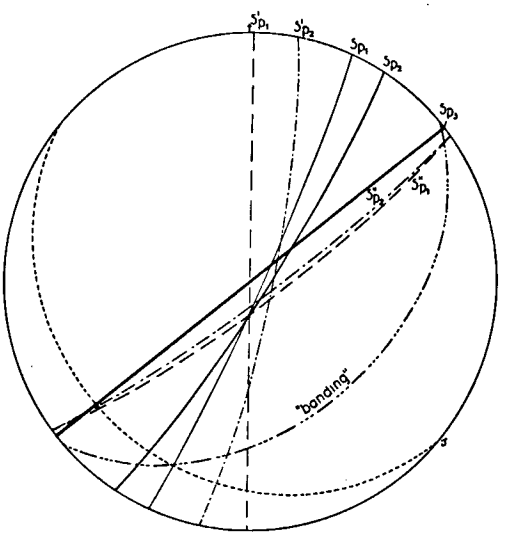

Figure 36.
Collective diagram of the structural features observed in the fabric diagrams of the Pyrenean lherzolite.
Sp_1, Sp_2, Sp_3: major vertical slip planes respectively in sample P. 1, P. 2, P. 3.
Sp_1' Sp_1'', Sp_2' Sp_2'': sets of rotated slip planes.
s: sub-horizontal slip plane.

concentrated in point maxima but they form girdles along the margins of the diagrams. The resulting slip planes which intersect at angles of about 30° can be observed in some of the thin sections where they are marked by zones of very fine grained, probably crushed olivine grains.

In the fabric diagrams of two of the three specimens (P. 1, P. 2) the rotated equivalents of the major vertical slip planes can be observed; the diagrams of the third specimen only show one probable vertical slip plane. Figure 36 represents a collective diagram of the major slip planes of the three specimens together with the above mentioned sets of rotated slip planes; the orientation of the supposed sub-horizontal slip plane system is also represented. This diagram proves the close agreement between the fabrics of the three specimens.

The enstatite fabric of specimen P. 3 can but lead to the conclusion that

the preferred orientation of this mineral is governed by the same rules as olivine. The theoretical basis and the data here collected are too restricted to permit any further conclusion regarding the specific deformation mechanism of this mineral.

Apart from the deformed aspect of the rock, the main argument that the observed fabric is secondary, has been based on the observation that the relation between the banding and the orientation of the crystal axes of olivine was not of the usual type, i. e. a strong concentration of X_{ol} normal to the lamination. It has already been mentioned that the banding has an almost constant orientation throughout the body. In specimen P. 2 it proved possible to measure the orientation of the banding in relation to the horizontal plane so that it could be represented in the fabric diagrams. Diagram 110 reveals that the Z_{ol} axes are almost parallel to the banding plane. By experience we know that the original fabric was probably dominated by an orientation of the Z_{ol} axes parallel to the plane of the lamination, and of the X_{ol} axes in the pole of the corresponding great circle. Although there are no indications for the direction of the original preferred orientation of Z_{ol} in this plane, it is not excluded that it did not differ much from the main Z_{ol} concentration now observed. This can probably account for the observed unusually strong Z_{ol} orientation. Furthermore it shows that the rotation of the olivine grains from their original to their new orientation has not necessarily been a very complex movement, a simple rotation around their long axis, Z_{ol}, may have been sufficient.

This petrotectonic study of the Pyrenean lherzolite indicates that the fabric of peridotites reacts easily upon deformative stresses. The resulting mineral orientation can be a lattice orientation in which the X_{ol} and Z_{ol} axes play a predominant role, a conclusion which is also supported by the nature of the tectonic fabric observed in the nodular inclusions in lavas. This observation implies that an interpretation of the usual olivine fabric in terms of a dimensional orientation of the composing crystals has to be handled with great reserve, especially because the alpine type peridotites occur in highly compressed areas.

CHAPTER VII

THE LATTICE ORIENTATION OF OLIVINE

The basic idea of the interpretation of the olivine fabric in the ultrabasic nodular inclusions in the lavas of Auvergne has been that the observed tectonic fabric can be interpreted as the result of the rotation of an earlier existing olivine fabric such as has been observed in many peridotites notably in the inclusions at Dreiser Weiher. The tectonic nature of the French nodules led to the conclusion that these rocks are not directly genetically related with the lavas in which they occur, but are probably fragments of the mantle of the earth, carried to the surface by means of the lavas. This conclusion is supported by the chemical and petrographical work of several other investigators.

Reasoning back from this conclusion we can now pay attention to the fabric observed in the sample from Dreiser Weiher which was supposed to be the same as the pre-deformational one in the samples from Auvergne. This olivine fabric, which is dominated by a strong X_{ol} concentration and a rather well developed parallel orientation of the Z_{ol} axes in the plane normal to X_{ol}, is mostly coupled with a dimensional orientation of the olivine crystals. The form of the crystals has been interpreted as the actual cause of the fabric by several authors. In such a view the parallel orientation of the crystals must have resulted from a mechanism of laminar flow which may have been attended by a gravitational settling of early crystallizing minerals to the bottom of the supposed magma chamber. In chapter II of this paper several objections have been formulated against such an interpretation. These objections were based on peculiarities of the observed mineral orientation which are difficult to reconcile with the idea of a dimensional orientation. The author then advanced the opinion that the dimensional orientation is probably the effect of the lattice orientation of the crystals. It is improbable that, if the nodular inclusions are fragments of the earth's mantle, the liquid phase from which the composing minerals crystallized, has in the not too distant past been so abundant that a laminar flow of the crystals could be the cause of their orientation. Consequently one should look for another mechanism which can account for the preferred orientation of olivine; and the only alternative of a dimensional orientation can be found in a lattice orientation of the crystals.

In chapter II attention has already been paid to the hypothesis that the ultrabasic nodules from Dreiser Weiher are S-tectonites. The data provided in the following chapters of this paper have demonstrated that the broad outlines of the microfabric of the sample concerned (the strong X_{ol} concentration normal to S, the parallel orientation of Z_{ol} and Z_{en} in S, as well as the Y_{en} girdle normal to this plane), correspond to the crystal orientation to be expected in a tectonite in which slip along a single or a couple of slip planes occurs. Despite this conclusion there remain still a few details (See chapter II) which are difficult to reconcile with the conclusion that the rocks in question are tectonites. Therefore it might be interesting to review two recent theories on

the possible structural orientation of olivine during crystallization.

Bautsch (1960) in his previously mentioned paper, has described an experiment during which a forsterite rock has been exposed to a temperature gradient provoked by hot gasses in a Siemens-Martin oven. For the experiment a specimen was used the composing olivine crystals of which did not show any sign of preferred orientation before the heating was started. Under the influence of the heat the rock recrystallized, thus giving rise to a rather strong preferred orientation of the crystals. The fabric diagrams of olivine published by Bautsch are very convincing regarding the orientation of the X_{ol} axes of the recrystallized olivine crystals parallel to the major temperature gradient. The Y_{ol} axes show this orientation to a minor extent. This experiment is interesting, for temperature gradients are likely to exist in the deeper parts of the earth, and could consequently be responsible for the often observed parallel orientation of the X_{ol} axes.

In chapter VI a passing reference has been made to the theory of Kamb (1959) which predicts the orientation of crystals in the case of (re)crystallization in a uniaxial stress field. According to Kamb the preferred orientation a crystal will assume in the case of recrystallization by solution and redisposition is that which minimizes the chemical potential required for equilibrium across the plane normal to the major axis of normal stress. Kamb has carried out the thermodynamical calculations for hexagonal and rhombohedral crystals, but the theory can also be applied to orthorhombic crystals and even to olivine since the elastic constants of this mineral are known (Verma 1960). The result of the pertinent calculations leads to the conclusion that the axes of olivine will tend to be aligned parallel to the major axis of normal stress [10]). These approaches to the problem of the possible lattice orientation of the X_{ol} axis are meant to demonstrate that other interpretations than the usually offered explanation, which is based on the dimensional orientation of olivine, can account for the often observed strong preferred orientation of X_{ol}. In the light of the conclusions reached in this paper these interpretations certainly gain in importance.

Kamb has also discussed the case of a recrystallization taking place without solution and redisposition, that is by the growth of crystals by diffusion in the solid state. It is found that hexagonal and rhombohedral crystals in a uniaxial stress field should grow preferentially with their strongest axis parallel to the unique stress axis. Olivine in such a case will show an alignment of the Z axes parallel to the unique stress axis. This is the case to which reference has been made in paragraph four of the foregoing chapter.

[10]) The said theory of preferred orientation of crystals growing in a stress field, and its application to olivine will be discussed by Hartman and den Tex in a paper to be published in the same volume of the Leidse Geologische Mededelingen.

SUMMARY

The solution of the problem whether the ultrabasic inclusions in lavas are accumulation products of early crystallized minerals of the lavas in which they occur, or fragments of the earth's peridotite shell carried to the surface by the eruptive force of the lavas, largely depends on the answer to the question whether these inclusions are tectonites or not.

The structure of the specimens from Auvergne (France), which formed the main subject of this study, has been proved conclusively to be of a tectonic nature, from the macroscopically visible intersecting slip planes which are definitely younger than the banding of the specimen, as well as from microscopic evidence that suggests that both the olivine and enstatite crystals are concentrated in the intersecting slip planes. The fabric of olivine and enstatite proved to be symmetrical in respect of these slip planes, although remnants of an initial, pre-deformational orientation related with the banding still persist. In order to establish the relation between the old and the new fabric a comparative study of the fabric of a nodule from Dreiser Weiher (chapter II) and the crystal orientation of the banded sample from Auvergne (chapter III) has been made. It was concluded that the tectonic fabric of the sample from Auvergne could be interpreted as the result of a mechanical rotation of the composing crystals around two rotation axes, from their earlier orientation which is observed in the German specimen, into their new orientation which is symmetrical in respect of the intersecting slip planes. The rotation axis of olivine proved to be parallel to the intersection of the banding and a slip plane (S_1), the rotation axis of enstatite is parallel to the intersection of the second slip planes (S_2) and a plane normal to the banding, which is characterized by the X_{ol}—Y_{en} girdle in the pre-deformational fabric. The geometry of the observed fabric further suggests that the crystals rotated in opposite sense over supplementary angles around the rotation axes.

The distribution of olivine in the intersecting planes as well as the above mentioned rotation were further proved in a second sample from Auvergne on which an axial distribution analysis was carried out. The results of this analysis confirmed the expectations that crystals of a specific orientation are concentrated in intersecting directions in the plane of observation. The lattice orientation of olivine proved to be dominated by an orientation of {010} parallel to S_1 and [010] sub-parallel to S_2, while the enstatite crystals showed a strong preferred orientation of [001] sub-parallel to S_1 and [100] in S_2. The comparison of the preferred orientation of the X_{ol} axes in five samples of different mineralogical composition has demonstrated that the preferred orientation of the X_{ol} axes increases with increasing olivine content. All these results point to a tectonic nature of the structure of the ultrabasic inclusions in the lavas of Auvergne. Since the Mg/Fe distribution in the pyroxenes of the nodules suggests that these minerals crystallized at temperatures well above those of magmatic assemblages, it was concluded that the studied specimens are not derived by crystal fractionation from the lavas in which they occur, but are likely to be fragments of the earth's peridotite shell.

The fabric of the type-locality of the lherzolites in the French Pyrenees proved to be secondary and symmetrical in respect of the local Alpine stress field in such a way that the Z axes of both olivine and enstatite are parallel to the major axis of the stress deviator. The interpretation of this tectonic fabric of olivine has been based on the translation mechanism of olivine, described by Chudoba and Frechen (1950).

In the last chapter attention has been paid to some recent theories and experiments which all lead to the conclusion that the orientation of crystals during growth, either in a uniaxial stress field or under a temperature gradient, is governed by the lattice of the crystals involved, a conclusion that might be useful for the interpretation of olivine fabrics, for the results of this study suggest that the crystal structure and not the grain shape governs he fabric of many ultrabasic rocks.

SAMENVATTING

Deze publikatie behandelt de struktuur van lherzolieten waarbij in het bijzonder aandacht is besteed aan het maaksel van ultrabasische insluitsels in de lava's van Auvergne. De orientatie van de kristallografische assen van olivijn en enstatiet in deze gesteenten werd vergeleken met die van de insluitsels van de bekende vindplaats Dreiser Weiher in de Eifel. De kernvraag voor de oplossing van het probleem of deze gesteenten kristal aggregaten zijn, ontstaan door de accumulatie van vroeg gekristalliseerde mineralen uit de lava's waarin zij thans worden aangetroffen, dan wel fragmenten van een veronderstelde peridotiet-laag in de aardmantel waaruit de lava's door opsmelting kunnen zijn ontstaan, wordt gevormd door de al dan niet tektonische aard van deze gesteenten.

De tektonische aard van de insluitsels uit Auvergne kon overtuigend worden aangetoond:

1e uit makroskopische eigenschappen van de gesteenten waarin elkaar snijdende bewegingsvlakken zichtbaar zijn die de oudere gebande struktuur van de handstukken verstoren.

2e uit een mikroskopisch onderzoek dat aantoonde dat de olivijn en enstatiet kristallen geconcentreerd zijn in richtingen die met deze schuifvlakken overeenkomen.

3e uit de gevonden kristal orientaties die merendeels symmetrisch bleken te zijn met de snijdende schuifvlakken, doch in één handstuk tegelijkertijd ook nog verband vertoonden met de oude gebande struktuur van het gesteente.

Teneinde nu een direct verband te kunnen leggen tussen het oorspronkelijke maaksel en datgene wat van de deformatie resulteerde, werden een handstuk uit de Eifel (hoofdstuk II) en een uit Auvergne (hoofdstuk III) onderzocht en vergeleken. Het is daarbij gebleken dat het maaksel dat in de gesteenten uit Auvergne wordt aangetroffen kan worden beschouwd als het resultaat van een draaiing van de kristallen vanuit hun originele orientatie, die in de gesteenten van de Eifel wordt aangetroffen, om rotatie assen. Deze assen zijn voor olivijn en enstatiet verschillend georienteerd, en wel zo dat die van olivijn evenwijdig is aan de snijlijn van een van het nieuwe schuifvlak (S_1) met de banding van het gesteente, terwijl die van enstatiet evenwijdig is aan de snijlijn van het tweede schuifvlak (S_2) met het vlak dat in het oorspronkelijke maaksel gekenmerkt wordt door een gordel van X_{ol} en Y_{en} assen. Een verdere uitwerking van de deformatie theorie maakt het dan waarschijnlijk dat deze draaiing om iedere rotatie as in tweeërlei zin plaats vond over hoeken die elkaars supplement zijn. De resulterende orientatie van de olivijn kristallen schijnt daarbij te worden bepaald door de ligging van het vlak {010} in het ene schuifvlak (S_1) en de richting [010] ongeveer in het snijdende vlak (S_2) terwijl enstatiet zich met [001] vrijwel parallel aan S_1 legt en met [100] in S_2. Deze gedachten vonden verdere bevestiging in een onderzoek van een tweede handstuk uit Auvergne waarop een zogenaamde „assen verdelings analyse" van olivijn werd uitgevoerd (hoofdstuk IV). Deze methode van onderzoek die erop gericht is na te gaan of er

een verband bestaat tussen de orientatie van de kristallografische assen van het betreffende mineraal en de ligging van de kristallen in het onderzochte gesteente, heeft aangetoond dat ook in een handstuk waarin makroskopisch geen richtingen te zien zijn, de olivijn kristallen met bepaalde rooster orientaties, in elkaar snijdende vlakken zijn geconcentreerd. Tenslotte leidde een verder onderzoek nog tot de conclusie dat de sterkte van de voorkeurs orientatie van de X assen van olivijn afneemt naarmate het gehalte olivijn in het gesteente afneemt.

De combinatie van de aldus bewezen tektonische aard van de gesteenten en de zeer hoge kristallisatie temperatuur en druk van de belangrijkste mineralen zoals die tot uiting komt in de Mg/Fe verdeling in de pyroxenen leidde tot de conclusie dat de uit Auvergne afkomstige ultrabasische insluitsels niet door fractionele kristallisatie ontstaan zijn uit de lava's waarin zij gevonden worden, waardoor het dan waarschijnlijk wordt dat dit ook niet het geval is voor de meeste van elders stammende ultrabasische insluitsels, met name die van Dreiser Weiher. In overeenstemming met de op geofysische, chemische, petrografische en vulkanologische onderzoekingen gebaseerde conclusies van andere onderzoekers werd besloten tot een herkomst van de onderzochte gesteenten uit de mantel van de aarde.

De type lokaliteit van de lherzolieten in de franse Pyreneeën werd eveneens in het onderzoek betrokken (hoofdstuk VI). De olivijn maaksels van drie, en het enstatiet maaksel van één handstuk hiervan werden onderzocht en hun verhouding tot de regionale tektonische struktuur bepaald. De Z assen van zowel olivijn als enstatiet bleken parallel te liggen aan de richting van sterkste compressie ten tijde van de alpiene deformatie. Een interpretatie gebaseerd op de gangbare verklaring van de translatie verschijnselen in olivijn bleek toepasbaar op het waargenomen maaksel.

Gezien het feit dat de resultaten van het onderhavige onderzoek erop wijzen dat de orientatie van olivijn in gedeformeerde gesteenten bepaald wordt door het kristalrooster van dit mineraal, werd in het laatste hoofdstuk een overzicht gegeven van enkele recente proeven en theorieën die het waarschijnlijk maken dat ook de orientatie van mineralen die onder gerichte druk of in een temperatuur gradient groeien, bepaald wordt door eigenschappen die nauw met de kristalstruktuur van deze mineralen samenhangen.

RÉSUMÉ

Cette étude traite de la structure des lherzolites. Attention a été donnée tout particulièrement à la structure des enclaves ultrabasiques dans les laves d'Auvergne. L'orientation des cristaux d'olivine et d'enstatite a été comparée avec celle des enclaves bien connues de Dreiser Weiher dans l'Eifel. La solution du problème si ces roches se sont formées par l'accumulation de cristaux de provenance des laves, ou bien qu'elles sont des fragments d'une couche de péridotite dans le manteau terrestre où les laves sont formées par fusion partielle, dépend largement de la réponse donnée à la question si la structure de ces roches est d'origine tectonique oui ou non. La nature tectonique de la structure des enclaves dans les roches volcaniques d'Auvergne a pu être démontrée de facons suivantes:

L'aspect macroscopique de ces roches révèle parfois des plans de glissement intersectant à des angles de 90°, ces plans sont certainement d'origine postérieure à la structure stratifiée des nodules.
L'étude microscopique a révélé que les cristaux d'olivine et d'enstatite sont concentrés dans ces plans.
L'orientation des axes cristallographiques de ces cristaux est symétrique par rapport à ces plans de glissement, quoique parfois des traces d'une orientation antérieure relative au rubanement persistent.

Enfin d'établir un rapport direct entre la structure ancienne et celle qui résulte de la déformation, un échantillon de l'Eifel a été comparé avec un autre d'Auvergne. Il en a résulté que l'orientation des cristaux dans le dernier peut être considérée comme le résultat d'une déformation qui a affecté une roche de structure analogue à celle trouvée ordinairement dans les nodules de l'Eifel. Cette déformation consiste d'une rotation des cristaux autour de l'un ou l'autre axe de rotation qui sont respectivement parallèles à la ligne d'intersection du premier plan de glissement (S_1) avec le plan de rubanement, et du second plan de glissement (S_2) avec le plan characterisé par l'orientation parallèle de X_{ol} et Y_{en} dans la structure ancienne. En outre il est probable que cette rotation se faisait en deux directions autour de chaque axe, sur des angles supplémentaires. Le résultat de cette rotation est tel que la face {010} d'olivine est parallèle à S_1 tandis que la direction [010] est quasi parallèle à S_2. [001] d'enstatite se met quasi parallèle à S_1 et [100] parallèle à S_2. Ces idées ont été confirmées par l'étude d'un second échantillon d'Auvergne dans lequel "une analyse de la distribution des axes" a été réalisée. Les résultats de cette analyse ont démontré que les cristaux d'olivine qui ont une certaine orientation sont concentrés dans des directions intersectantes dans le plan d'observation. En outre il a été démontré que l'orientation préférée d'olivine, en ce qui concerne la face {010} augmente avec l'augmentation de la teneur en olivine des nodules.

Toutes ces observations convergent vers la conclusion que la structure des enclaves volcaniques d'Auvergne est d'origine tectonique. Comme la distribution de Mg et Fe dans les pyroxènes édifiants est telle qu'on peut en déduire une température de cristallisation bien supérieure à celle des pyroxènes magmatiques

il en résulte qu'il est probable que les enclaves volcaniques de composition ultrabasique étudiées sont des fragments du manteau terrestre.

La localité type des lherzolites dans les Pyrénées françaises a aussi fait l'objet d'une analyse structurelle. Il en a résulté que la symétrie de l'orientation des axes d'olivine et enstatite est congruente avec la disposition des axes tectoniques Alpines, dans ce sens que Z_{ol} et Z_{en} sont parallèles à la direction de compression. L'interprétation de cette structure tectonique a pu être basée sur la théorie courante des phénomènes de translation dans l'olivine.

Enfin l'auteur a prêté attention à des théories et expériments récents qui ont démontré que l'orientation préférée adoptée par des cristaux pendant leur cristallisation dans un milieu de poussée unilatérale ou dans un gradient de température dépend de la structure de ces cristaux, une conclusion qui a été confirmée par les résultats de cette étude.

LIST OF ROCK SAMPLES

First column: notation mentioned in text.
Second column: registration number of the Rijksmuseum van Geologie en Mineralogie te Leiden.

D.W. 1.	St. 109431.
A. 1.	St. 109432.
A. 2.	St. 109433.
A. 3.	St. 109434.
A. 4.	St. 109435.
A. 5.	St. 109436.
A. 6.	St. 109437.
A. 7.	St. 109438.
P. 1.	St. 109439.
P. 2.	St. 109440.
P. 3.	St. 109441.

SELECTED BIBLIOGRAPHY

ADAMS, G., 1926. The compressibilities of dunite and of basalt glass, and their bearing on the composition of the earth. Proc. Natl. Acad. Sci. U. S. A., **12**, 275—283.

ANDREATTA, C., 1934. Analisi strutturali di rocce metamorfiche, V. Oliviniti. Period. Min., Anno V., 237—253.

—— 1946. La regola di orientazione dei cristalli di olivina nelle tettoniti. Rend. Soc. Min. Ital., **Anno III**, 41—42.

BARTHOLOMÉ, P., 1960. L'interprétation pétrogénétique des associations d'olivine et d'orthopyroxène. An. Soc. Géol. Belg., **83**, 319—345.

—— 1961. Co-existing pyroxenes in igneous and metamorphic rocks. Geol. Mag., **98**, 346—348.

BATTEY, M. H., 1960. The relationship between preferred orientation of olivine in dunite and the tectonic environment. Am. Jour. Sci., **258**, 716—727.

—— 1962. Reply to the discussion by Brothers. Am. Jour. Sci., **260**, 313—315.

BAUER, M., 1891. Der Basalt vom Stempel bei Marburg und einige Einschlüsse desselben. N. Jahrb. Min. Geol. Palaeont., IIe Band, 156—205, 231—271.

BAUTSCH, H. J., 1960. Mineralogisch-petrographische Untersuchungen an Chrommagnesit- und Forsteritsteinen. Freib. Forsch. H., **C 106**, 1—75.

BECKER, A., 1881. Ueber die Olivinknollen im Basalt. Deutsche Geol. Ges. Zeitschr., **33**, 31—65.

BLEIBTREU, K., 1883. Beiträge zur Kenntnis der Einschlüsse in den Basalten mit besonderer Berücksichtigung der Olivinfels-Einschlüsse. Deutsche Geol. Ges. Zeitschr., **35**, 489—556.

BOULE, R., 1892. Description géologique du Velay. Bull. Ser. Carte Géol. Fr., **28**.

BOWEN, N. L., 1927. Ultrabasic and related rocks. Am. Jour. Sci. 5th ser., **29**, 89—108.

BOWEN, N. L. & SCHAIRER, J. F., 1933. The problem of the intrusion of dunite in the light of the olivine diagram. 16th Internat. Geol. Congr. Rept., **1**, 391—396.

—— —— 1935. The system MgO-FeO-SiO_2. Am. Jour. Sci. 5th ser., **29**, 151—217.

BOWEN, N. L. & TUTTLE, O. F., 1949. The system MgO-SiO_2-H_2O. Bull. Geol. Soc. Am., **60**, 439—460.

BOYD, F. R. & ENGLAND, J. L., 1960. Minerals of the mantle. Yearb. Carnegie Inst., **59**, 47—52.

—— —— 1961. Melting of silicates at high pressures. Yearb. Carnegie Inst. **60**, 113—125.

BROTHERS, R. N., 1959. Flow orientation of olivine. Am. Jour. Sci., **257**, 574—585.

—— 1960. Olivine nodules from N. Zealand. Rep. Intern. Geol. Congr., 21e Session, Norden, **13**, 68—81.

—— 1962. Discussion: The relationship between preferred orientation of olivine and the tectonic environment. Am. Jour. Sci., **260**, 310—312.

BROUSSE, R., 1961. Analyses chimiques des roches volcaniques tertiaires et quaternaires de la France. Bull. Serv. Carte Géol. Fr., **263**, T. 58.

BROWN, G. M., 1961. Co-existing pyroxenes in igneous assemblages, a re-evaluation of the existing data on tie-line orientations. Geol. Mag., **98**, 333—343.

BROWN, P. E., 1961. Co-existing pyroxenes. Geol. Mag., **98**, 531.

CASTERAS, M., 1933. Recherches sur la structure du versant Nord des Pyrénées. Bull. Serv. Carte Géol. Fr., **189**, T. 37, 1—524.

CHUDOBA, F. K. & FRECHEN, J., 1941. Die frühmagmatische Bildung der Olivinausscheidungen von Finkenberg (Siebengebirge) und Dreiser Weiher (Eifel). Geol. Rundschau, **32**, 257—278.

—— —— 1950. Ueber die plastische Verformung von Olivin. N. Jahrb. Min. Abh. Abt. A, Bd. **81**, 183—200.

COLLETTE, B. J., 1959. On helicitic structures and the occurrence of elongate crystals in the direction of the axis of a fold. Proc. Kon. Ned. Akad. Wet., ser. B, **62**, 161—171.

DACHILLE, F. & ROY, R., 1960. High pressure studies of the system Mg_2GeO_4-Mg_2SiO_4 with special reference to the olivine-spinel transition. Am. Jour. Sci., **258**, 225—246.

DAVIS, G. L., ALDRICH, L. T., TILTON, G. R., WETHERILL, G. W. & JEFFERY, P. M., 1956. Geochemistry of uranium and lead. Carnegie Inst. Wash. Year Book, **1955—1956**, 99—100.

Diriu, M., 1959. Olivini e pirosseni di noduli inclusi in basalti della Sardegna centro-occidentale. Period. Min., **28**, 259—283.

Drescher-Kaden, F. K., 1954. Zur Darstellung des Regelungsgrades eines Gefüges. Tschermaks Min. Petr. Mitt. 3e F., B. **4**, 159—177.

Eaton, J. P. & Murata, K. J., 1960. How volcanoes grow. Science, **132**, no. 3432, 925—938.

Ernst, Th., 1935. Olivinknollen der Basalte als Bruchstücke alter Olivinfelse. Nachr. Ges. Wiss. Göttingen, Math.-Phys. Kl., N. F. Fachgr. IV, 1e B., 147—154.

—— 1936. Der Melilith-Basalt des Westberges bei Hofgeismar, nördlich von Kassel, ein Assimilationsprodukt ultrabasischer Gesteine. Chem. d. Erde, **10**, 631—666.

—— 1948. Die Olivinfels-Einschlüsse der Basalte. Zusammenfassung einer Entgegnung an F. K. Chudoba and J. Frechen. Geol. Rundschau, B. **36**, 39.

Fairbairn, H. W., 1949. Structural Petrology of deformed rocks. Addison-Wesley Press. Inc., Cambridge, Mass.

Frechen, J., 1948a. Die Genese der Olivinausscheidungen von Dreiser Weiher (Eifel) und Finkenberg (Siebengebirge). N. Jahrb. Min. Geol., B. **79**, Abt. A, 317—406.

—— 1948b. Zur Gefügeausbildung der basaltischen Olivinknollen. Zusammenfassung einer Entgegnung an Th. Ernst. Geol. Rundschau, B. **36**, 40.

Gorshkov, G. S., 1957. On some theoretical problems of volcanology. Bull. Volc. ser. II, T. **19**, 105—115.

Griggs, D. T., Turner, F. J. & Heard, H. C., 1960. Deformation of rocks at 500°—800°C. Rock deformation. Mem. Geol. Soc. Am., **79**, 39—62.

Hamilton, J., 1957. Banded olivines in some Scottish Carboniferous olivine-basalts. Geol. Mag., **94**, 135—139.

Harris, P. G. & Rowell, J. A., 1960. Some geochemical aspects of the Mohorovic discontinuity. Jour. Geophys. Res., **65**, 2443—2459.

Hartman, P. & Perdok, W. G., 1955. On the relation between structures and morphology of crystals. Acta Cryst., **8**, 49—52.

Harumoto, A., 1952. Melilite-nepheline basalt, its olivine nodules, and other inclusions from Nagahama, Japan. Mem. Coll, Sci. Univ. Kyoto, ser. B, **20**, 69—88.

Heritsch, F., 1908. Ueber einige Einschlüsse und vulkanische Bomben von Kapfenstein in Oststeiermark. Centralbl. Min., Geol. Palaeontol., 297—305.

Hess, H. H., 1938. A primary peridotite magma. Am. Jour. Sci., 5th ser., **35**, 321—344.

—— 1941. Pyroxenes of common mafic magmas, part 2. Am. Min., **26**, 573—594.

—— 1949. Chemical composition and optical properties of common clinopyroxenes. Am. Min., **34**, 621—666.

—— 1955. Serpentines, orogeny, and epeirogeny. Geol. Soc. Am. Spec. Paper, **62**, 391—408.

—— 1960. Stillwater igneous complex, Montana, a quantitative mineralogical study. Geol. Soc. Am., Mem. **80**, 1—230.

Hoffer, A., 1961. Discussion of the paper by Barclay Kamp: The thermodynamic theory of non-hydrostatically stressed solids. Jour. Geophys. Res., **66**, no. 8, 2600.

Huang, W. T. & Merritt, C. A., 1952. Preferred orientation of olivine crystals in troctolite of the Wichita mountains Oklahoma. Am. Min., **37**, 865—868.

Isshiki, N., 1958. Petrology of plutonic cognate ejecta from Nishi-Yama volcano, Hachijo Jima. Jap. Jour. Geol. Geogr., **29**, 55—75.

Jackson, E. D., 1961. Primary textures and mineral associations in the ultramafic zone of the Stillwater Complex Montana. Geol. Surv. Prof. Paper, **358**, 1—106.

Kamb, W. B., 1959. Theory of preferred crystal orientation developed by crystallization under stress. Jour. Geol., **67**, 153—171.

—— 1961. The thermodynamic theory of non-hydrostatically stressed solids. Jour. Geophys. Res., **66**, no. 1, 259—273.

Knopf, I. & Ingerson, E., 1938. Structural petrology. Geol. Soc. Am. Mem. **6**.

Koark, H. J., 1954. Ueber einen diagonalgeschichteten chromitdunit. Tschermaks Min. Petr. Mitt., 3e F., B. **IV**, 216—225.

Kretz, R., 1961a. Some applications of thermodynamics to co-existing minerals of variable composition: orthopyroxene-clinopyroxene and orthopyroxene-garnet. Jour. Geol., **69**, 361—387.

—— 1961b. Co-existing pyroxenes. Geol. Mag., **98**, 344—345.

Kuno, H., 1959. Discussion of the paper by J. F. Lovering: The nature of the Mohorovicic discontinuity. Jour. Geophys. Res., **64**, no. 8, 1071.

Kushiro, J., 1960. A possible origin of the tholeiitic magma. Jap. Jour. Geol. Geogr., **32**, 31—39.

Lacroix, A., 1893. Les enclaves des roches volcaniques. Extrait Ann. Acad. Mâcon, T. 10.

—— 1894. Etude minéralogique de la lherzolite des Pyrénées et ses phénomènes de contact. Nouv. Arch. Mus. Hist. Nat., 3e sér., T. 6, 209.

LADURNER, J., 1953. Zur Regelung von Olivingefüge. Fortschr. Min., B. 32, 82.

—— 1956. Das Verhalten des Olivins als Gefügekorn in einigen Olivingesteinen. Tschermaks Min. Petr. Mitt. 3e F., B. 5, 21—36.

LAUSEN, C., 1927. The occurrence of olivine bombs near Globe, Arizona. Am. Jour. Sci. 5th ser., 14, 293—306.

LOVERING, J F., 1958. The nature of the Mohorovicic discontinuity. Trans. Am. Geophys. Un., 39, 947—955.

—— 1959. Reply to discussion by H. Kuno. Jour. Geophys. Res., 64, no. 8, 1073.

MACDONALD, G. A., Volcanology. Science, 133, no. 3454, 673—679.

MACDONALD, G. J. F., 1960. Orientation of anisotropic minerals in a stress field. Geol. Soc. Am., Mem. 79, 1—8.

—— 1961. Discussion of the paper by W. Barclay Kamb. Jour. Geophys. Res., 66, no. 8, 2599.

MACKENZIE, D. B., 1960. High-temperature Alpine-type peridotite from Venezuela. Bull. Geol. Soc. Am., 71, 303—317.

MARINOS, G. & MARATOS, G., 1957. Greek Olivinites. Geol. Geoph. Res. (Athens), 5, 2, 1—12.

MURATA, K. J., 1960. A new method of plotting chemical analyses of basaltic rocks. Am. Jour. Sci., 258 A, 247—252.

O'HARA, M. J., 1960. Co-existing pyroxenes in metamorphic rocks. Geol. Mag., 97, 498—503.

PAULITSCH, P., 1953. Olivinkornregelung und Genese des Chromitführenden Dunits von Anghida auf der Chalkidike. Tschermaks Min. Petr. Mitt. 3e F., B. 3, 158—167.

PEACEY, J. S., 1961. Rolled garnets from Morar, Inverness-shire. Geol. Mag., 98, 77—80.

PHILLIPS, F. C., 1938. Mineral orientation in some olivine-rich rocks from Rum and Skye. Geol. Mag., 75, 130—135.

POLDERVAART, A., 1955. The crust of the earth. Sp. Pap. 62, Geol. Soc. Am.

POWERS, H. A., 1955. Composition and origin of basaltic magma of the Hawaiian Islands. Geochim. Cosmochim. Acta, 7, 77—107.

RAGAN, D. M., 1959. Mode of emplacement of the Twin Sister dunite. Bull. Geol. Soc. Am., 70. 1742—1743.

RAMBERG, H. & DE VORE, G. W., 1951. The distribution of Fe++ and Mg++ in co-existing olivines and pyroxenes. Jour. Geol., 59, 193—210.

RAVIER, J., 1959. Le métamorphisme des terrains secondaires des Pyrénées. Mém. Soc. Géol. Fr. Nouv. Sér., T. 38, no. 86.

REED, J. J., 1959. Chemical and modal composition of dunite from Dun Mountain, Nelson. N. Zealand Jour. Geol., 2, 916—919.

RINGWOOD, A. E., 1958. The constitution of the mantle. I. Geochim. Cosmochim. Acta, 13, 303—321.

—— 1959. Id. II—III. Ibidem, 15, 18—29, 195—212.

ROEVER, W. P. DE, 1957. Sind die Alpinotypen Peridotitmassen vielleicht tektonisch verfrachtete Brüchstücke der Peridotitschale? Geol. Rundschau, B. 46, 137—146.

—— 1960. Beitrage der Petrographie zur Kenntnis der tieferen Teile der Erde. Verh. Geol. Bundesanst. Wien, 1960, 23—31.

—— 1961. Mantelgesteine und Magmen tiefer Herkunft. Fortschr. Min., 39, 96—108.

ROSS, C. S. & FOSTER, M. D. & MYERS, A. T., 1954. Origin of dunites and of olivine-rich inclusions in basaltic rocks. Am. Min., 39, 693—737.

ROST, F., 1959. Probleme ultrabasischer Gesteine und ihrer Lagerstätten. Freib. Forsch. H., C. 58, 28—65.

—— 1961. Zur Stellung der Granatultrabasite des Sächsischen Grundgebirges. Freib. Forsch, H., C. 119, 119—135.

SANDER, B., 1930. Gefügekunde der Gesteine. Wien, Springer Verlag.

—— 1948. Einführung in de Gefügekunde der geologischen Körper. Wien-Innsbruck, Springer Verlag.

SANDER, B. & KASTLER, D. & LADURNER, J., 1954. Zur Korrektur des Schnitteffektes in Gefügediagrammen heterometrischer Körper. Sitz. Ber. Osterr. Akad. Wiss., Math. Naturw. Kl., Abt. I, B. 163, 400—424.

—— —— —— 1957. Tabellen zur Arbeit: Zur Korrektur des Schnitteffektes in Gefügediagrammen heterometrischer Körper. Ann. Univ. Saraviensis Naturw.-Sci. VI-4/2, 337—358.

SCHADLER, J., 1913. Zur Kenntnis der Einschlüsse in den südsteirischen Basalttuffen und ihrer Mineralien. Tschermaks Min. Petr. Mitt., **32**, 485—511.

SCHMIDT, W., 1932. Tektonik und Verformungslehre. Berlin, Verlag von Gebr. Borntraeger.

SCHWANTKE, A., 1923. Differenzierungerscheinungen an Hessischen Basalten. N. Jahrb. Min. Geol., Beil. B. **48**, 260—273.

SITTER, L. U. DE & ZWART, H. J., 1959. Explanatory text to the geological maps of the Palaeozoic of the Central Pyrenees, sheet 3, Ariège, France, 1 : 50.000. Leidse Geol. Med., **22**, 351—419.

SÖLLNER, K., 1960. Der Olivinnephelinit vom Teichelberg bei Groschlattengrün (Fichtelgebirge). N. Jahrb. Min. Abh., **93**, 324—388.

SØRENSEN, H., 1953. The ultrabasic rocks at Tovqussaq, West Greenland. Grønlandse Geol. Unders, **4**, 1—86.

TILLEY, C. E., 1947. The dunite-mylonites of St. Paul's rocks, Atlantic. Am. Jour. Sci., **245**, 483—491.

TILTON, G. R. & REED, G. W., 1960. Concentration of lead in ultramafic rocks by neutron activation analysis. Jour. Geophys. Res., **65**, 2529.

TURNER, F. J., 1942. Preferred orientation of olivine crystals in peridotites, with special reference to N. Zealand examples. Trans. Proc. Roy. Soc. N. Zealand, **72**, 280—300.

TURNER, F. J. & VERHOOGEN, J., 1960. Igneous and metamorphic petrology. McGraw-Hill Inc.: New York.

VERMA, R. K., 1960. Elasticity of some high density crystals. Jour. Geophys. Res., **65**, no. 2, 757—766.

VOLL, G., 1960. New work on petrofabrics. Liverpool, Manchester, Geol. Jour., **2**, 503—598.

WAGER, L. R., 1956. A chemical definition of fractionation stages as a basis for comparison of Hawaiian, Hebridean, and other basic lavas. Geochim. Cosmochim Acta, **9**, 217—248.

—— 1958. Beneath the earth crust. Adv. Sci., **15**, no. 58, 31—46.

WARREN, B. E. & MODELL, D. I., 1930. The structure of enstatite. Zeitschr. Krist., B. **75**, 1—15.

WEISKIRCHNER, W., 1958. Il comportamento delle Olivine alle temperature alte. Rend. Soc. Min. Italica, **14**, 355—358.

WILSHIRE, H. G. & BINNS, R. A., 1961. Basic and ultrabasic xenoliths from volcanic rocks of New South-Wales. Jour. Petr., **2**, 185—208.

WILSON, A. F., 1960. Co-existing pyroxenes: Some causes of variation and anomalies in the optically derived compositional tie-lines, with particular reference to charnocktitic rocks. Geol. Mag., **97**, 1—17.

WYLLIE, P., 1960. The system CaO-MgO-FeO-SiO_2 and its bearing on the origin of ultrabasic and basic rocks. Min. Mag., **32**, 459—470.

YODER, H. S. & SAHAMA, TH. G., 1957. Olivine X-ray determinative curve. Am. Min. **42**, 475—491.

YOSHINO, G., 1961. Structural-petrological studies of peridotite and associated rocks of the Higashi-akaishi-yama district, Shikoku, Japan. Jour. Sci. Hiroshima Univ., Ser. C, **3**, 343—408.

ZIRKEL, F., 1903. Ueber Urausscheidungen in rheinischen Basalten. Abh. Math. Phys. Kl. Königl. Sächs. Ges. Wiss., **28**, 101—198.

ZWART, H. J., 1954. Sur les lherzolites et ophites des Pyrénées. Leidse Geol. Med., **18**, 281—286.